GEOMORPHIC CONTROLS ON SPATIAL DISTRIBUTIONS OF COBBLES AND BOULDERS IN STREAM-CHANNEL NETWORKS

A thesis submitted to the faculty of
San Francisco State University
In partial fulfillment of
The Requirements for
The Degree

Master of Science
In
Geosciences

by

Eric Thomas Donaldson

San Francisco, California

August, 2011

CERTIFICATION OF APPROVAL

I certify that I have read *Geomorphic Controls on Spatial Distributions of Cobbles and Boulders in Stream-Channel Networks* by Eric Thomas Donaldson, and that in my opinion this work meets the criteria for approving a thesis submitted in partial fulfillment of the requirements for the degree: Master of Science in Geoscience at San Francisco State University.

Dr. Leonard Sklar

Associate Professor of Geosciences

Dr. Jason Gurdak

Assistant Professor of Geosciences

Dr. Tim Janssen

Assistant Professor of Geosciences

GEOMORPHIC CONTROLS ON SPATIAL DISTRIBUTIONS
OF COBBLES AND BOULDERS IN STREAM-CHANNEL NETWORKS

Eric Thomas Donaldson
San Francisco, California
2011

Cobbles and boulders (CoBo) in stream channels provide overwintering habitat for juvenile steelhead trout (*Oncorhynchus mykiss)*. Lack of overwintering habitat may be a key limiting factor causing dwindling steelhead populations. Here, I develop a model for predicting the spatial distribution of CoBo in Pescadero Creek, San Mateo County, northern California, which could be used to estimate the watershed-scale extent of overwintering habitat. The model is based on the theoretical expectations that (1) bed sediment is at threshold of motion at bankfull discharge, (2) debris flows deliver large material to predictable locations in stream channel networks, (3) shallow landsliding is a primary source for debris flows, and (4) that durable source bedrock is necessary for CoBo to occur. I develop and test the model with a combination of field reconnaissance, laboratory rock strength testing, and GIS analysis of the channel network and upstream shallow landsliding potential and rock type. The model correctly predicts the occurrence or lack of CoBo at 90% of the field-verified sites using criteria for channel slope, drainage area, and upstream extent of either hillslope instability or durable bedrock. From measurements of refugia density in two reaches, I estimate that CoBo can support 0.5 fish/m^2 for juvenile steelhead.

I certify that the abstract is a correct representation of the content of this thesis.

______________________________ ____________________
Chair, Thesis Committee Date

ACKNOWLEDGEMENTS

This thesis would not have been possible without the help and support provided by my advisor, Dr. Leonard Sklar. His guidance and encouragement from the ambitious beginnings of this project have facilitated my growth as a scientist. I thank my committee members, Jason Gurdak and Tim Janssen for the thoughtful insight and patience. I thank the members of the Pescadero TMDL team, specifically Jill Marshall, Mike Napolitano, Frank Ligon, and Bill Dietrich for their collective assistance and guidance. Thanks to the following for help performing fieldwork: Jeff Prancevic; Nelle Donaldson; Jon Beyeler; Leslie Ferguson; Alan Kuoch; Nariman Safizadeh; Russell Macarthur; Eric Huber; Charles Post; Sam Kayed. I'd like to extend gratitude to Doug Ley, Matt Bissell, and Fred Keesaw of RedTree Lumber for facilitating access to the many stream channels on their property. Gratitude goes to the California State Water Resources Control Board and the Doris and David Dawdy Foundation for their financial support. I am grateful to my mother and father, Pat and Doug Donaldson, for always sustaining my intellectual curiosity and supporting me and my family through this adventure. I thank my intelligent and beautiful wife, Nelle Donaldson, for her unending patience, flexibility, emotional support, quality editing, and for being an amazing mother to our son, Kaj. Lastly, I thank Kaj, for putting this experience in perspective.

TABLE OF CONTENTS

LIST OF TABLES

LIST OF FIGURES

LIST OF APPENDICES

1. INTRODUCTION

1.1 BACKGROUND

Wild steelhead trout (*Oncorhynchus mykiss*) populations in California have declined 80% since European settlement [*Busby*, 1996; *Busby et al.*, 2000] due to climate change, overfishing, dams, and loss of habitat due to land use practices and development. Along the western coast of the United States, steelhead are listed as threatened or endangered by the National Oceanic and Atmospheric Administration (NOAA) Fisheries Division. Recently, many biologists and geomorphologists have focused their efforts on restoring and preserving salmonid species as a natural resource, influencing public policy, attracting substantial funding and generating an industry of professional scientists dedicated to studying salmonids [*e.g. Cui et al.*, 2006].

A great number of studies have focused on spawning habit, where adult fish create nests (redds) and deposit eggs into the streambed, however, very little emphasis has been placed on rearing habitat for juvenile salmonids as a limiting factor for the species. Cobble-boulder channel beds (hereafter, "CoBo") are a critical habitat feature for juvenile Steelhead, who overwinter in freshwater streams prior to migrating to the ocean [*Meyer and Griffith*, 1997]. CoBo can be defined (Ligon, pers. com) as channel beds dominated by cobbles and boulders (median grain size ≥128mm), with open interstices free of fine sediment, where constituent bed particles have a low recurrence interval of motion. Fish use CoBo as refuge from high velocity stream flow events [*Reiser and Bjornn*, 1979]. In addition to protecting fish from being displaced downstream, these features also provide cover from predators and help improve fish bioenergetic performance during a period marked by poor growth. As a result of widespread removal of large woody debris from streams [*e.g. Sedell and Luchessa*, 1982], it is likely that the interstitial spaces provided by CoBo have gained importance for overwintering salmonids. CoBo are correlated with higher densities of juveniles steelhead [*Chapman and Bjornn*, 1969; *Hartman*, 1965; *Meyer and Griffith*, 1997], yet none have quantitatively identified the landscape-scale geologic and geomorphic conditions necessary to generate CoBo habitat. Because overwintering habitat could be a limiting factor for steelhead, it is important to assess the physical controls on the distribution of CoBo in stream channel networks and develop a predictive model that can help guide land management and stream restoration efforts.

Many workers have used the assumption that the bed sediment grains are at the threshold of motion for some dominant discharge, often referred to as bankfull flow, to successfully predict the caliber of stream bed sediment for sand and gravel bedded streams[*e.g. Parker*, 1978a; *Wilcock*, 1993; *Buffington*, 1999]. This approach is based on the expectation that smaller particles will be winnowed from the bed during lower, more frequent flows. Only recently have workers begun to study how threshold of motion predictions can be applied to steep channels [*Church*, 2006; *Yager et al.*, 2007; *Lamb et al.*, 2008; *Recking*, 2009]. While these studies have done an excellent job identifying the mechanisms that control the threshold of motion in steep mountain channels, none attempt to apply the results in the field to predict bed grain size in steep mountain streams where bed grain size is influenced by debris flows and other hillslope properties.

The threshold-of-motion approach assumes that local hydraulic conditions control bed particle size, and that variations in sediment supply from upstream can be neglected. In contrast, *Sklar et al.* [2006] posit that supply of sediment from hillslopes, and the abrasion of particles as they move downstream, also influence the grain size distribution of channel beds. The theoretical model set forth by *Sklar et al.* [2006] introduces a fundamental paradigm shift from the threshold of motion at bankfull flow bed grain size prediction: In order to fully understand why channel beds have a certain grain size, we must look upstream at the sediment supply conditions.

Debris flows are an important mechanism that delivers sediment from hillslopes to channels, particularly the coarse particles that form CoBo. Debris flows typically originate as landslides on hillslopes that mobilize a heterogeneous mixture of rock particles, soil and woody material in a slurry that is delivered to and eventually deposited in stream channels. Debris flows strongly influence channel long profile in steep mountain streams by eroding bedrock and mobilizing and depositing sediment [*Stock and Dietrich*, 2003]. The dominance of incision into bedrock by debris flows in steep mountain streams causes a scaling break in the relationship between drainage area and channel slope, compared to reaches downstream where fluvial processes dominate incision [*Montgomery and Buffington*, 1997; *Montgomery and Foufoula-Georgiou*, 1993;

Stock and Dietrich, 2003]. This scaling break in drainage area-channel slope relationships has potential as a predictive tool. If debris flows come to rest where the drainage area-channel slope scaling shifts from incision into bedrock by debris flows to incision into bedrock by fluvial processes, it is reasonable to assume that large cobbles and boulders will be most common at the scaling break.

To predict where debris flows deposit in the landscape it may also be helpful to predict where debris flows originate in the landscape. Shallow landsliding on hillslopes is an important process for generating debris flows. SHALSTAB, a shallow hillslope stability model, has been used to predict shallow landsliding potential [*Dietrich et al.*, 1998]. SHALSTAB was designed to help timber companies and other land managers reduce erosion by identifying hillslopes that are prone to landsliding. SHALSTAB may be useful in predicting which watersheds are likely to have CoBo beds formed from landslide-derived debris flow deposits.

The strength of bedrock underlying hillslopes that supply sediment to channels may also be an important factor in the spatial distribution of CoBo. Although there is very little scholarly literature on the role of rock durability in bed grain size distributions, it is reasonable to expect that channel bed median grain size should be larger in basins with more durable lithologies [*Attal and Lave*, 2006; *Attal*, 2009; *Sklar et al.*, 2006]. Basins underlain by weak or highly fractured rocks may not produce particles in the cobble and boulder size range and would therefore be unlikely to provide CoBo overwintering habitat.

The goal of my master's thesis research is to develop an empirical model to predict where cobbles and boulder bedded channels occur in stream-channel networks. Currently, there are no tools to predict the distribution of CoBo habitat in stream channel networks. This research is the first step is solving this important geomorphic and ecologic problem. Here, I analyze four possible approaches to predicting the distribution of cobble and boulder bedded channels: bankfull threshold of motion criteria; debris flow deposition zones; extent of shallow landsliding potential; and bedrock durability. I combine multiple approaches to propose a predictive empirical model that can be used by land managers to estimate the extent of CoBo, and by extension, the amount of available over-wintering habitat.

There is very little published work on the carrying capacity of CoBo channel beds for juvenile salmonids [*Coulombe-Pontbriand and Lapointe*, 2004; *Finstad et al.*, 2007], and even less work has been done for juvenile steelhead [*Cover,* In Press]. To translate the predicted spatial distribution of CoBo into the spatial distribution of habitat, work must been done to analyze the potential carrying capacity of CoBo. I report here the initial results of field work linking the geomorphic observations presented in this study to theoretical juvenile steelhead carrying capacity.

1.2 STUDY SITE: PESCADERO CREEK

1.2.1 Geology and Geography

Pescadero Creek, in Santa Cruz and San Mateo Counties is about 80 km south of San Francisco on the coast of California. Pescadero Creek, and its tributary, Butano Creek, transport water and sediment off the northwestern flank of the Santa Cruz Mountains to the Pacific Ocean (Figure 1-1 and Figure 1-2). The western portion of the basin is underlain predominantly by Tertiary sedimentary rocks and the eastern portion of the basin is underlain by mixed Tertiary sedimentary and volcanic rocks (Figure 1-3) [*Noguchi*, 1972]; map compiled by *Brabb et al.* [1998]. The variability of the underlying bedrock lithologies creates the opportunity to examine possible links between rock durability and the distribution of cobble and boulder bedded channels in the Pescadero Creek watershed.

Shallow landslides and debris flows occur in the Pescadero Creek watershed [*Ellen et al.*, 1997]. The presence of shallow landslides and debris flows creates the opportunity to examine possible links between shallow landslides and debris flows and the distribution of cobble and boulder bedded channels in the Pescadero Creek watershed.

The Pescadero Creek watershed experiences Mediterranean climate patterns typical of the central California coast, with a mild, wet winter season (November-April) and a warm, dry summer season (May-October) [*Gasith and Resh*, 1999]. The watershed receives approximately 100 cm of precipitation annually, with nearly all precipitation falling during the 6-month wet season. Typically, the highest flows occur as a result of high intensity, long duration rainfall events, when antecedent soil saturation prevents infiltration into the shallow subsurface and a higher proportion of rainfall rapidly enters the stream channel network.

1.2.2 Land Use History

Logging has impacted the redwood forests within the Pescadero Creek basin. Intensive logging in the watershed began during the second half of the 1800s and then resumed in the 1950s and 1960s [*Barbic et al.*, 2004]. Today, the upper quarter of the watershed is a managed forest harvested for timber, using modern, low-impact forest practices by RedTree Lumber Company, LP [*Barbic et al.*, 2004]. Much of the remaining uplands are now part of different regional and state parks, including Memorial Park, Portola Redwoods State Park, and parcels managed by the Mid-Peninsula Open Space District. Relict logging roads and various public and private roads continue to influence the basin hydrology and sediment flux [*Barbic et al.*, 2004].

Pescadero Creek historically hosted a healthy steelhead trout population, and in 1912, was classified as one of four high quality steelhead producing streams in San Mateo County [*Becker and Reining*, 2008]. The Department of Fish and Game (DFG) estimated that the steelhead run in 1967 consisted of 1,500 individuals [*Becker and Reining*, 2008]. There are currently no data on the size of the steelhead run in Pescadero creek, but it is generally considered to be only a fraction of the already reduced numbers observed in 1967 [*Barbic et al.*, 2004; *Becker and Reining*, 2008].

2. THEORETICAL FRAMEWORK

2.1 STEELHEAD OVERWINTERING

A limiting factor describes the most critical factor for the survival of a given population of steelhead. Limiting factors can range from spawning habitat, to turbidity and water quality and water temperature that hinder the successful rearing, to fish passage barriers and over fishing that limits the number of returning adult fish to a given stream. Steelhead can spend an extended time in freshwater streams before they smolt, therefore, rearing habitat is a likely limiting factor, where other factors, such as stream temperature, spawning habitat and water quality, are not a concern [*Reiser and Bjornn*, 1979].

During floods, juvenile steelhead seek refuge from the high velocity, highly turbulent flood waters in the interstitial space between immobile cobbles and boulders. Additionally, CoBo provides cover from predators and hosts numerous benthic macro-invertebrates, which constitute the primary food source for juvenile steelhead trout. *Reiser and Bjornn* [1979] compiled the findings of many studies and found that cobble and boulder channel beds are the most productive areas in stream channels for benthic macro-invertebrates. *Meyer and Griffith* [1997] performed experiments designed to identify the ideal arrangement of bed grains for rainbow trout, a sub-species of

Oncorhynchus mykiss that does not migrate to the sea. Figure 2-1 summarizes the ideal bed arrangement for refugia preferred by juvenile steelhead [*Bjornn*, 1977, Ligon, pers. comm.]. *Ligon et al.* define CoBo as a channel bed with a minimum median grain size (D_{50}) of 128mm, with open interstitial spaces to a depth of 150mm, and this definition was borrowed for this study.

Geomorphic habitat modeling is an emerging field. *Coulombe-Pontbriand and Lapointe*[2004] and *Wilkins and Snyder* [2010] pursued landscape based habitat prediction for Atlantic salmon (*Salmo salar*) in post-glacial terrain and found the glacial history in their respective study sites was a first order control on the distribution of cobbles and boulders. Prior to this research, no such efforts have been undertaken for non-glacial terrains.

2.2 THRESHOLD OF BED SEDIMENT MOTION

In flume experiments using uniform sand grains, *Shields* [1936] established an empirical bedload transport threshold based on the assumption that bedload transport occurs when shear stress at the bed cross above a threshold of motion. The Shields equation is a tool commonly used to estimate median grain size (D_{50}) of channel beds:

$$D_{50} = \frac{\rho h S}{(\rho_s - \rho)\tau_c^*} \tag{1}$$

where ρ_s is the density of bed material, here assumed to be 2650 kgm^{-3}, ρ is the density of the mobilizing fluid, in this case water with a density of 1000kgm^{-3}, g is the acceleration due to gravity, h is the flow depth, and S is the slope the channel bed. The critical Shields number (τ_c^*) is a dimensionless ratio of the mobilizing forces acting on a particle (drag, lift, buoyancy) on the channel bed and the force of gravity acting to hold that particle in place, and a value of 0.03-0.06 is commonly used [*Buffington and Montgomery*, 1997]. To estimate the D_{50} of the bed at a given reach-averaged channel slope is measured, either in the field or from a DEM. To estimate h, many workers assume that the bed sediment is at the threshold of motion during bankfull flow conditions and that bankfull flow depth is proportional to the upstream accumulation area, or drainage area, for a given reach [*Leopold and Maddock*, 1953].

Theory and empirical observation supports the notion that, for gravel bedded streams, bed material is mobilized primarily during bankfull discharge [*e.g. Andrews*, 1984; *Carling*, 1988; *Parker*, 1978b]. Bankfull discharge is defined as the dominant discharge that, over time, transports the greatest amount of sediment down a river. Bankfull discharge represents a trade-off between the frequency of flow events and the sediment transport that accompanies those events. Typically, the distribution of storm flow events has a mode that describes very frequent storms, with a long and narrow tail that represents large floods that occur infrequently. Sediment transport increases as a function of discharge. When storm frequency and sediment transport are multiplied the maxima of the union function describes bankfull discharge [*Wolman and Miller*, 1960].

The seminal work of *Leopold and Maddock* [1953] introduced the concept that bankfull stream characteristics vary downstream as a function of discharge:

$$h = cQ^f \tag{2}$$

where h is depth, Q is discharge, and c and f are empirical coefficients. *Leopold et al.* [1995] note that discharge scales with drainage area, and it follows that:

$$h = aA^b \tag{3}$$

where A is drainage area and a and b are empirical coefficients. To determine a and b typically depth is observed for a sub-sample of locations in the field and the resulting relationship regressed to drainage area derived from a map. This relationship describes the downstream hydraulic geometry and is often use to interpolate bankfull channel dimensions from a sub-sample of observed reaches.

The critical Shields number (τ_c^*) was developed in flumes with highly mobile bed sediment of a single grain size and it is not mechanistically valid in steep mountain streams where step-pools and boulder cascades form structures of interlocking bed clasts. However, recent work has refined the relationships between the threshold of motion for stream channel beds in steep headwater channels, bed sediment structure and bed sediment caliber [e.g. *Yager et al.*, 2007; *Zimmermann and Church*, 2001]. *Lamb et al.* [2008] analyzed flume and field data compiled by *Mueller and Pitlick* [2005] and found that the critical Shields number (τ_c^*) increases as a power function of slope. They proposed that grain emergence, energy dissipation by boulders, aeration of flow and wall drag increase the critical shear necessary to move particles in steep mountain streams. They observed that the Shields number (τ_c^*) is slope dependent (i.e. variable as a function of slope). Their data demonstrate a slope (*S*) dependent best-fit relationship to non-dimensional shear stress:

$$\tau_c^* = 0.15S^{0.25} \tag{4}$$

Figure 2-1 is adapted from *Lamb et al.* [2008] and presents their empirical dataset regressing critical Shields number as a function of slope. Substituting Equation 4 into Equation 1 results in:

$$D_{50} = \frac{6.67\rho h S^{0.75}}{(\rho_s - \rho)} \tag{5}$$

Prior to this research, no one has attempted to predict median bed grain size by modifying the Shields equation (Equation 1) with the empirical data fit introduced by *Lamb et al.* [2008] (Equation 5). Even with recent advancements, it is still difficult to apply Equation 5, because in steep headwater streams, Equation 5 will predict that the median grain size is greater than the depth of water, *h*. When estimated bankfull depth is less than the predicted median grain size, the exposed bed grains are not subject to the drag force across their entire surface and therefore the shear stress is less than predicted by Equation 5.

2.3 DRAINAGE AREA-SLOPE ANALYSIS

Flint's law is an empirical observation that there is a power law relationship between drainage area and channel slope for steady-state channels:

$$S = k_s A^{-\theta} \tag{6}$$

where S is slope, A is drainage area, k_s is a steepness coefficient, and θ is the concavity coefficient. Flint's law is only valid for steady state landscapes, and where incision into bedrock occurs through fluvial processes [*Flint*, 1974; *Whipple*, 2004]. Steady-state landscapes arise when erosion occurs at the same pace as tectonic uplift. Based on cosmogenic radionuclide denudation rate data collected in the Pescadero Creek watershed and surrounding watersheds, *Hilley et al.*[2010] argue that the steady-state assumption is tenable for Pescadero Creek.

Numerous workers [*Montgomery and Foufoula-Georgiou*, 1993; *Seidl and Dietrich*, 1993; *Sklar and Dietrich*, 1998] have subsequently observed a deviation from this power law relationship in steep headwater channels. The deviation is attributed to the transition from fluvial driven incision downstream, to debris flow driven incision upstream. The zone of transition, where the slope of the regression shifts, is thought to be the zone in any given basin where debris flows terminate and deposit material. Generally this zone occurs between 1 km^2 and 10 km^2 in forested soil-mantled landscapes [*Stock and Dietrich*, 2006]. Theoretically, coarse material should be supplied along stream channels periodically, at or upstream of the inflection in drainage area-slope relationship. Figure 2-

2, adapted from *Stock and Dietrich* [2006] shows a conceptual model in log-drainage area, log-slope space. Importantly, the theoretical power function of slope in a pure fluvial channel typically traces a straight line in the log-slope log-drainage area space, but the influence of debris flows as the dominant tool for channel incision in headwater channels creates the upper limb where slope changes more slowly as a function of decreasing drainage area.

Figure 2-3 illustrates three theoretical pathways for sediment carried from hillslopes to channels. First, a landslide (A) can generate debris flows that can come to rest and deposit the load material as the bed reduces in slope (B) [*Stock and Dietrich*, 2003]. Second, a debris flows can continue from the hillslope down the stream channel until it reaches a confluence between the small debris flow channel and a larger stream channel, where the rapid reduction if slope results in the debris flow coming to rest (C) [*Benda and Cundy*, 1990; *May and Gresswell*, 2004]. Rock fall (D) can also produce CoBo source material where conditions produce unstable bare rock hillslopes.

2.4 SHALLOW LANDSLIDING

Shallow landsliding is a principle source for debris flows. SHALSTAB was developed as a way to rapidly assess shallow landslide potential. SHALSTAB is a coupled steady-state runoff and infinite-slope stability model presented in *Dietrich et al.* [1998]. SHALSTAB calculates the ration of effective precipitation to predicted soil transimissivity, which is a metric for the stability of a hillslope at any given point. The following equation can be applied to a DEM in a GIS, and the output is a mapped distribution of shallow landsliding potential:

$$\frac{q}{T} = \frac{\rho_s}{\rho_w}\left(1 - \frac{tan\theta}{tan\phi}\right)\frac{bsin\theta}{a} \tag{7}$$

where q is the effective precipitation, T is soil transimissivity, a is the drainage area that drains through unit contour length, b. The ratio of q/T describes the potential rainfall conditions necessary at a given cell for hillslope failure to occur, where low values of q/T represent regions that are inherently stable or need a very large amount of rainfall to become unstable and high values of q/T represent regions that need very little to no rain become unstable. For a given point in the landscape that has a large contributing area, there is higher likelihood that the subsurface flow at that cell will exceed the transimissivity through the cell in the shallow subsurface, resulting in increased pore pressure and potential hillslope failure. In their model calibration study, *Dietrich et al.* [1998] proposed a shallow hillslope stability threshold where log(q/T) equals -2.8. Cell values of less than -2.8 indicate that the cell is instable.

2.5 BEDROCK DURABILITY

In addition to the influence of deposition by debris flows on the spatial distribution of cobbles and boulders in channel networks, theoretical work by *Sklar et al.* [2006] emphasizes that rock durability affects channel bed grain size. While no scholarly work has defined the effect of rock strength on abrasion of clasts in debris flows, intuition dictates that more durable rocks would be more likely to survive transport by debris flows to stream channels. Debris flow deposition generates a poorly sorted initial grain size distribution. Fluvial processes transport finer particles more rapidly, leaving larger, more immobile particles on the stream bed [*Brummer and Montgomery*, 2006]. Some of the coarser particles are transported downstream, but many are abraded in place. Regardless of the pathway, we can infer from work by *Sklar and Dietrich* [2001] that rock tensile strength is a primary control on erosion rate, that durable rocks wear less rapidly than soft rocks, and that more durable rock favor the production of CoBo.

2.6 RESEARCH QUESTIONS AND HYPTHOTHESES

To frame my MS Thesis research I asked the following questions which motivated my hypotheses:

Question 1: Does the slope dependent Shields equation (Equation 5) accurately predict the spatial distribution of cobbles and boulders in the Pescadero Creek watershed?

Hypothesis 1: The Shields equation modified by the work of *Lamb et al.* [2008] (Equation 5) will not accurately predict the spatial distribution of cobbles and boulders in stream channel networks because sediment supply is not considered.

Question 2: Can modeling of shallow landslides and debris flows be used to predict the distribution of cobbles and boulders in the Pescadero Creek watershed?

Hypothesis 2: Shallow landsliding and debris flows can be used to predict the spatial distribution of cobbles and boulders in stream channel networks. Cobble boulder channel beds require a threshold quantity of unstable terrain upstream and must be located within the portion of the stream channel networks where debris flows deposit material.

Question 3: Can spatial analysis of bedrock durability be used to predict the distribution of cobbles and boulders in the Pescadero Creek watershed?

Hypothesis 3: Cobble-boulder bedded stream channels in stream channel networks require a threshold quantity of durable bedrock upstream.

2.7 STUDY DESIGN

To approach the problem of predicting where cobble and boulder bedded channels occur in stream channel networks, I explored four explanatory variables:

1. Prediction of bed sediment caliber based on the slope dependent Shields equation (Equation 5) and the assumption that sediment is at the threshold of motion during bankfull flow conditions.
2. Cobble and boulder bedded channels occur where debris flows deposit material, described here as the inflection in scaling between drainage area and channel slope.
3. Spatial distribution of predicted upstream hillslope instability based on the SHALSTAB shallow landsliding potential model.
4. Spatial distribution of durable bedrock lithologies.

I developed my hypotheses during initial field reconnaissance, then collected field data to test the 4 variables outlined above. I used a GIS to run Equation 5 for all stream arcs in the Pescadero Creek watershed, extract slope and drainage area, run and sample SHALSTAB, and sample mapped bedrock lithologies. I used statistical analysis to determine, individually, if the four predictor variables predicted the distribution of cobble and boulder bedded stream-channels, then with multiple logistic regression. I calibrated the predictive models initially with observations from the field. I then took the calibrated models back to the field to test the predictions of each. After model testing the calibration, model testing data were combined to formulate the final models. Ultimately, I explored a nested modeling approach that combined filtering the data through a drainage area-channel slope criteria, followed by filtering of the data through threshold quantities of predicted upstream shallow landsliding and the quantity of durable rock upstream, respectively.

3. METHODS

3.1 STREAM CHANNEL NETWORK MODELING

I extracted data from a digital stream channel network provided to me by Stillwater Sciences, Berkeley, California. To build the stream network model, Stillwater Sciences analyzed a 10 m DEM from the seamless United States Geologic Survey (USGS) data server. They used standard hydrologic tools in ArcGIS 9.3 (ESRI Corp.), and compared their data to the blue line dataset from the National Hydrography dataset. Stillwater

Sciences digitized the vector polylines, divided the polylines into arcs with 10 m of vertical elevation change, and further sub-divided at arcs at stream confluences. I paired my field-based observations with attributes exported from the GIS to build a database in JMP statistical package developed by the SAS Corporation (Appendix I).

3.2 FIELDWORK

I conducted field work between Fall 2009 and Spring 2011, visiting many sub-basins within the Pescadero Creek watershed (Figure 1-3). I performed initial reconnaissance to develop the hydraulic geometry relationship and begin generating hypotheses about the genesis of CoBo bedded channels. After initial reconnaissance, I selected reaches to visit representing 1) a wide variety of expected bed grain sizes based on the threshold of motion predictions, 2) a wide variety of channel slopes and drainage areas 3) a wide variety of predicted upstream hillslope instability values, 4) a wide variety of upstream lithologies, and 5) where I was granted access.

I collected data in two phases: The first was the model calibration phase. Data I collected during phase 1 were used to build the empirical models and to determine if there was a statistically significant relationship between drainage area-slope relationships, hillslope stability, rock durability and the distribution of CoBo in the Pescadero Creek watershed. I then used the predictions from the model calibration phase to perform phase II, model testing. To test the models, I used the calibrated models to make predictions, then selected two previously unvisited stretches along Lambert Creek and Oil Creek to visit and check the validity of the predictions.

I collected data at 134 arcs. Eighty-four of the arcs visited as part of this study are located on nine tributaries: Bradley Creek; McCormick Creek; Jones Gulch Creek; Towne Creek; Tarwater Creek Peters Creek; Lambert Creek; Slate Creek Little Boulder Creek and Oil Creek. These sub-basins are generally the larger tributary basins within the Pescadero Creek Basin. The remaining sites I visited were within six other tributaries: Little Butano Creek; Hoffman Creek; Dark Gulch Creek; Hooker Creek; Fall Creek and Waterman Creek. Generally, these basins are quite small with only 1-6 sample reaches within each.

I made ocular estimates of median grain size and classified an arc as a CoBo arc when median grain size was determined to be equal to or greater than 128 mm, and the channel bed was dominated by step-pool morphology [*Montgomery and Buffington*, 1997]. At 37 reaches, channel slope measurements were taken using and MDL Laser Ace, laser range finder/inclinometer to compare to DEM derived slopes. For 28 reaches, I estimated bankfull width and depth. For each bankfull width and depth estimate entered into the database, I measured 2-10 times to establish a reach average measurement. In addition to channel features, I observed hillslope and valley bottom conditions, looking for evidence of debris flows/rock fall. Where possible, I identified debris flow deposits in canyon bottoms. Debris flow deposits typically form a bench above one or both stream banks consisting of diamicton: a mix of angular and rounded clasts supported by a matrix of fine sediment. I identified rock fall deposits by coupling observation of angular clasts in the bed with bare, inner gorge hillslopes that connect directly to the adjacent channel. Where possible, I walked long reaches of channel to develop a qualitative sense of each sub-basin's geomorphic attributes and to insure that reaches that were locations where measurements were taken and observations made were representative of the corresponding arc in the GIS.

3.3 THRESHOLD OF BED SEDIMENT MOTION

To estimate h for the Shields equation, I generated a hydraulic geometry rating curve by collected estimates for bankfull depth within the Pescadero stream network at reaches with drainage areas varying over multiple orders of magnitude at 28 locations and regressed the data to derive a best-fit power function hydraulic geometry relationship in the form of Equation 3. With this equation, I converted drainage area for reaches in the digital stream network model to predicted water depths at bankfull for the entire basin.

I predicted grain size using the Shields equation (Equation 1), the Lamb modified Shields equation (Equation 5) and finally, the Lamb modified Shields equation (Equation 5) where I also eliminated reaches from the prediction where the predicted D_{50} was greater than the depth, h. For all three threshold of motion predictions, I used slope derived from the digital stream network, and estimated depth based on the hydraulic geometry relationship developed for this study. I produced a reach-averaged median grain size prediction for each arc in the digital stream network, and classified all channels with predicted grain size equal to or greater than 128mm as predicted CoBo reaches. For reaches visited in the field and recorded in the database, I entered the median grain size predicted by Equation 5. I analyzed the median grain size predicted by Equation 5 using logistic regression to determine the statistical significance of the relationship between the prediction and the observations of CoBo in the field. Logistic regression is discussed later in this section.

3.4 DRAINAGE AREA-SLOPE ANALYSIS

To analyze the drainage area and channel slope relationships of the arcs I visited in the Pescadero Creek watershed, I calculated the drainage area for all arcs in the digital drainage network using standard ArcGIS hydrology tools. Arc-averaged slope was calculated for each arc in the digital drainage network. For analysis, I plotted the arcs I visited during field work, and compared the drainage area to reach averaged channel slope for each.

3.5 SHALLOW LANDSLIDING

I implemented SHALSTAB with the model default soil density and internal angle of friction parameters of 1,700 g/L and 45°, respectively. I analyzed a 10 m DEM down-sampled from 1.4 m gridded LiDAR data. The 1.4 m gridded data was down-sampled using bilinear interpolation to 10 m gridded data using the raster conversion tool in ArcGIS. The larger grid size was necessary in order to facilitate running SHALSTAB with limited available computing power. For each arc I visited in the field and recorded in the database, I created a sub-basin mask in ArcGIS using the flow direction and flow accumulation tools as well as a watershed pour point placed at the reach. I used the sub-basin masks to sample the cells within each sub-watershed. In Figure 3-1, I present a sample of sub-basin extraction masks I generated in ArcGIS. For each sub-basin I calculated the cumulative distribution of *log[q/T]*. I calculated the percentage of cells within each sub-basin where $log[q/T] \leq -2.8$. The percentage of each sub-basin predicted by SHALSTAB to be unstable was entered into the database for analysis. I used logistic regression to determine if the relationship between upstream shallow hillslope instability and CoBo observations was statistically significant, selecting a threshold predictor value that minimized false model predictions. Logistic regression is described later in the methods section.

3.6 BEDROCK DURABILITY

I collected cobble samples from six observed CoBo reaches for strength testing, noting the location and mix of lithologies at each sample location. Using a Brazilian splitting tensile strength tester I measured the force required to split two inch diameter rock disks cut from the cobble samples. The samples were soaked in water until saturation to emulate conditions in the stream bed. I determined saturation by successively weighing disks until their weight ceased to increase. The force needed to fracture the rock disks was converted to Megapascals (MPa), based on the precise dimension of each disk. Each cobble produced 5-12 discs. I recorded the mean strength of all samples from each cobble.

To supplement field data, I compiled data from *Ellen and Wentworth* [1995]. Their compendium presents a survey of geologic material properties found throughout the San Francisco Bay Area, including the Pescadero Creek watershed. *Ellen and Wentworth* [1995] estimated rock hardness using the rebound of their rock hammer upon striking fresh and weathered rock, as well as fracture spacing and bedding thickness at outcrops around the San Francisco Bay Area, and developed a rating scheme. *Ellen and Wentworth* [1995] proposed a descriptive scheme for rock "hardness". In order to compare different lithologies in their compendium and determine if their data could help identify potential CoBo-forming lithologies, I replaced their descriptive scheme with an ordinal rating scheme, rating hardness of one through nine; nine representing the "hardest" rocks on their scale and one, the softest (Table 1). In addition to the rock strength estimates, they present data on fracture spacing and bedding thickness, which I also converted to ordinal ratings, rating each one through six, with six representing wide fracture spacing and bedding planes and one representing close fracture spacing and bedding planes (Tables 2 and 3). I compared their assessments to my field and laboratory observations.

In ArcGIS, I converted mapped lithologies digitized from *Brabb et al.* [1998] to raster data, which divided the mapped distribution of lithologies into cells of equal size. To quantify the extent of varying bedrock lithologies upstream of each reach visited in the field, I sampled the cells within each sub-basin upstream of each reach using standard watershed delineation tools in ArcGIS (Figure 3-1). I entered the lithologies with the greatest spatial extent within each sub-basin into the database, accounting for at least 90% of each sub-basin, and labeling the remainder as "other" (Appendix 1). I entered the rock types into the database as percent coverage and then binned them into three categories: strong; weak; unknown (See Table 5). I used logistic regression to determine if there was a statistically significant relationship between percent coverage of durable bedrock upstream of each observed reach and the presence of lack of CoBo. I chose a threshold predictor value that minimized the number of false model predictions.

3.7 STATISTICAL ANALYSIS

Logistic regression is a statistical data analysis method for assessing the significance of a relationship between a continuous independent predictor variable and a binomial dependent outcome variable [*Helsel and Hirsch*, 1993]. Here, the binomial dependent variable is whether or not a given channel reach was CoBo bedded. To determine their suitability for predicting the spatial distribution of CoBo, I regressed the Lamb modified Shields equation (Equation 5) predictions, the predicted percentage of the landscape upstream of each reach with a *log[q/T]* value less than -2.8, and the percentage of the landscape upstream of each reach underlain by durable bedrock.

Contrary to linear regression, where the magnitude of a response variable is modeled relative to one or more continuous predictor variables, logistic regression models the probability (*p*) of being in one of the two categorical responses [*Helsel and Hirsch*, 1993]. The logistic regression plot transforms the estimated probabilities into a continuous response variable. The plot of estimated probabilities forms an S-shape, where probability estimates rapid change at the center of the plot, therefore the data range of the continuous predictor variable should be scaled so that the maximum rate of change in the probabilities occurs away from the limbs of the plot. For a binary response, the probability, or slope of the line is best described by

$$\log\left(\frac{p(y=1)}{p(y=2)}\right) = X\beta \tag{8}$$

where $X\beta$ reflects the change in response y, per unit change in the value of the predictive independent predictor, 1 and 2 represent the positive and negative nominal responses, in this case whether or not a channel is CoBo bedded, and p is the probability of the response [*Helsel and Hirsch*, 1993]. I calculated p using JMP and compared the models using their receiver operator characteristics.

To determine if the models were significant, I chose a maximum p-value of 0.05. The p-value indicates the likelihood that the relationship between the independent and dependent variables is random, a low p-value indicates a strong case for rejecting the null hypothesis, which is that the binomial dependent variable does not occur as a result of the independent variable being analyzed. In other words, the p-value simply states the reliability of the regression.

I used receiver operator characteristic (ROC) plots to assess the logistic regression models. ROC plots show the rate of true positives as a function of false positives as one works through the independent predictor variable data, with each scale varying from 0 to 1 [*Hosmer and Lemeshow*, 2000]. Independent predictor variables with large areas underneath the ROC line have a more distinct threshold of differentiation of data along the continuous predictor variable that defines whether or not a given reach is CoBo bedded.

In addition to ROC plots, I compared the predictive power of the models I tested here by calculating the α-values and β-values for the proposed predictive models, where:

$$\alpha = \frac{false\ positive\ predictions\ (type\ I\ error)}{total\ positive\ predictions} \tag{9}$$

$$\beta = \frac{false\ negative\ predictions\ (type\ II\ eroor)}{total\ positive\ observations} \tag{10}$$

In other words, α represents the probability that a model will wrongly reject the null hypothesis and β is the probability that a model will wrongly retain the null hypothesis.

Once I modeled the predictor variables independently and determined that each was significant, I used multiple logistic regressions to isolate the best explanatory variables [*Hosmer and Lemeshow*, 2000]. I preformed multiple logistic regressions of the three primary continuous variables: threshold of motion bed grain size prediction; predicted upstream hillslope instability; and upstream bedrock durability. I iteratively removed variables with p values greater than 0.05. The output is a linear equation that assigns an intercept and coefficients for each statistically significant explanatory variable.

3.8 MODEL TESTING

After calibrating the predictive models I performed model testing by using the calibrated models to predict the bed character of unknown stream reaches. I tested the models at Lambert Creek on November 22, 2010 and Oil Creek on January 21. 2011. In ArcGIS, I selected arcs along Lambert and Oil Creeks, and determined the channel slope and drainage area. For each arc, I determined the percentage of each sub-basin characterized as unstable (cells with values for *log[q/T]* less than or equal to -2.8) using SHALSTAB, and the upstream extent of durable rocks.

3.9 OVERWINTERING HABITAT ASSESSMENT

The goal of this phase of the research was to count the number of refugia within CoBo channel beds and connect the channel bed surface texture to over-wintering habitat value. In collaboration with scientists from Stillwater Sciences and United States Forest Service Redwood Sciences Lab in Arcata, California, I developed a sampling method to count the number of refugia. Data collected included reach length and channel length for different bed types (pool, step, and cascade), channel width of active channel as well as bankfull width and depth. At two sample locations, I quantified the number of refugia, produced a facies map, measured bed slope and channel width, and estimating winter base flow and bankfull width. I matched each sample reach to the reach represented by an arc in the GIS stream channel layer to allow for comparison to the digital representation of the stream channel. Each single-entry interstitial space is counted as one refuge (i.e. a Y-shaped interstitial space between 3 cobbles or boulders will be counted as 3 refugia) [*Finstad et al.*, 2007]. I probed refugia with a 1.5cm diameter 40cm long flexible plastic tube. I estimated the number of potential steelhead parr based on the width of the refugia compared to the plastic probe. I recorded the number of holes with a depth greater than 15 cm, which is adequate to provide shelter for most 0+ and 1+ steelhead parr [*Reiser and Bjornn*, 1979]. Figure 3-2 shows a field assistant probing the bed to locate potential refugia. I estimated the number of potential juvenile that the Pescadero Creek watershed can support during winter storm flow using the mean estimate of refugia/m2 of bed area, bankfull width based on hydraulic geometry, and channel length for all the arcs in the dataset. I extended these results to the entire basin by finding all channels that satisfy the drainage area-slope model and then assuming that the sample dataset was a proportional representation of CoBo and non-CoBo channel beds, by length.

4. RESULTS

4.1 OVERVIEW

My dataset consisted of 135 arcs in the Pescadero Creek watershed. Forty-four sample arcs were classified as CoBo and 90 were classified as non-CoBo. The 134 total reaches cover 24.2 km of channel out of the 252 km of stream channel, if only the basins from which the samples reaches were taken are considered. For 100 of these reaches, I analyzed upstream shallow landsliding potential and upstream bedrock durability. There were a total of 543 km of channel in the Pescadero Creek basin, based on the digital stream network prepared by Stillwater Science. In Figure 4-1, I present a map of all reaches visited in the field. Appendix I presents the database of attributes for the reaches shown in Figure 4-1.

I calibrated the threshold of motion, shallow landsliding potential, and bedrock durability models using 73 reaches consisting of 25 field-verified CoBo reaches and 48 non-CoBo reaches. I included an additional 35 non-CoBo reaches for calibration of the drainage area-slope debris flow runout model, for which I did not collect upstream data. Within the calibration dataset, slopes vary between 0.002 m/m and 0.5 m/m while drainage areas vary from 0.1 km^2 to 110 km^2. During the model testing phase, I visited 27 reaches, 19 CoBo reaches and 8 non-CoBo reaches. Channel slopes vary through these reaches from 0.017 to 0.53, while the drainage area varies from 2.2-12.3 km^2. The percentage of the basin with *log[q/T]* values less than -2.8 varies from 7.5% to 15.8% and the percentage of strong bedrock within each sub-basin varies from 21-56%. For a complete summary of model test data, see Appendix I.

For the final model, the entire calibration and model testing datasets were combined into one. The sample reaches are in basins that cover the full range of upstream area underlain by the durable bedrock materials: the Butano and Vaqueros Sandstones and the Mindego Volcanics. The combined model calibration and test basins reflect a range of values for SHALSTAB predictions. The percent of the basin with *log[q/T]* values less than -2.8 varies between 1.8% and 15.7%.

4.2 THRESHOLD OF BED SEDIMENT MOTION

Using measurements from 28 reaches within Pescadero Creek, I developed a hydraulic geometry relationship following the form of Equation 3:

$$h = 0.0028A^{0.35} \tag{11}$$

where h is water depth at bankfull in meters and A is the drainage area in meters. The exponent is similar to the exponent of 0.4 observed by [*Leopold and Maddock*, 1953]. Figure 4-2 presents the data and the hydraulic geometry relationship for Pescadero Creek.

The standard Shields equation (Equation 1) predicts 84%, by length, of the channel network in the Pescadero Creek watershed to be cobble or boulder bedded. The Shields equation modified by the slope dependent τ_c^* regression from Lamb et al. [2008] predicts 74% of the channel length in Pescadero Creek is CoBo. However, when Equation 5 is used to predict grain size, predicts D_{50} is greater than estimated bankfull depth (h) for 40% of the channel network, by length; in this case the physics are not described well by the Shields equation (Equation 1) or the Lamb modified Shields equation (Equation 5).

I recorded the prediction from the Lamb modified Shields equation for all the reaches observed in the field and used logistic regression with a threshold for predicted median grain size of 128 mm. The model threshold of 128 mm predicts the field observations for 58% of the reaches visited, when both calibration and model testing data are considered (Figure 4-3). For the combined calibration and test dataset, 40% of the predictions are false positives. The p-value for the logistic regression of the entire data set is 0.0005, the α-value is 0.49, and the β-value is 0.05. The Lamb modified Shields prediction is presented in Table 6, Model 1 for the calibration and model testing datasets, separately and in Table 7, Model 1. The receiver operator characteristic value for the area under the curve is 0.79 (Figure 4-4).

4.3 DRAINAGE AREA-SLOPE ANALYSIS

Figures 4-5 and 4-6 show the locations of a representative sample of field observations in drainage area-slope space, relative to the drainage area-slope envelope for the whole dataset, including the calibration and model test datasets. Figure 4-5 shows the primary location for CoBo reaches is at the inflection of the data cloud on the drainage area-slope plot with a secondary location at a very large drainage area where small debris flow tributaries deposit cobbles and boulders into the main stem of Pescadero Creek. Importantly, notice that Figure 4-5, Panel D, Fall Creek, is surrounded in slope area space by both CoBo and non-CoBo reaches. In Figure 4-6 presents seven examples of non-CoBo reaches visualized in the context of drainage area-slope relationships. The pictured reaches were selected to emphasize that course material is generally deposited by debris flows within a drainage area-slope envelope, but that simply falling in the drainage-area slope envelop is not necessarily enough to define predict whether cobbles and boulders are present or absent in a stream reach. Figure 4-6, Panel A, shows a reach of Lambert Creek where the channel slope is too steep at a drainage area of 2 km^2. Figure 4-6 Panel D, shows a reach of Tarwater Creek at the same drainage area, yet the channel is gravel bedded. CoBo occurs at this drainage area only at intermediate slopes of about 4-25%. Figure 4-5, Panel F, shows a reach along the main stem of Pescadero Creek at 100 km^2 CoBo at this location is derived from Dark Gulch a very small tributary channel that periodically delivers sediment directly to Pescadero Creek.

I constructed an envelope bounding the location of the observed CoBo channel reaches, defining the envelope using minimum and maximum drainage area boundaries, and a drainage area dependent slope value that relates drainage area to slope through a negative power function. Initially, I defined a drainage area envelope between the lines $S=0.065DA^{-0.65}$ and $S=0.45DA^{-0.65}$ with drainage areas varying between 0.8 km^2 and 5.65 km^2. This model correctly predicts 68% of the calibration sample dataset with an α-value of 0.48 and a β-value of 0.08 (Table 6). During model testing, I found that Peters and Oil Creek had cobble and boulder bedded channels at 9-10 km^2, and subsequently extended the drainage area of the model envelope to 10 km^2. When both model calibration data and test observations are considered, the resulting drainage area-slope envelope model correctly predicts 76% of the sample data with an α-value of 0.34 and a β-value of 0.05 (Table 6). The final drainage area-slope envelop model predicts 22 false positives. I did not perform logistic regression analysis on the drainage area-slope model because there were two thresholds per variable instead of one. The final drainage area-slope envelope developed from the whole dataset is shown in Figure 4-7

4.4 HILLSLOPE STABILITY ANALYSIS

I present the cumulative distribution of predicted instability values from sub-basins within the Pescadero Creek watershed in Figure 4-8. Each line represents an individual sub-basin within the Pescadero Creek watershed and the plot indicates that for the sampled sub-basins, choosing the representative threshold of stability where log[q/T] is -2. 8for each basin is a meaningful method for comparing instability between sub-basins.

Basins where SHALSTAB predicts greater shallow landsliding potential are more likely to have CoBo bedded channels. Logistic regression yields a statistically significant relationship ($p<0.0002$) between the percentage of each sub-basin that is unstable and the spatial distribution of CoBo in the stream channel network. The logit is presented in Figure 4-9. I selected a threshold of 6%, where sub-basins with ≥6% unstable terrain are likely to predict CoBo bedded channels at their mouth and sub-basins with <6% unstable terrain are not likely to have CoBo bedded channels at their outlet. I chose the 6% upstream-unstable threshold to minimize the number of false predictions, nonetheless there are twenty-two false positives predicted at that threshold. The upstream hillslope stability model correctly predicted the distribution of CoBo in 78% of the calibration reaches and 70% for the model test reaches (Table 6, Model 3) and 76% for the whole dataset (Table 7, Model 3). The combined model calibration and test dataset has an α-value of 0.34 and a β-value of 0.05. The receiver operator characteristic value for the area under the curve is 0.84 (Figure 4-4).

4.5 ROCK DURABILITY

I sampled cobbles from CoBo deposits at Slate Creek, Fall Creek and Waterman Creek and found samples from the Butano Sandstone, the Vaqueros Sandstone and the Mindego Basalt. At these three locations I did not find samples that I could reliably correlate with other known bedrock formations in the Pescadero Creek watershed. Tensile strength for CoBo clasts varied between 1.2 and 8.5 megapascals (MPa) (Tables 1 and 5). Rock strength testing performed by *Beyeler and Sklar* [2010] illustrates that the minimum tensile strength from CoBo samples of 1.2 (MPa) is similar to other moderately cemented sandstones (Figure 4-10).

I classified bedrock materials as either durable or weak. Based on field observations of bank and bed material in Tarwater Creek, Towne Creek, Jones Gulch Creek and McCormick Creek, I classified Purisima Formation as weak. *Ellen and Wentworth* [1995] describe the Lambert Shale classified the Lambert Shale as weak (Table 5). Because of limited access during model calibration, I compiled my tensile strength data with data collected by *Ellen and Wentworth* [1995] (Table 5). Field sampling indicates that the stronger, more durable rocks consist primarily of Vaqueros Sandstone (Tvq), Butano Sandstone (Tb), and Mindego Basalt in the Pescadero Creek watershed. Durable bedrock materials were correlated with the spatial distribution of CoBo bedded channels. The logit comparing the percent of each sub-basin underlain by durable bedrock material and the presence of CoBo is presented in Figure 4-11. For the calibration, test and whole datasets, there was statistically significant correlation between mapped lithology and CoBo channel types ($p < 0.0001$). For the calibration and whole datasets, I selected a threshold value for upstream areal fraction of strong rock of 0.25 to minimize false responses. The rock durability model correctly predicted the channel bed character for 88% of the calibration reaches and 70% for the model test reaches (Table 6, Model 4) and 83% for the whole dataset, with an α-value of 0.26 and a β-value of 0.05 (Table 7, Model 4). The receiver operator characteristic value for the area under the curve is 0.83 (Figure 4-4).

4.6 MULTIPLE LOGISTIC REGRESSION MODEL

To find the best model to predict the spatial distribution of CoBo in the stream channel network, I used multiple logistic regression to compare the independent variables for the combined model calibration and model testing datasets. I entered three independent variables into the multiple logistic model: The threshold of motion prediction based on the Lamb modified Shields equation, the SHALSTAB prediction of upstream unstable terrain and the upstream extent of durable bedrock materials. The threshold of motion prediction using the Lamb modified Shields equation (Equation 5) had a p-value of 0.16 and was rejected from the multiple logistic regression model. When upstream unstable terrain and upstream durable bedrock are combined in multiple logistic regressions, each parameter has p-values of 0.0037 and 0.0016, respectively. The following equation results:

$$E = -3.49 + 21.94[Percent\ Uptream\ Unstable] \\ + 4.10[Percent\ Upstream\ Durable\ Bedrock] \tag{12}$$

where highly positive values of *E* predict a high likelihood of finding CoBo channel beds and highly negative values predict a low likelihood of finding CoBo channel beds, and when *E* equals zero there is equal likelihood of finding or not finding CoBo bedded channels. The *E* model is statistically significant ($p<0.0001$) and the area under the ROC curve is 0.85 (Figure 4-4). The *E* Model correctly predicts the channel bed character for 79% of the calibration dataset and 70% of the model test dataset (Table 6, Model 5). The *E* model correctly predicts 80% of the sample data when the calibration and model testing data are combined, with a α-value of 0.29 and a β-value of 0.18 (Table 7, Model 5).

4.7 APPLIED MODELS

In addition to logistic regression, I explored a two part modeling procedure to predict the spatial distribution of CoBo. For this approach, I utilized the drainage area-slope envelope model (debris flow incision/deposition) in tandem with both the upstream analysis of shallow landsliding and rock durability. I found the best models performed best when I maximized the size of the drainage area-slope envelope to include all the observed CoBo reaches that are located at the inflection, or kink, in drainage area-slope space. The maximized drainage area-slope envelope includes numerous false negatives, which are mostly detected both by the analysis of the predicted fraction of unstable terrain upstream and the fraction of upstream durable bedrock. As a result, only when a sample arc satisfied the drainage area-slope envelope model and the threshold value for predicted upstream unstable terrain or upstream fraction of durable bedrock, was an arc predicted to be CoBo bedded. These combined models resulted in excellent predictions. When the drainage area-slope model is combined with the upstream fraction of predicted unstable terrain, the resulting model (Table 6, Model 2+3) correctly predicted channel bed conditions 88% of the time for the calibration dataset and 74% of the time for the test dataset, respectively. For the whole dataset the paired model predicted the bed conditions of the sample data 90% correctly, with α and β values of 13% and 9%, respectively (Table 6, Model 2+3). When the drainage area-slope model is combined with the upstream fraction of durable bedrock, the resulting model (Table 6, Model 2+4) predicts the same result, and correctly predicted channel bed conditions 88% of the time for the calibration dataset and 74% of the time for the test dataset, respectively. For the whole dataset the paired model predicted the bed conditions of the sample data 90% correctly, with α and β values of 13% and 9%, respectively.

4.8 OVERWINTERING HABITAT ASSESSMENT

To estimate the amount of habitat available to juvenile salmonids during winter storm flow I surveyed two CoBo bedded reaches. At Little Boulder Creek I surveyed 165 m of channel. The reach slope is 0.045 and the drainage area is 2.7 km^2 and a mean width of approximately 3.6 m. Over the entire reach, I counted 356 refugia, which equates to 0.601 refugia/m^2. Figure 4-12 presents two pictures of the surveyed reach.

At Oil Creek, I surveyed 153m of channel. The reach slope is 0.028, the drainage area is 9.3 km^2 and the mean width was approximately 4.6 m. Over the entire reach, I counted 327 refugia which equates to 0.46 refugia/m^2. During my work at Oil Creek, the flow was approximately at winter base flow conditions, as observed from stream data at the Pescadero Creek Stream Gage (Station 11162500). Of the 327 refugia observed at this site, 284 were submerged, indicating that 90% of the refugia at this reach are available at winter base flow conditions. Figure 4-13 shows two pictures of the surveyed reach.

Based on the resulting potential number of refugia/m^2, I estimate the potential number of juvenile salmonids that can seek refuge in Pescadero Creek during high velocity storm flow. If I assume that the sample dataset reflects the correct proportion of CoBo to non-CoBo channel bed, by length, I estimate the Pescadero Creek watershed can potentially support 28,000 juvenile steelhead trout during winter storm flow. This estimate ignores fish passage barriers. Ligon (pers. comm.) suggests that steelhead can be found in channels with slopes up to 0.07. If all reaches with slopes greater than 0.07 and reaches cutoff from the ocean by passage barriers are removed, the remaining reaches in the sample dataset will potentially support 10,500 juvenile steelhead trout during winter storm flow conditions.

5. DISCUSSION

5.1 THRESHOLD OF MOTION PREDICTION

While prediction of the spatial distribution of CoBo made using Equation 5 is statistically significant, the model does not perform well. This suggests that there is more influencing channel bed grain size than simply the available shear at a given reach during bankfull discharge. In channels with limited supply from hillslopes, or where supply from hillslopes is generally fine grained, the sheer applied to the channel bed might be estimated well using Equation 5, but the bed may be scoured to bedrock.

5.2 DRAINAGE AREA-SLOPE ENVELOPE

The drainage area-slope model predicts the distribution of CoBo well, although there are twenty-two false positives. Within the drainage area-slope envelope there are both observed CoBo and observed non-CoBo reaches overlapping within the modeled envelope, which suggests that the envelope does not entirely describe the runout of debris flows in the landscape. It appears that some channels within the drainage area-slope envelope either aren't subject to debris flows, or are subject to debris flows but aren't CoBo bedded. At 10 km^2 drainage area, the model suggests a process shift where it is less common to find cobbles and boulders delivered by debris flows. This agrees with published literature on observed debris flow runout [*e.g. Montgomery and Buffington*, 1997; *Stock and Dietrich*, 2003].

There are two false negatives predicted by the drainage area-slope model that are important to discuss. These reaches occur at very large drainage areas on the main stem of Pescadero Creek. The first occurs where Dark Gulch, a small debris flow channel, deposits coarse debris into Pescadero Creek at about 100 km^2 (Figure 4-5, Panel F). This reach and others like may be very important for juvenile steelhead because they are closer to the mouth of Pescadero Creek and less prone to being cut off by fish passage barriers. CoBo beds that occur as a function of small-meets-large tributary confluences are not accounted for in the drainage area-slope envelope model and more explicit modeling of debris flow runout would likely resolve this shortcoming. The second false negative prediction occurs in a gorge section of the main stem of Pescadero Creek at nearly 110km^2 where rock fall has deposited large boulder debris in the channel. Inner gorge rock fall processes are not accounted for in the drainage area-slope model.

Debris flows happen periodically, but recurrence of shallow landsliding is highly variable and hard to predict. Here, I address the inherent stochasticity of shallow landsliding and debris flows by adopting a statistical approach. The stochasticity may be partly responsible for errors in the model. Further work might improve our understanding of debris flow recurrence and the time scale of channel bed recovery from debris flow events and improve our ability to interpret the landscape to find CoBo bedded channels.

More data should be collected to explore the role of bedrock durability, uplift rate and climate in sizing the drainage area-slope envelope. The modeling approach taken here maximizes the size of the drainage area-slope envelope to include all observed CoBo reaches; more data may warrant expansion of the drainage area-slope envelope.

5.3 HILLSLOPE STABILITY ANALYSIS

When SHALSTAB is implemented as a secondary filter to the drainage area-slope debris flow runout model, the combined model predicts 90% of the observed CoBo reaches within the Pescadero Creek watershed. This implies that the drainage area-slope model and the hillslope instability model represent different, uniquely important aspects of delivery of sediment by debris flows. I suggest that SHALSTAB is a suitable proxy for debris flow source areas in the landscape, and the drainage area-slope envelope implies information about debris flow runout and deposition.

SHALSTAB is designed to locate filled colluvial hollows and assess their relative instability. However, there is a temporal disconnect: SHALSTAB predicts the instability based on the moment in time when the data was collected to construct the DEM. Because I am interested in the past distribution of shallow landslide debris flow source areas, I must assume that the landscape is in steady state. This is complicated by variability in anthropogenic influences and possible resulting transient behaviors. Nonetheless, the model predicts the observed bed conditions well, which suggests that anthropogenic forcing is perhaps not always a critical factor for DEM interpretation.

Small tributaries that are prone to debris flows also provide source material to main stem channels with large drainage areas. Along the north flank of Butano Ridge (Figure

1-2), a series of small basins enter the main stem of Pescadero Creek. These tributary junctions are injection points for large boulder material. Mathematically, the high *q/T* predicted for these basins lifts the overall basin distribution of *q/T* below the tributary junction, but they have such a low drainage area, the model currently doesn't reflect the effect of source proximity on channels downstream of these tributary junctions.

Rock fall is a debris source that is not accounted for in the model. On the main stem of Pescadero Creek there is an inner gorge reach. Inner gorges can result from responses to uplift, knick-points, and differential bedrock strength. The Pescadero inner gorge has a drainage area greater than 100 km^2, and a reach averaged slope of less than 1%; yet the steep slopes adjacent to the channel supply the channel with large angular material. SHALSTAB predicts these inner gorge walls accurately as unstable but again, because the stability is currently averaged over the entire drainage area, the proximity of the source is poorly represented by the model.

Many false positives in the model results occur at reaches along Slate Creek. The upstream basins surpassed the threshold instability and durable bedrock models, and therefore the channel was predicted to be cobble and boulder bedded, yet surprisingly, the bed substrate between 0.75km^2 and 2km^2 did not have high quality CoBo habitat. Occasional boulders and cobbles were dominated by alluvial gravels and short steep sections of bedrock. There are reports of historic logging infrastructure in the headwaters of Slate Creek [*Keesaw,* pers. comm.] which may be influencing coarse sediment delivery to the reaches in question.

5.1 ROCK DURABILITY

The rock durability model performs very well, suggesting supply of durable rock fragments from hillslopes is a first order control on the spatial distribution of CoBo in stream channel networks. A primary goal of this study is to provide planners with a simple methodology to predict the spatial distribution of CoBo bedded channels. Unfortunately, rock durability data is not common and methodologies for data collection vary from region to region, making comparisons difficult. More generally, rock durability data relies heavily on accurate mapping of bedrock formations, which is quite difficult in forested terrain and is often interpolated from sporadic observations. Finally, bedrock materials are inherently heterogeneous, even within a single geologic formation. I observed mudstone lens in the Butano Sandstone and sandy lens in the Purisima Formation; not even the most detailed geologic maps account for these small-scale heterogeneities. A reach I visited along Oil Creek at 6 km^2 drainage area further illustrates this point: The reach drains an area underlain almost predominantly by Lambert Shale. The stream bed was dominated by cobbles and boulders, and the majority of step forming clasts are angular to sub-angular limey-mudstone clasts, suggesting a short travel distance. The likely provenance of these clasts is a durable sub-member of the Lambert Shale, because the closest bedrock materials that I classified as durable upstream of the reach were the Vaqueros Sandstone and the Mindego Basalt, which were likely not the parent rock. Without intensive field work, implementation of rock durability to predict the distribution of CoBo in other watersheds may not be reliable.

Rock durability correlates with the shallow hillslope instability as predicted by SHALSTAB. Theoretically, SHALSTAB models process, and rock strength mapping determines the amount of source material. I plotted each of the samples and test reaches to see if there was a relationship between basin instability and basin rock strength in Figure 5-1. The R^2 value of 0.38 percent is low, but there is a very slight possibility that the observed pattern arose at random ($p<0.0001$). The data indicates a positive correlation between the percentage of a given basin that is predicted to be prone to shallow land sliding and the percentage of the basin underlain by strong rocks. *Whipple* [2004] suggests that rock durability is one factor controlling basin steepness. Because hillslope angle is a primary control on the outcome of SHALSTAB (steeper hillslopes are more likely to be unstable), I propose that the correlation between rock durability and predicted hillslope instability observed in this study results from the steeper angle of repose imposed by strong rocks.

Abrasion of bed clasts during transport is highly dependent on rock durability, and is not explicitly accounted for in this model. The life history of cobbles and boulders in stream channel networks is complex and abrasion is difficult to account for because large clasts are typically abraded in place and then transported downstream only rarely, during very large flow events or successive debris flows. Future work should focus on constraining how colluvially deposited cobbles and boulders breakdown and weather in stream beds.

5.2 MULTIPLE REGRESSION ANALYSIS

The multiple logistic regression model presented here uses a combination of upstream rock durability and fraction of upstream unstable terrain, yet does not perform as well as the upstream rock durability model performs alone. I reject the multiple logistic regression model in favor of the applied model discussed in the next section.

5.3 APPLIED MODEL

Together, coupling the drainage area-slope envelope model with the fraction of upstream unstable landsliding prediction is the best tool for predicting the spatial distribution of CoBo in stream channel networks. The drainage area-slope model and fraction upstream unstable model also pair well in a mechanistic sense: SHALSTAB predicts where shallow landsliding, a primary source for debris flows, is most likely to occur in the landscape, and the drainage area-slope model predicts where in the landscape debris flow are likely to deposit material. Statistically, the model performs equally as well as the coupled drainage area-slope envelope and upstream durable bedrock model, but avoids many of the pitfalls of the upstream durable bedrock model discussed earlier in this section. SHALSTAB is easy to implement in GIS with very little to no field work and a basic understanding of the landscape (must be forested and prone to shallow landsliding). I propose that SHALSTAB incorporates the influence of bedrock durability through topography and may interpret the influence of bedrock material variability on the distribution of CoBo in stream channel networks more accurately.

5.4 OVERWINTERING HABITAT ASSESSMENT

The habitat quantification performed as part of this work is a pilot study aimed to begin the necessary work of tying my predictive model to actual fish population numbers. Current work underway by Cover (in press) will further refine the potential overwintering carrying capacity of CoBo bedded channels for different juvenile fish size-classes and for channels with varying amounts of embedded fines.

5.5 SEDIMENT ROUTING

Predicting the spatial distribution of CoBo in stream channel networks is useful not only for quantifying fish habitat; constraining the spatial organization of sediment delivery to channels has implications for bedrock incision models [*e.g. Ouimet et al.*, 2009; *Whipple and Meade*, 2006]. *Sklar et al.* [2006] assert that sediment supply from hillslopes exerts a strong control on the caliber and arrangement of channel beds; my research strongly supports this claim. Additionally, this study begins to develop a key goal for future work laid out by *Sklar et al.* [2006]: the need for a more predictive model for hillslope processes that deliver sediment to channels. *Marshall* [2009] characterized the size distribution of rock fragments on hillslopes and compared the fragment grain size distributions with other landscape metrics in an effort to develop a model for predicting the grain size distribution of sediment that channels receive from hillslopes. *Attal and*

Lave [2006] compared grain size distributions of channels and hillslopes to track the evolution of grain size distributions and account for fluvial abrasion, tributary contribution, and hillslope contribution. This study highlights the effectiveness of using lithologic properties and the distribution and debris flows in a given basin to predict channel bed grain size. Armed with this knowledge, future workers should refine the mechanistic links between rock fragment generation, emplacement on the stream bed, and eventual abrasion and transport, and eventually we may make better predictions about the way sediment is routed through channels.

6. CONCLUSIONS

There are few tools available to predict the character and caliber of bed sediments in steep channels. Beds dominated by cobble-and-boulder-sized particles provide over-wintering habitat to salmonids that use the interstitial space as refuge from high flows. Here, I developed and tested an empirical model to predict the occurrence and distribution of cobble-boulder channels. My primary findings are:

1. The spatial distribution of CoBo in stream channel networks can be predicted 90% of the time using a combination of predicted fraction of upstream shallow landsliding and a drainage area-slope envelope.

2. Sediment supply matters. Predictions of bed caliber based on the threshold of motion for bankfull flow using a Lamb modified Shields equation do not resolve the spatial distribution of CoBo because they don't consider supply.
3. CoBo occurs in a distinct part of the channel network, described as a parallelogram in log slope - log drainage area space. Observations of CoBo can be explained as the region where debris flows deposit coarse material.
4. As a predictive tool for whether a channel will be CoBo or not, there are two types of errors, non-CoBo in the drainage area-slope parallelogram and CoBo outside of the parallelogram.
   a. False positives can be identified by the lack of upstream slope instability, and/or the lack of upstream strong rock.
   b. False negatives occur because of tributary supply to main stem and inner-gorge local hillslope supply.
5. Analyzing upstream unstable fraction and upstream durable bedrock fraction both predict the spatial distribution of CoBo in stream channels well, but using SHALSTAB to predict the upstream unstable fraction is easier and more reliable to implement than analysis of upstream durable bedrock fraction.
6. I estimate that CoBo bedded channels support about 0.5 fish/m^2, although more work needs to be done to define habitat extent and quality within correctly predicted CoBo reaches.

7. RECOMMENDATIONS

I propose a coupled empirical model, whereby drainage area-slope envelope is used to assess debris flow runout and SHALSTAB is used to assess the potential within a watershed to generate shallow landslides that deliver cobbles and boulders to channels. Further work needs to be done to make the findings of this study into an easily implemented predictive model. The drainage area-slope envelope is not an elegant way to handle debris flow runout, as I suggest in the discussion section. A more accurate approach might be to alter SHALSTAB to transmit predicted unstable hillslopes to channels using the flow accumulation function in ArcGIS, then calibrating and selecting a minimum channel slope where debris flows deposit. A model like this would explicitly predict the location of CoBo in stream channel networks by accounting for proximal debris flow sources, pathways and eventual deposition.

This work also highlights that a hybrid approach must be taken using hydraulic sediment transport theory, as well as hillslope sediment transport and engineering geology approaches to predict the character of channel beds. Furthermore, I have benefited greatly from many fruitful discussions with fishery biologists on the topics of fish behavior and habitat. Many interesting problems in geomorphology stem from questions about the influence of geomorphology on biology and I recommend that further efforts be made to support collaboration between these two interrelated fields.

The failure of the model to accurately predict the bed state in upper Slate Creek actually highlights its potential utility in the future. Whether or not I hypothesize correctly about why upper Slate Creek deviates from the rest of the model calibration data, the deviation itself leads to inquiry about possible explanations, very much in the spirit of this predictive model. There is great strength in hypothesis testing models as a way of discovering problems and bringing focus to future investigations.

Generating predictions for the spatial distribution of CoBo holds great value. This model can be used to estimate the intrinsic potential of a basin to support CoBo habitat. Basins with high intrinsic potential should be preserved or restored. Understanding which basins in a given watershed have high intrinsic potential to support CoBo can help prioritize dam and fish passage barrier removal, thereby efficiently using precious financial resources to maximize benefit to steelhead populations.

8. REFERENCES CITED

Andrews, E. D. (1984), Bed-material entrainment and hydraulic geometry of gravel-bed rivers in Colorado, *Bulletin of the Geological Society of America*, *95*(3), 371.

Attal, M., and J. Lave (2006), Changes of bedload characteristics along the Marsyandi River (central Nepal); implications for understanding hillslope sediment supply, sediment load evolution along fluvial networks, and denudation in active orogenic belts, *Geol. Soc. Am. Spec. Pap.*, *398*, 143.

Attal, M. (2009), Pebble abrasion during fluvial transport; experimental results and implications for the evolution of the sediment load along rivers, *J GEOPHYS RES*, *114*(F4).

Barbic, N., D. Sicular, D. Hagans, M. O'Connor, C. Blount,, and D. Jackson (2004), *Pescadero-Butano Watershed Assessment*, Environmental Science Associates. [online] Available from: montereybay.noaa.gov/resourcepro/reports/sedrep/pescadero.pdf (Accessed 22 March 2010)

Becker, G., and I. Reining (2008), *Steelhead/Rainbow trout (Oncorhynchus mykiss) Resources South of the Golden Gate, California*, Center for Ecosystem Management and Restoration., Oakland, CA.

Benda, L. E., and T. W. Cundy (1990), Predicting deposition of debris flows in mountain channels, *Canadian Geotechnical Journal*, *27*(4), 409–417.

Beyeler, J. D., and L. S. Sklar (2010), Bedrock resistance to fluvial erosion: the importance of rock tensile strength, crystal grain size and porosity in scaling from the laboratory to the field, in *AGU Fall Meeting Abstracts*, vol. 1, p. 0740.

Bjornn, T. C. (1977), Wild fish production and management, *American Fisheries Society Special Publication*, *10*, 65–71.

Brabb, E. E., R. W. Graymer, D. L. Jones, and G. Explanation (1998), Geology of the onshore part of San Mateo County, California: A digital database, *US Geological Survey Open File Report*, 98–137.

Brummer, C. J., and D. R. Montgomery (2006), Influence of coarse lag formation on the mechanics of sediment pulse dispersion in a mountain stream, Squire Creek. North Cascades, Washington. United States, *Water Resources Research*, *42*(7), 7412.

Buffington, J. M. (1999), The legend of AF Shields, *Journal of Hydraulic Engineering*, *125*, 376–387.

Buffington, J. M., and D. R. Montgomery (1997), A systematic analysis of eight decades of incipient motion studies, with special reference to gravel-bedded rivers, *Water Resources Research*, *33*(8), 1993-2029.

Busby, P. J. (1996), *Status review of west coast steelhead from Washington, Idaho, Oregon, and California*, US Dept. of Commerce, National Oceanic and Atmospheric Administration, National Marine Fisheries Service, Northwest Fisheries Science Center, Coastal Zone and Estuarine Studies Division.

Busby, P. J., T. C. Wainwright, and G. J. Bryant (2000), Status review of steelhead from Washington, Idaho, Oregon, and California, *Knudsen, EE, CR Steward, DD MacDonald, JE Williams, and DW Reiser. Sustainable fisheries management: Pacific salmon. Lewis Publishers. Boca Raton, Florida*, 119–132.

Carling, P. (1988), The concept of dominant discharge applied to two gravel-bed streams in relation to channel stability thresholds, *Earth Surface Processes and Landforms*, *13*(4), 355–367.

Chapman, D. W., and T. C. Bjornn (1969), Distribution of salmonids in streams with special reference to food and feeding, in *Symposium on Salmon and Trout in Streams: papers*, p. 153.

Church, M. (2006), Bed material transport and the morphology of alluvial river channels, *Annual Review of Earth and Planetary Sciences*, *34*, 325-354.

Coulombe-Pontbriand, M., and M. Lapointe (2004), Landscape controls on boulder-rich, winter habitat availability and their effects on Atlantic salmon (Salmo salar) parr abundance in two fifth-order mountain streams, *Canadian Journal of Fisheries and Aquatic Sciences*, *61*(4), 648–658.

Cui, Y., G. Parker, C. Braudrick, W. E. Dietrich, and B. Cluer (2006), Dam Removal Express Assessment Models (DREAM)., *Journal of Hydraulic Research*, *44*(3), 291–307.

Dietrich, W. E., R. R. de Asua, J. Coyle, B. Orr, and M. Trso (1998), A validation study of the shallow slope stability model, SHALSTAB, in forested lands of Northern California, *Prepared for Louisiana-Pacific Corporation, Calpella, CA, 29.*

Ellen, S. D., S. E. Graham, and G. S. (US) (1997), *Map Showing Principal Debris Flow Source Areas in the San Francisco Bay Region, California*, The Survey.

Ellen, S. D., and C. M. Wentworth (1995), Hillside materials and slopes of the San Francisco Bay region, California, in *International Journal of Rock Mechanics and Mining Sciences and Geomechanics Abstracts*, vol. 33, p. 274A–275A.

Finstad, A. G., S. Einum, T. Forseth, and O. Ugedal (2007), Shelter availability affects behaviour, size-dependent and mean growth of juvenile Atlantic salmon, *Freshwater Biology*, *52*(9), 1710–1718.

Flint, J. J. (1974), Stream gradient as a function of order, magnitude, and discharge, *Water Resources Research*, *10*, 969-973.

Gasith, A., and V. H. Resh (1999), Streams in Mediterranean Climate Regions: Abiotic Influences and Biotic Responses to Predictable Seasonal Events, *Annual Review of Ecology and Systematics*, *30*, 51-81.

Hartman, G. F. (1965), The role of behavior in the ecology and interaction of underyearling coho salmon (Oncorhynchus kisutch) and steelhead trout (Salmo gairdneri), *Journal of the Fisheries Research Board of Canada*, *22*(4), 1035–1078.

Helsel, D. R., and R. M. Hirsch (1993), *Statistical methods in water resources*, Elsevier Science Ltd.

Hilley, G. E., R. Burgmann, T. A. Dumitru, Y. Ebert, J. C. Fosdick, K. Le, N. M. Levine, A. Wilson, and M. H. Gudmundsdottir (2010), Tectonics and Unroofing of the Santa Cruz Mountains, California, from Low-Temperature Thermochronology and Catchment-Averaged 10Be-Derived Denudation Rates, in *AGU Fall Meeting Abstracts*, vol. 1, p. 07.

Hosmer, D. W., and S. Lemeshow (2000), *Applied logistic regression*, Wiley-Interscience.

Lamb, M. P., W. E. Dietrich, and J. G. Venditti (2008), Is the critical Shields stress for incipient sediment motion dependent on channel-bed slope, *Journal of Geophysical Research*, *113*, 2008.

Leopold, L. B., and T. Maddock (1953), *The hydraulic geometry of stream channels and some physiographic implications*, US Govt. Print. Off.

Leopold, L. B., M. G. Wolman, and J. P. Miller (1995), *Fluvial processes in geomorphology*, Dover Pubns.

Marshall, J. A. (2009), Hillslope Rock Fragment Production: Grain Size Distributions, Abundance and Climatic Influences, San Francisco State University, San Francisco, California.

May, C. L., and R. E. Gresswell (2004), Spatial and temporal patterns of debris-flow deposition in the Oregon Coast Range, USA, *Geomorphology*, *57*(3-4), 135–149.

Meyer, K. A., and J. S. Griffith (1997), Effects of cobble-boulder substrate configuration on winter residency of juvenile rainbow trout, *North American Journal of Fisheries Management*, *17*(1), 77–84.

Montgomery, D. R., and J. M. Buffington (1997), Channel-reach morphology in mountain drainage basins, *Geological Society of America Bulletin*, *109*(5), 596-611, doi:10.1130/0016-7606(1997)109<0596:CRMIMD>2.3.CO;2.

Montgomery, D. R., and E. Foufoula-Georgiou (1993), Channel network source representation using digital elevation models, *Water Resources Research*, *29*(12), 3925–3934.

Mueller, E. R., J. Pitlick, and J. M. Nelson (2005), Variation in the reference Shields stress for bed load transport in gravel-bed streams and rivers, *Water Resources Research*, *41*(4), W04006.

Noguchi, N. (1972), Quantitative Geomorphology and Relative Rate of Erosion, Pescadero Creek Basin, San Mateo County, California, Master of Science, University of California, Santa Cruz, Santa Cruz, California.

Ouimet, W. B., K. X. Whipple, and D. E. Granger (2009), Beyond threshold hillslopes: Channel adjustment to base-level fall in tectonically active mountain ranges, *Geology*, *37*(7), 579.

Parker, G. (1978a), Self-formed straight rivers with equilibrium banks and mobile bed. Part 1 - The sand-silt river., *Journal of Fluid Mechanics*, *89*(1), 109-125.

Parker, G. (1978b), Self-formed straight rivers with equilibrium banks and mobile bed. Part 2 - The gravel river., *Journal of Fluid Mechanics*, *89*(1), 127-146.

Recking, A. (2009), Theoretical development on the effects of changing flow hydraulics on incipient bed load motion, *Water Resources Research*, *45*(4), W04401.

Reiser, D. W., and T. C. Bjornn (1979), Habitat requirements of anadromous salmonids, *USDA Forest Service General Technical Report PNW-96*, *54*.

Roering, J. J., J. W. Kirchner, and W. E. Dietrich (2005), Characterizing structural and lithologic controls on deep-seated landsliding: Implications for topographic relief and landscape evolution in the Oregon Coast Range, USA, *Geol Soc America Bull*, *117*(5), 654, doi:10.1130/B25567.1.

Sedell, J. R., and K. J. Luchessa (1982), Using the historical record as an aid to salmonid habitat enhancement, *Acquisition and utilization of aquatic habitat inventory information. American Fisheries Society, Western Division, Bethesda, Maryland*, 210–223.

Seidl, M. A., and W. E. Dietrich (1993), The problem of channel erosion into bedrock, *Catena Supplement*, *23*, 101–101.

Shields, A. (1936), Application of similarity principles and turbulence research to bed-load movement, U.S. Dept. of Agr., Soil Conservation Service Cooperative Laboratory, California Institute of Technology, Pasedena.

Sklar, L. S., and W. E. Dietrich (2001), Sediment and rock strength controls on river incision into bedrock, *Geology*, *29*(12), 1087.

Sklar, L. S., and W. E. Dietrich (1998), River longitudinal profiles and bedrock incision models; Stream power and the influence of sediment supply, in *Rivers Over Rock: Fluvial Processes in Bedrock Channels*, vol. 107, edited by K. J. Tinkler and E. E. Wohl, pp. 237-260, AGU, Washington D.C.

Sklar, L. S., W. E. Dietrich, E. Foufoula-Georgiou, B. Lashermes, and D. Bellugi (2006), Do gravel bed river size disributions record channel structure?, *Water Resources Research*, *42*, doi:10.1029/2006WR005035.

Stock, J. D., and W. E. Dietrich (2006), Erosion of steepland valleys by debris flows, *Geol Soc America Bull*, *118*(9), 1125, doi:10.1130/B25902.1.

Stock, J., and W. E. Dietrich (2003), Valley incision by debris flows: Evidence of a topographic signature, *Water Resources Research*, *39*(4), 1089.

Whipple, K. X. (2004), Bedrock rivers and the geomorphology of active orogens, *Annu. Rev. Earth Planet. Sci.*, *32*, 151–185.

Whipple, K. X., and B. J. Meade (2006), Orogen response to changes in climatic and tectonic forcing, *Earth and Planetary Science Letters*, *243*(1-2), 218-228, doi:10.1016/j.epsl.2005.12.022.

Wilcock, P. R. (1993), Critical shear stress of natural sediments, *Journal of Hydraulic Engineering*, *119*(4), 491–505.

Wilkins, B. C., and N. P. Snyder (2010), Geomorphic comparison of two Atlantic coastal rivers: Toward an understanding of physical controls on Atlantic salmon habitat, *River Res. Applic.*, doi:10.1002/rra.1343. [online] Available from: http://doi.wiley.com/10.1002/rra.1343 (Accessed 14 April 2010)

Wolman, M. G., and J. P. Miller (1960), Magnitude and frequency of forces in geomorphic processes, *The Journal of Geology*, *68*(1), 54–74.

Yager, E. M., J. W. Kirchner, and W. E. Dietrich (2007), Calculating bed load transport in steep boulder bed channels, *Water Resources Research*, *43*(7), W07418.

Zimmermann, A., and M. Church (2001), Channel morphology, gradient profiles and bed stresses during flood in a step-pool channel, *Geomorphology*, *40*(3-4), 311–327.

Table 1: Adaptation of Rock Hardness from Ellen and Wentworth [1995]

Hardness, from Ellen and Wentworth	Code, from Ellen and Wentworth	**Assigned Rank**
hard	h	**9**
	h-qf	**8**
quite firm	qf	**7**
	qf-f	**6**
firm	f	**5**
	f-fas	**4**
firm aprch soft	fas	**3**
	fas-s	**2**
soft	s	**1**

I assigned an ordinal ranking for hardness based on classifications presented in *Ellen and Wentworth* [1995]. Ordinal rank is used to relate material properties to bedrock materials in the Pescadero Creek Watershed (Table 5).

Table 2: Adaptation of Fracture Spacing from Ellen and Wentworth [1995]

Fracture Spacing, from Ellen and Wentworth	Code, Ellen and Wentworth	Spacing (cm), from Ellen and Wentworth	**Assigned Rank**
v. close	vc	0-1cm	**1**
close	c	1-5cm	**2**
moderate	m	5-30cm	**3**
wide	w	30-90	**4**
v wide	vw	>90	**5**
absent	a		**6**

I assigned ordinal values for qualitative descriptions presented in *Ellen and Wentworth* [1995]. Ordinal rank is used to relate material properties to bedrock materials in the Pescadero Creek Watershed (Table 5).

Table 3: Adaptation of Bedding Thickness from Ellen and Wentworth [1995]

Bedding Thickness from Ellen and Wentworth	Code From Ellen and Wentworth	Thickness (cm) from Ellen and Wentworth	**Assigned Rank**
v. thin/ lam	vn	0-1cm	**1**
thin	n	1-5cm	**2**
med	m	5-30cm	**3**
thick	k	30-90	**4**
v thick	vk	>90	**5**
absent	a		**6**

I assigned ordinal values for qualitative descriptions presented in *Ellen and Wentworth* [1995]. Ordinal rank is used to relate material properties to bedrock materials in the Pescadero Creek Watershed (Table 5)

Table 4: Rock Strength of Cobble Samples

Sample Number	Lithology	Strength (MPa)	Number of samples (n)	Standard Deviation
WD-1	Vaqueros Sandstone	4.4	11	0.31
F-1	Butano Sandstone	1.17	8	0.31
SL-1	Mindego Basalt	2.87	9	0.25
SL-2	Mindego Basalt	8.07	6	2.23
SL-3	Vaqueros Sandstone	6.05	8	1.43
SL-4	Vaqueros Sandstone	2.3	8	0.28

Table 5: Summary of Rock Strength Data

THIS STUDY					*Ellen and Wentworth* [1995]										
CoBo Observed ?	**Map Symbol**	**Name**	**Classification:**	**Measured Tensile Strength (MPa)**	**Number from *Ellen and W'worth***	**Alt.Number from *Ellen and W'worth***	**Strength**			**Bedding Thickness**		**Fracture Spacing**			
							***Ellen and W'worth* Classification**	**Weathered**	**Fresh**	***Ellen and W'worth* Classification**	**Rank**	***Ellen and W'worth* Classification**	**Weathered**	**Fresh**
Yes	Tmb	Mindego Basalt	Durable	2.9-8.5	232		f-s, h blocks (m)w/h	3	9	vk	5	(c-m)w	2.5	2.5
Yes	Tvq	Vaqueros Sandstone	Durable	4.4	369		f-s/f-h	3	7	m(k-10ft) tens of ft	4	c(m-w)6ft	3.5	3.5
Yes	Tb	Butano Sandstone	Durable	1.2	323	460	f-s/f-h	3	7	m-30ft	4	c(m-vw)	4	4
Yes	Tbu	Butano Sandstone	Durable	1.2	369		f-s/f-h	3	7	m(k-10ft) tens of ft	4	c(m-w)6ft	3.5	3.5
No	Tpp	Pomponio Mudstone Member of the Purisma	Weak		500		h-f	7	7	m-vk	4	(c-vc)m	1.5	1.5
Yes and No	Tla	Lambert Shale	Weak		460	500	f-s/f?	3	5	vk-a	5.5	(c-vc)m/m-w	1.5	3.5
No	Tpt	Tahana Member of the Purisima	Weak		380		f-s/f	3	5	a-vk	5.5	vc-m/m-vw	2	4
N/A	Tsr	Rices Mudstone member of the San Lorenzo Formation	Unknown		460		f-s/f?	3	5	vk-a	5.5	(c-vc)m/m-w	1.5	3.5
N/A	Tsl	San Lorenzo Formation	Unknown		460		f-s/f?	3	5	vk-a	5.5	(c-vc)m/m-w	1.5	3.5
N/A	Tm	Monterey Formation	Unknown		500		h-f	7	7	m-vk	4	(c-vc)m	1.5	1.5
N/A	Tsc	Santa Cruz Mudstone	Unknown		500		h-f	7	7	m-vk	4	(c-vc)m	1.5	1.5

Table 6: Summary of Models, Calibration and Test Datasets

		MODEL NUMBER	1	2	3(0.06)	4 (0.20)	2+3	2+4	5
Preliminary Models	Calibration	Correct +	23	23	23	23	21	21	16
		Correct -	16	27	34	41	43	43	42
		False +	32	21	14	7	5	5	6
		False -	2	2	2	2	4	4	9
		α	0.58	0.48	0.38	0.23	0.19	0.19	0.27
		β	0.08	0.08	0.08	0.08	0.16	0.16	0.41
		percent correct prediction	0.53	0.68	0.78	0.88	0.88	0.88	0.79
	Model Test	Correct +	19	12	19	19	12	12	19
		Correct -	0	8	0	0	8	8	0
		False +	8	0	8	8	0	0	8
		False -	0	7	0	0	7	7	0
		α	0.30	0.00	0.30	0.30	0.00	0.00	0.30
		β	0.00	0.37	0.00	0.00	0.37	0.37	0.00
		percent correct prediction	0.70	0.74	0.70	0.70	0.74	0.74	0.44

Results of predictive models based on model calibration and test data presented separately.

Model 1: Prediction based on Shields equation modified with data for slope dependent critical shear [*Lamb et al.*, 2008]. Threshold set to 128mm for D_{50}.
Model 2: Slope and drainage area "envelope" where the slope is drainage area dependent between the lines 0.065[Drainage Area]$^{-0.65}$ and 0.45[Drainage Area]$^{-0.65}$ for drainage areas between 0.8 and 5.65 km^2.
Model 3: Two versions of model 3 are presented here. The first utilizes a threshold value for percent of watershed instable of 5% and the second utilizes a threshold of 6%.
Model 4: Two versions of model 3 are presented here. The first utilizes a threshold value for percent of watershed underlain by strong lithologies of 25% and the second utilizes a threshold of 20%.
Model 2+3: This model combines the slope and drainage area "envelope" with the percent of the watershed instable (at a 6% threshold) in a nested approach.
Model 2+4: This model combines the slope and drainage area "envelope" with the percent of the watershed underlain by strong lithologies (at a 6% threshold) in a nested approach.
Model 5: Utilizes multiple logistic regression where the equation $E = -3.49 + 21.94[Percent\ Uptream\ Unstable] + 4.10[Percent\ Upstream\ Durable\ Bedrock]$

Table 7: Final Model Results

		MODEL NUMBER	1	2	3 (0.05)	3(0.06)	4 (0.25)	4 (0.20)	2+3	2+4	5
Final Models	All Database	Correct +	42	42	42	42	37	42	40	40	35
		Correct -	16	34	30	34	41	41	50	50	42
		False +	40	22	26	22	15	15	6	5	14
		False -	2	2	2	2	7	2	4	4	9
		α	0.49	0.34	0.38	0.34	0.29	0.26	0.13	0.13	0.29
		β	0.05	0.05	0.05	0.05	0.16	0.05	0.09	0.09	0.18
		percent correct prediction	0.58	0.76	0.72	0.76	0.78	0.83	0.90	0.90	0.77

These results are based on the finalized models that include data from both the calibration and testing datasets. Most notably, the downstream edge of the drainage area envelope has been changed to 10km2.

Model 1: Prediction based on Shields equation modified with data for slope dependent critical shear [*Lamb et al.*, 2008]. Threshold set to 128mm for D_{50}.
Model 2: Slope and drainage area "envelope" where the slope is drainage area dependent between the lines 0.065[Drainage Area]$^{-0.65}$ and 0.45[Drainage Area]$^{-0.65}$ for drainage areas between 0.8 and 10 km^2.
Model 3: Two versions of model 3 are presented here. The first utilizes a threshold value for percent of watershed instable of 5% and the second utilizes a threshold of 6%.
Model 4: Two versions of model 3 are presented here. The first utilizes a threshold value for percent of watershed underlain by strong lithologies of 25% and the second utilizes a threshold of 20%.
Model 2+3: This model combines the slope and drainage area "envelope" with the percent of the watershed instable (at a 6% threshold) in a nested approach.
Model 2+4: This model combines the slope and drainage area "envelope" with the percent of the watershed underlain by strong lithologies (at a 6% threshold) in a nested approach.
Model 5: Utilizes multiple logistic regression where the equation $E = -3.49 + 21.94[\mathit{Percent\ Uptream\ Unstable}] + 4.10[\mathit{Percent\ Upstream\ Durable\ Bedrock}]$

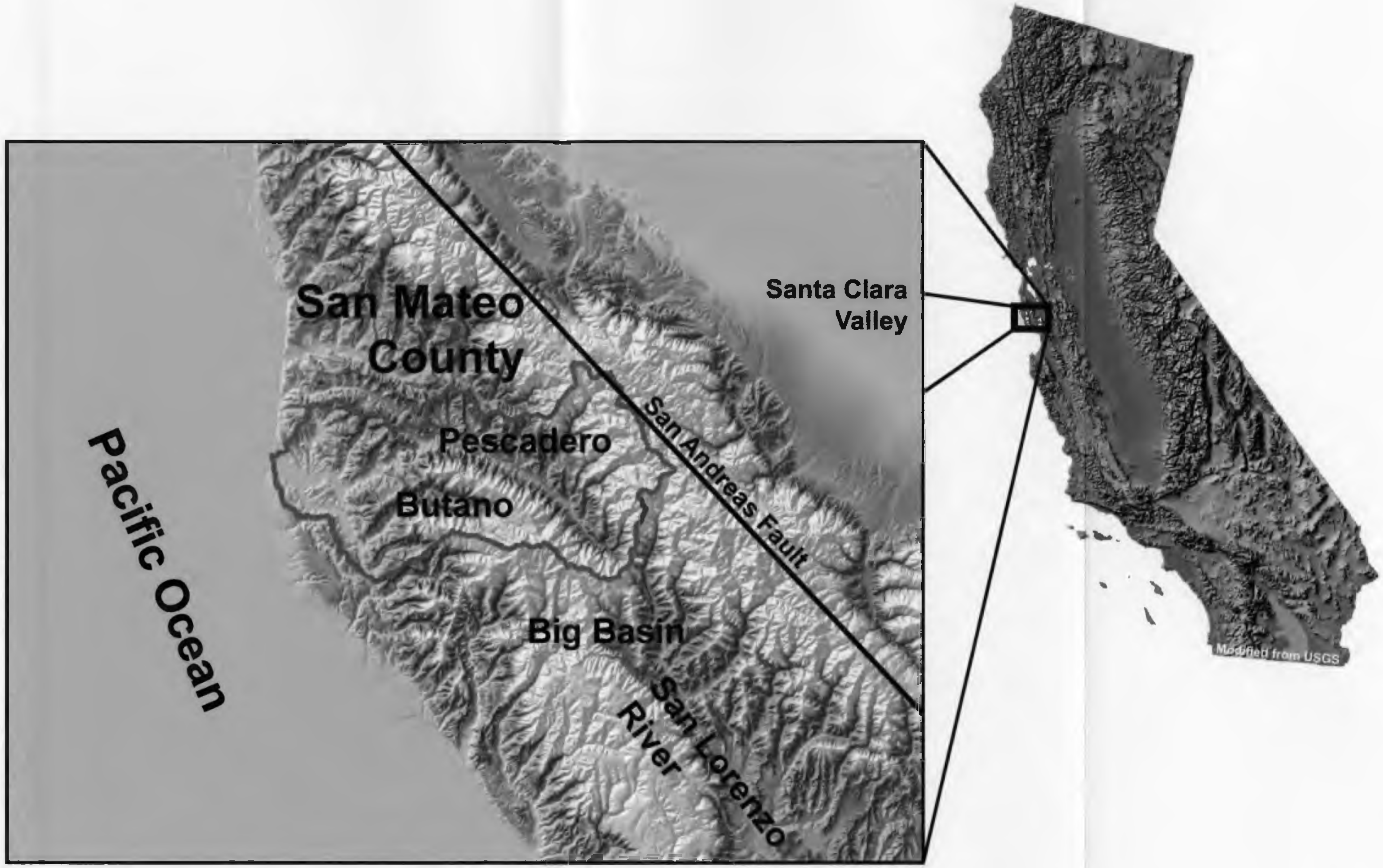

Figure 1-1 Location Map, Pescadero Creek

Map of Pescadero and Butano Creeks, San Mateo County, California. Pescadero and Butano Creeks drain the western flank of the northern Santa Cruz Mountains, a restraining bend along the San Andreas Fault (SAF). The SAF approximately follows the ridge crest of the Santa Cruz Mountains in the vicinity of the Pescadero Creek.

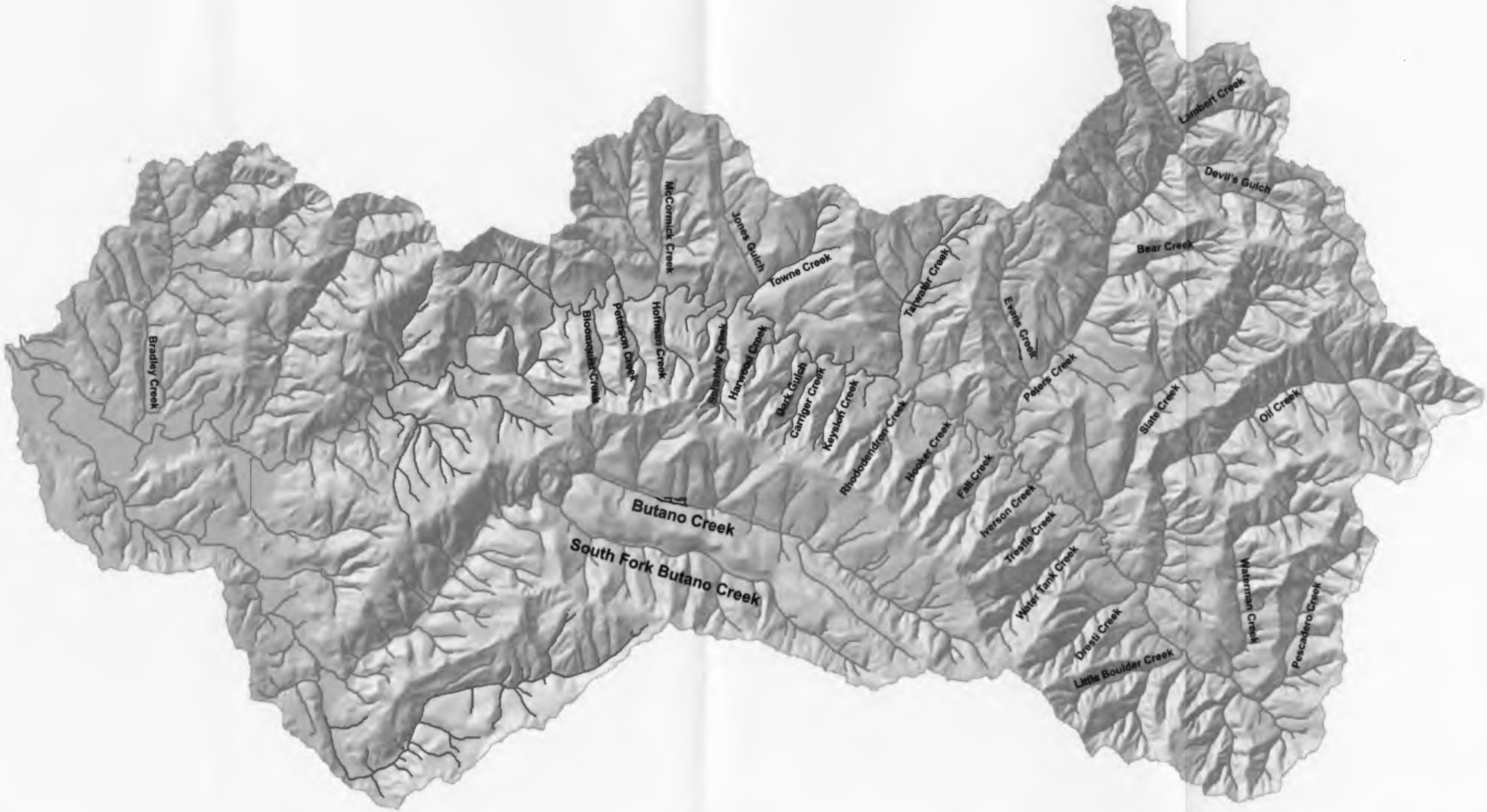

Figure 1-2 Pescadero Creek Channel Network

Map of Pescadero and Butano Creeks, San Mateo County, California. Names of Creeks.

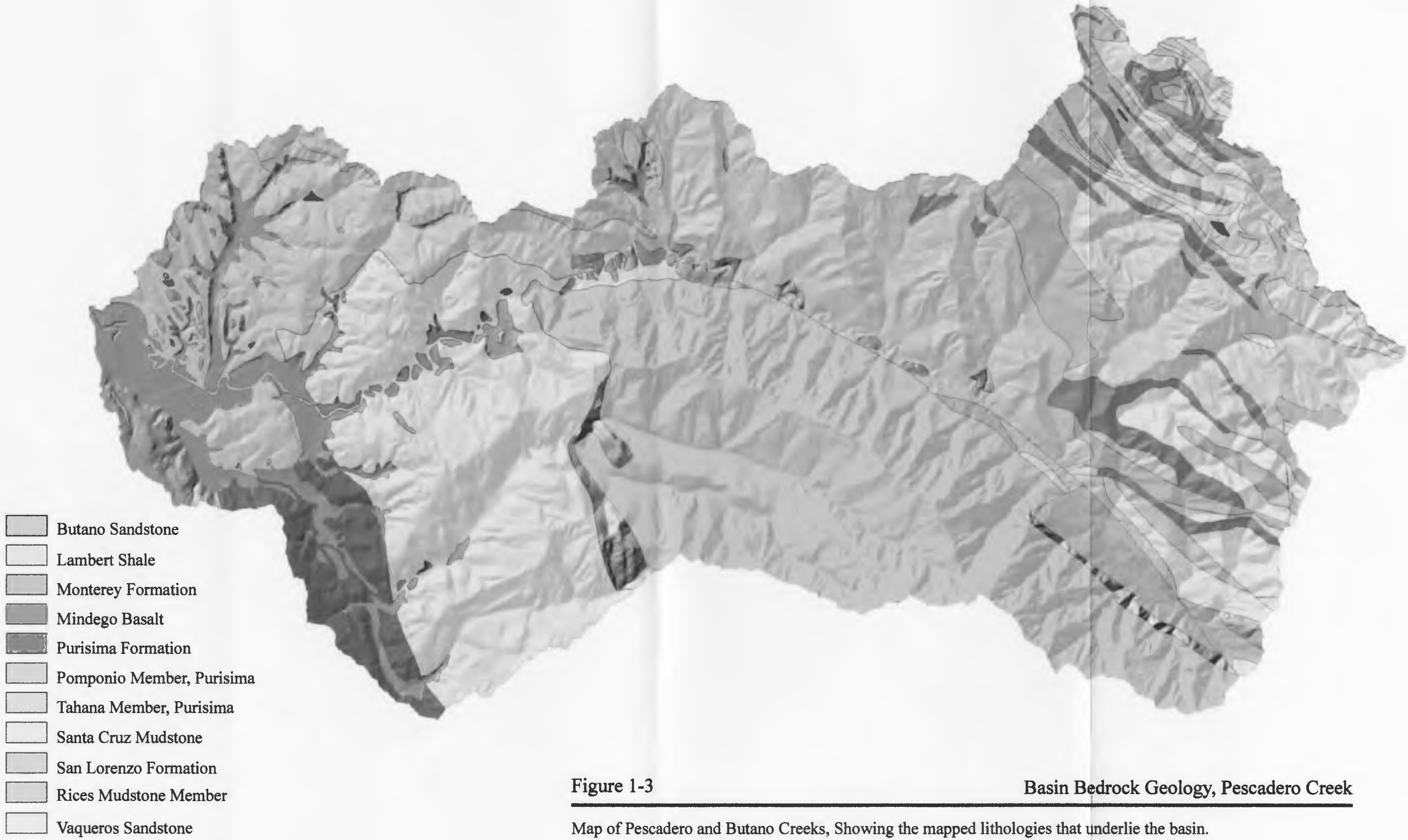

Figure 1-3 **Basin Bedrock Geology, Pescadero Creek**

Map of Pescadero and Butano Creeks, Showing the mapped lithologies that underlie the basin.

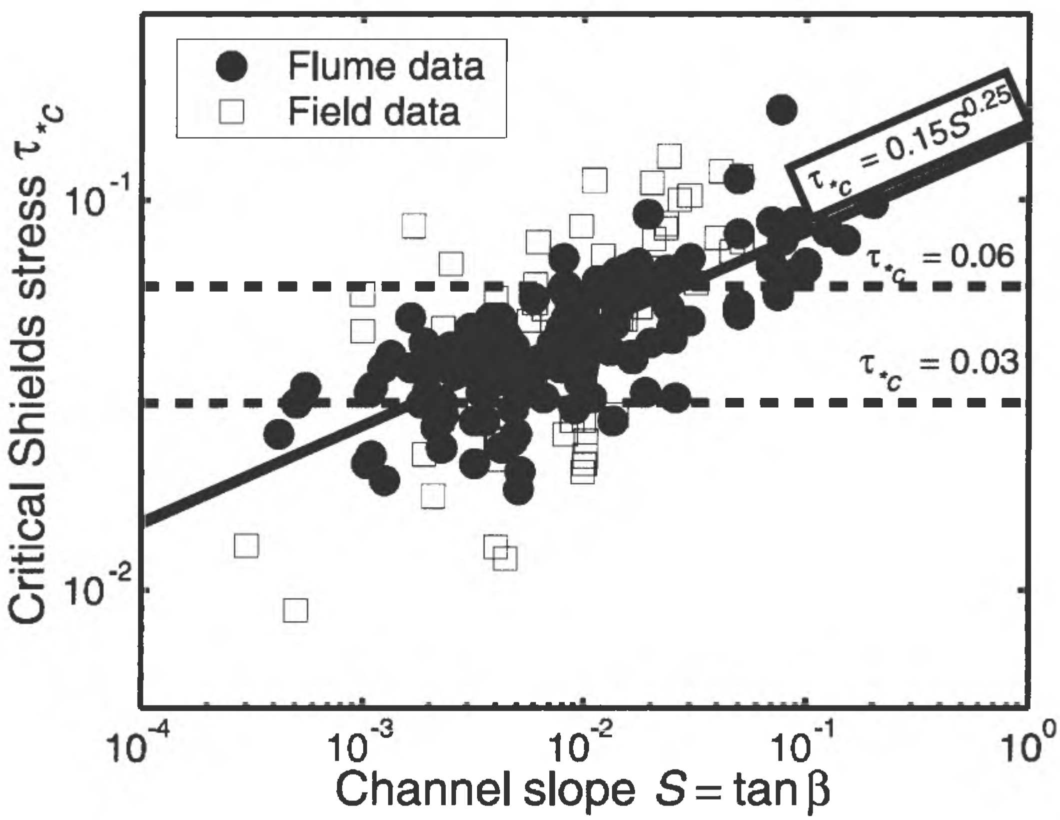

Figure 2-1 Channel Slope vs. Critical Shields Number

Adapted from *Lamb et al.* [2008], this plot forms the rationale for altering estimating channel bed grainsize in steep mountainous channels. The plot indicates that, from flume and field studies, there is substatially more sheer stress needed to mobilize the D50 in steep mountainous channels, which is thought to be a result of form drag imposed by large boulder structures, emergence of grains above the water surface and aeration of flow.

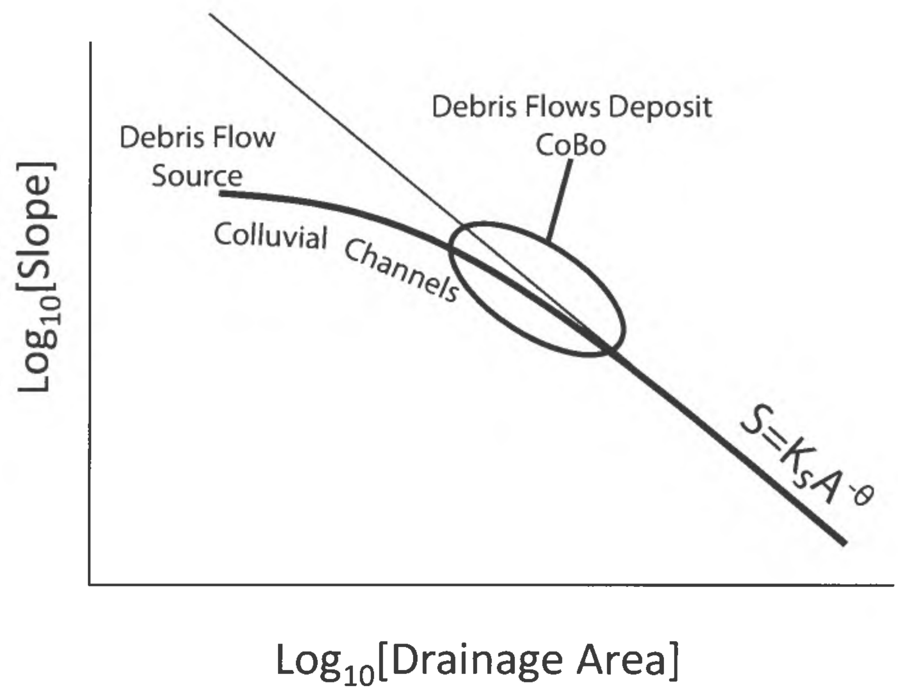

Figure 2-2 Drainage Area Channel Slope Relationships

This plot, adapted from *Stock and Dietrich* [2006], illustrates the trend in steep headwater channels with low drainage area, for slope to change less quickly as a function of drainage area. This is thought to be a result of different incision processes that dominate in colluvial channels. Debris flow material is deposted most commonly, where the colluvial channels give way to alluvial dominated channels.

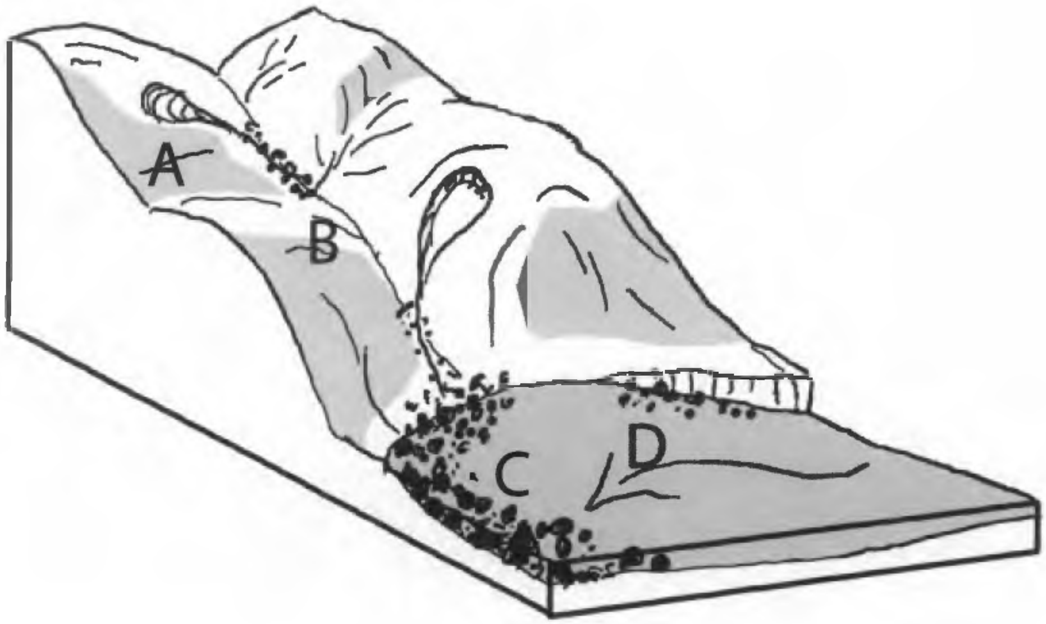

Figure 2-3 Schematic: Shallow Landslides, Debris Flows, Rockfall

Debris flows typically originate in colluvial hollows (A) and travel downslope until they reach the stream channel network. Depending on the conditions within the channel, debris flows will either come to rest in the headwater channel (B) or continue until it reaches a larger channel (C). Rock fall can also generate coarse material where steep threshold hillslopes are adjacent to channels (D)

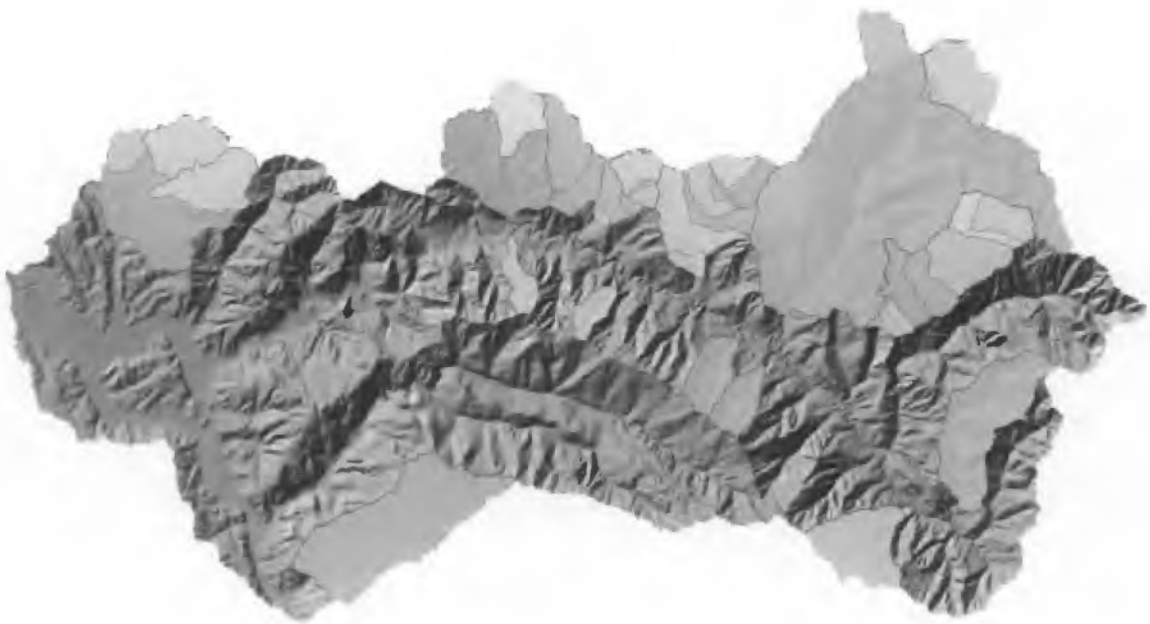

Figure 3-1 Sub-basin Sampling Masks, Pescadero Creek

The colored polygons in this figure show a sample of the basin clips. Sites along the main stem Pescadero Creek and the model testing are excluded for clarity.

Figure 3-2 Sampling Channel Bed for Refugia

Field assistant sampling refugia with probe (submerged in flow).

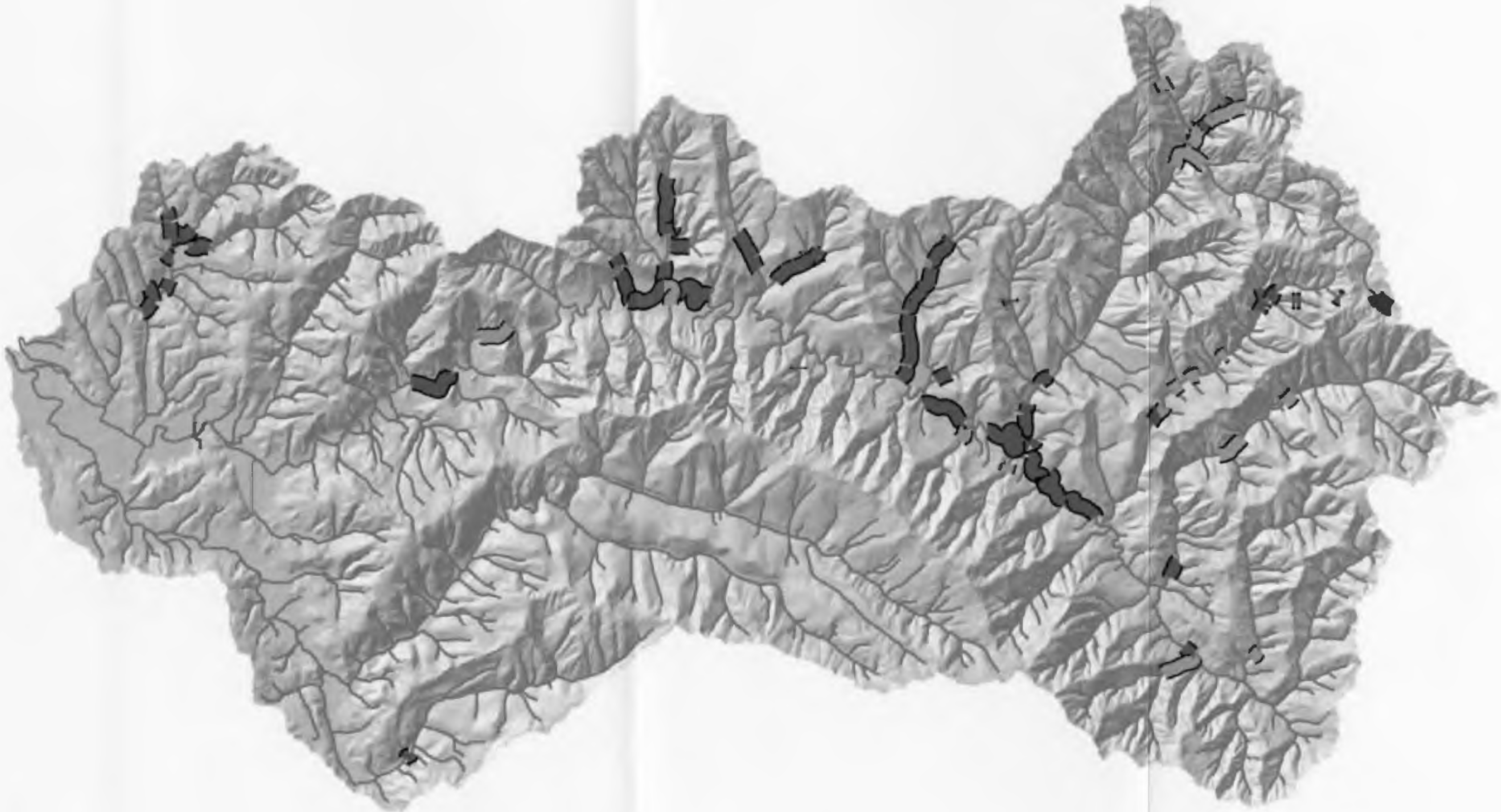

Stream Channel Network
Arcs where CoBo was observed in the field
Arcs where no CoBo was observed in the field

Figure 4-1 Map of Study Reaches, Pescadero Creek

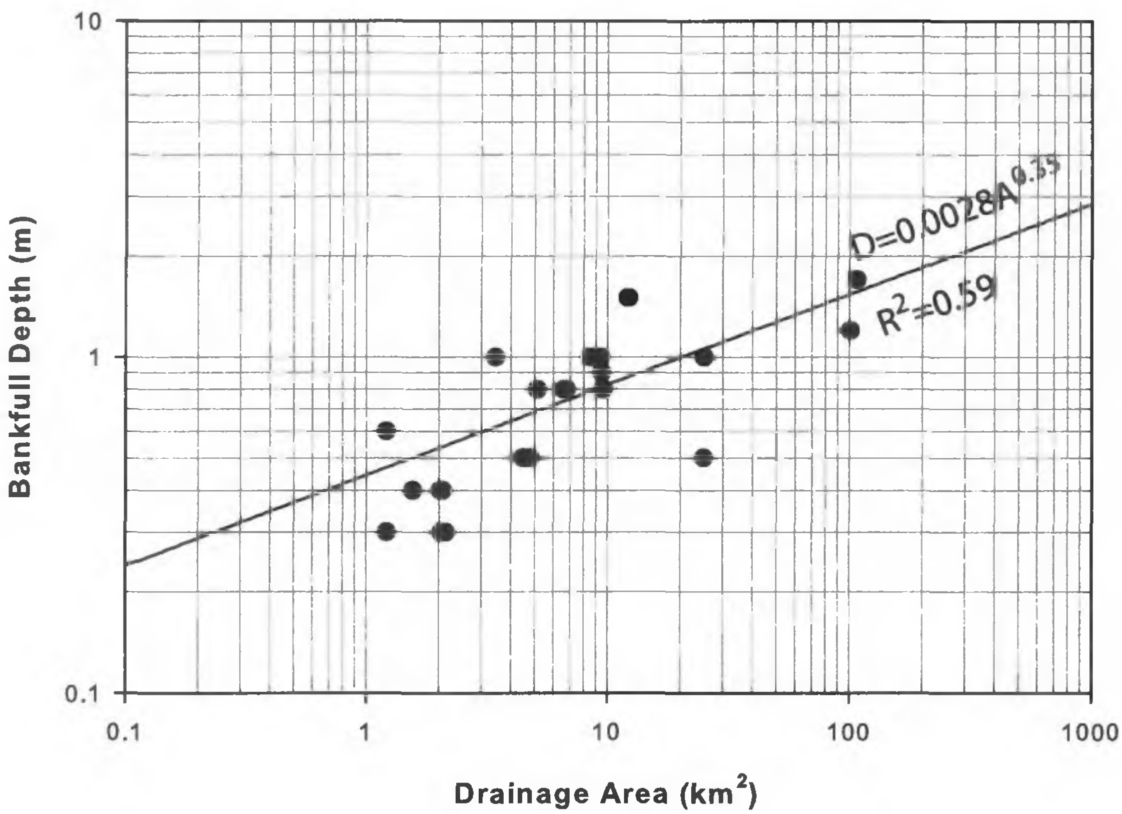

Figure 4-2 Plot of Drainage Area (km^2) versus Bankfull Depth (m)

I estimated bankfull depth in the field at 28 reaches and compared the results to drainage area extracted from the DEM in ArcGIS. I used the resulting regression presented here to estimate depth and solve the Lamb modified Shields equation to estimate median grain size for arcs with the the Pescadero Creek watershed.

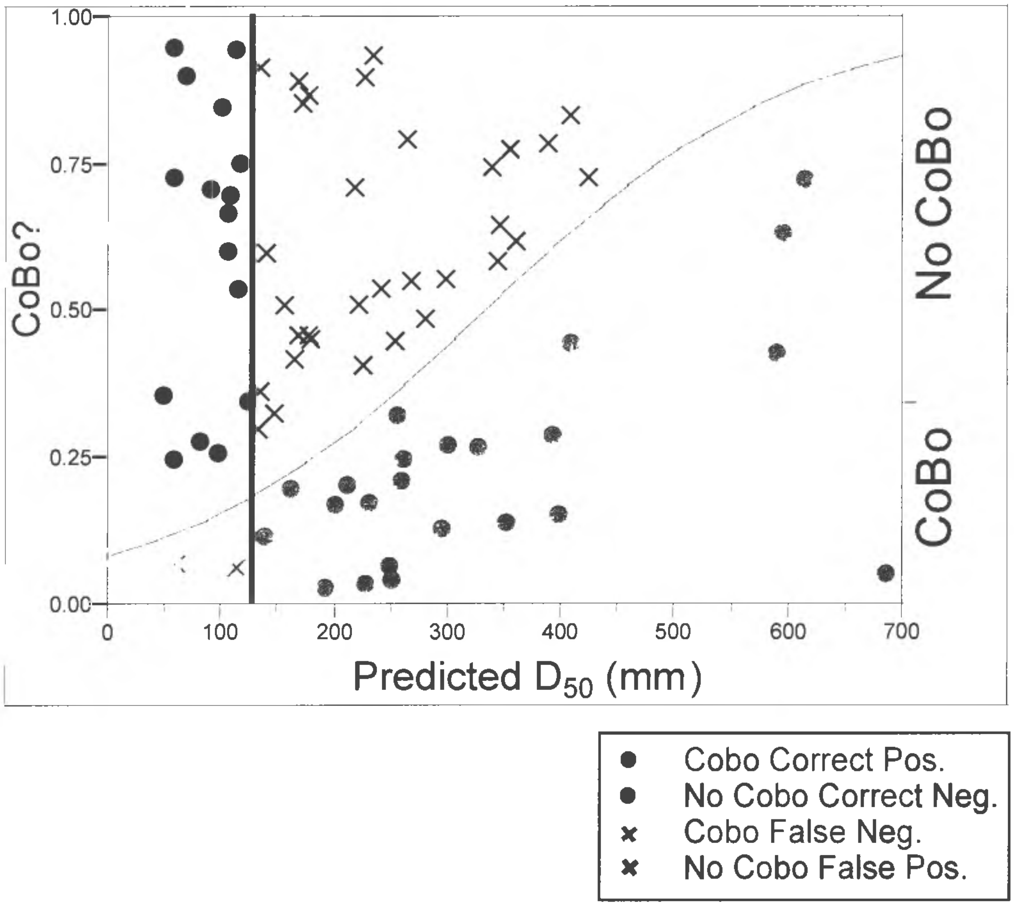

Figure 4-3 Logit, Threshold of Motion Predictions vs. Observed CoBo

Logit depicts the relationship between the prediction of grain size based on the threshold of motion for bed sediment at bankfull discharge using the Shields equation with the slope dependent critical shear stress relationship introduced by Lamb et al. [2008] for the calibration dataset. P=value is 0.0005, therfore the relationship is significant. Red line indicates the minimum median grain size to be deifned as CoBo, 128mm. Note that the threshold of 128 mm produces very few false negative predictions, but

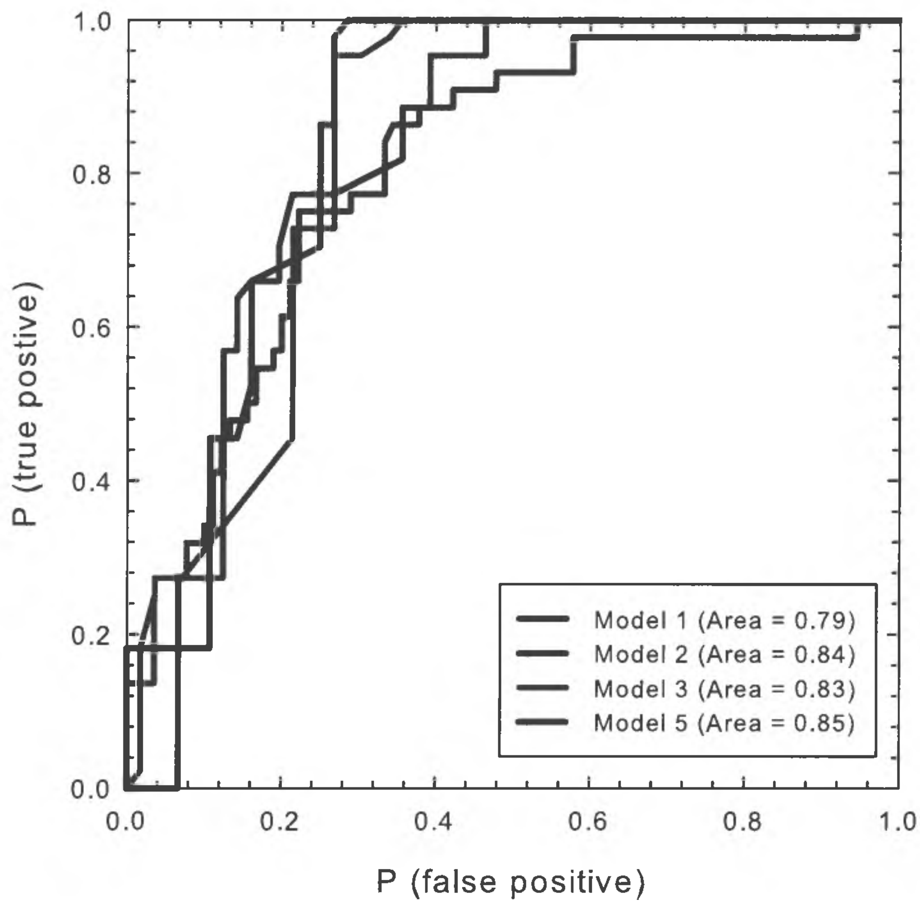

Figure 4-4 Receiver Operator Characteristics Hydraulic, Lithologic, and debris flow models

Reciever operator characteristics are a common indicator of the statistical significance of logistic regression models, where a larger area under the curve represents more favorable explanitory power for a given independent variable. Here we see that the rock strength model performs the best and the modified Shields hydraulic prediction performs the worst of the three models.

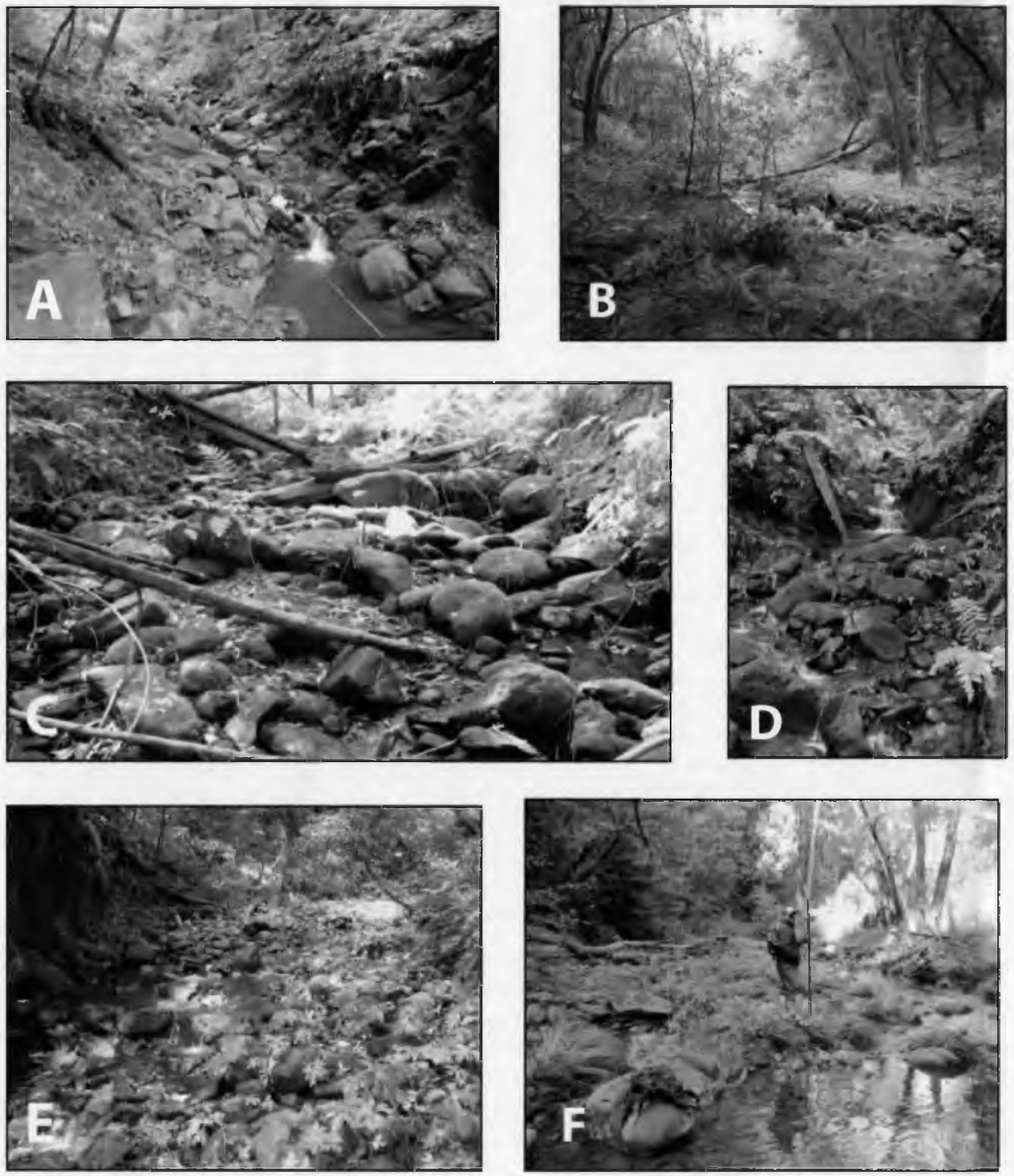

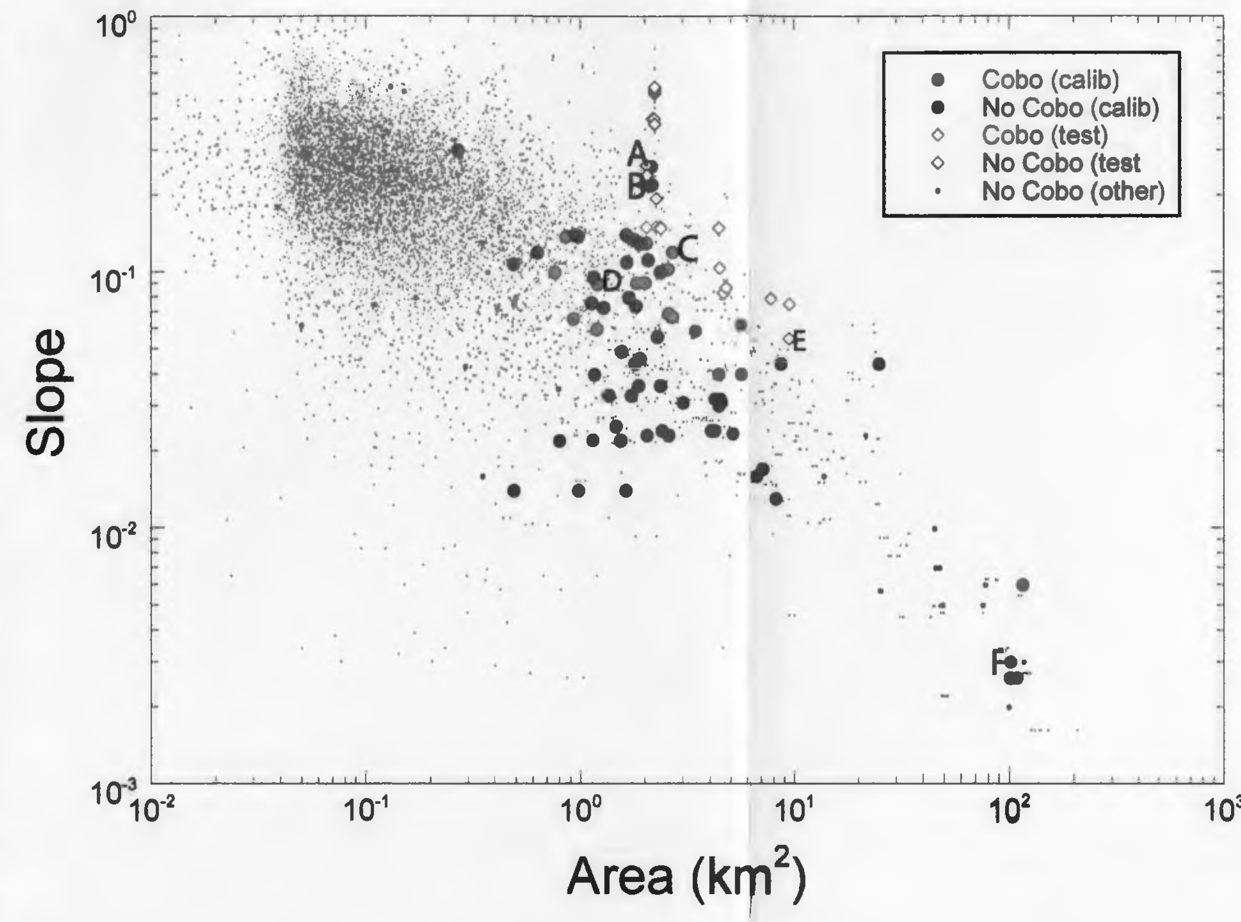

Figure 4-5 Field Tested Cobo Locations in Slope-Area Plot, Pescadero Creek

The six reaches pictures are a sample of the locations visited as part of this study. These sites are classified as CoBo reaches. Reach A and B are on Lambert Creek, Reach C is on Little Boulder Creek, Reach D is on Fall Creek, Reach E is on Peters Creek and reach F is on the main stem Pescadero Creek. Observe Reach F, located on the main stem of Pescadero Creek occurs where Dark gulch has deposited a debris fan adjacent to the channel. This provides a source for large bed material. In this basin, these fans have a limited effect downstream. The current model does work for predicting tributary junctions where channels with small draiange areas meet channels with large drainage areas.

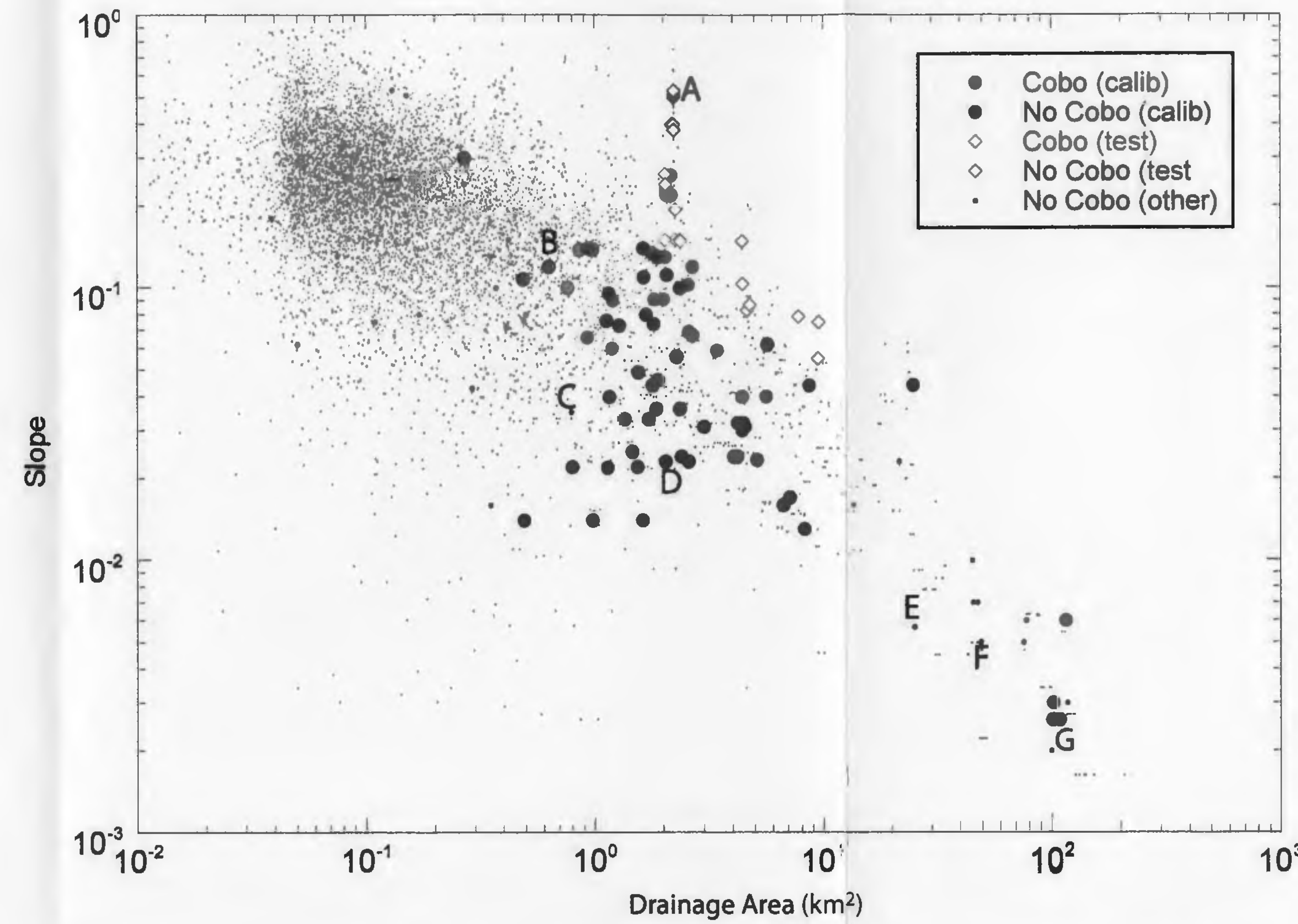

Figure 4-6 Field Tested No Cobo Locations in Slope-Area Plot, Pescadero Creek

The seven reaches depicted pictures are a sample of the locations visited as part of this study. These sites are classified as No CoBo reaches. Reach A is on Lambert Creek, this reach is underlain by the Vaqueros Sandstone. This bedrock cascade reach represents a convexity in the channel long profile. Reach B is on Dark Gulch Creek. At this reach, there is a very small drainage area. This area was logged in the 1950's and it is possible that in its natural state there might be more course material. Reach C is on McCormick Creek, near the confluence with the main stem, this is local knick point where the channel steepens, instead of a CoBo armored channel, this reach, which drains a basin underlain by the soft Tahana member of the Purisima Formation, scours to bedrock. Reach D is on Tarwater Creek. Tarwater Creek is dominated by the weak Tahana member of the Purisima Formation. Reach E is on Peters Creek at a drainage area of approximately 29 km^2. There is ample strong rock upstream, but few local source areas, notice the bed material is generally well rounded. Reach F is on the Pescadero Creek Main stem, just downstream of a tributary draining Butano ridge. This tributary injects large boulders into the channel, but there is not enough supply to create good CoBo. Reach G is characteristic of the main stem Pescadero Creek near La Honda.

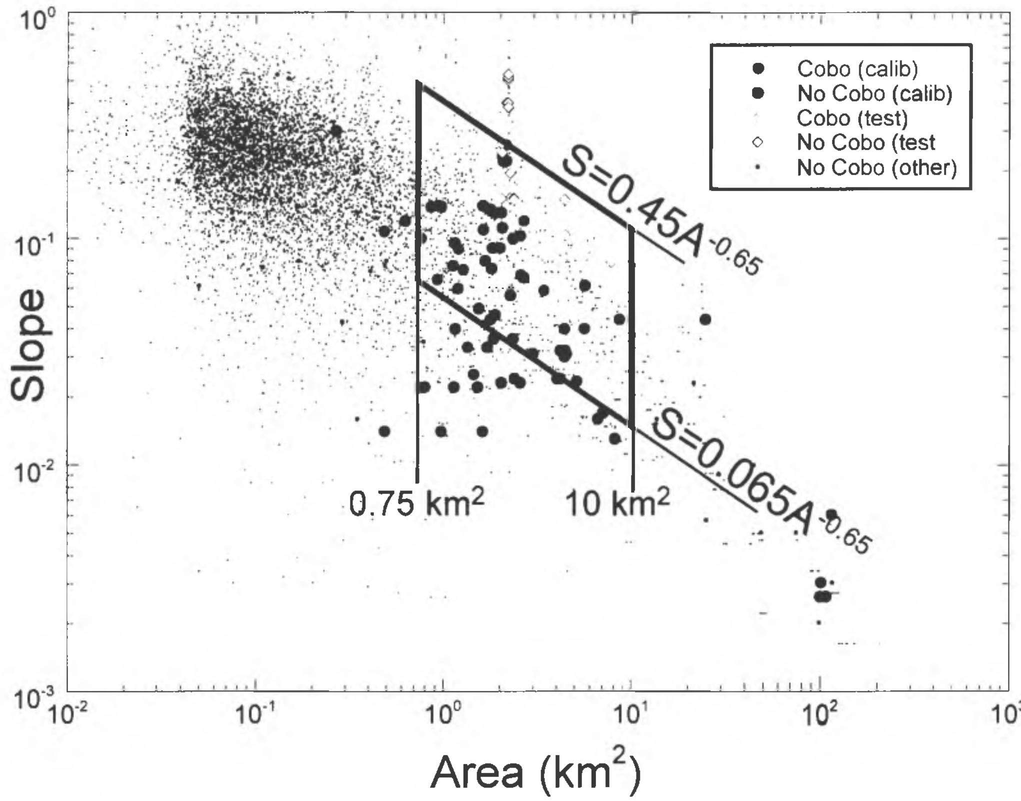

Figure 4-7 Drainage Area-Slope Envelope Model

Using the combined calibration and model testing datasets, I constructed a drainage-area slope envelope that is optimized to include all the true CoBo bedded channel reaches except two CoBo reaches on the main stem of Pescadero Creek where small colluvial tributaries form short, CoBo beds.

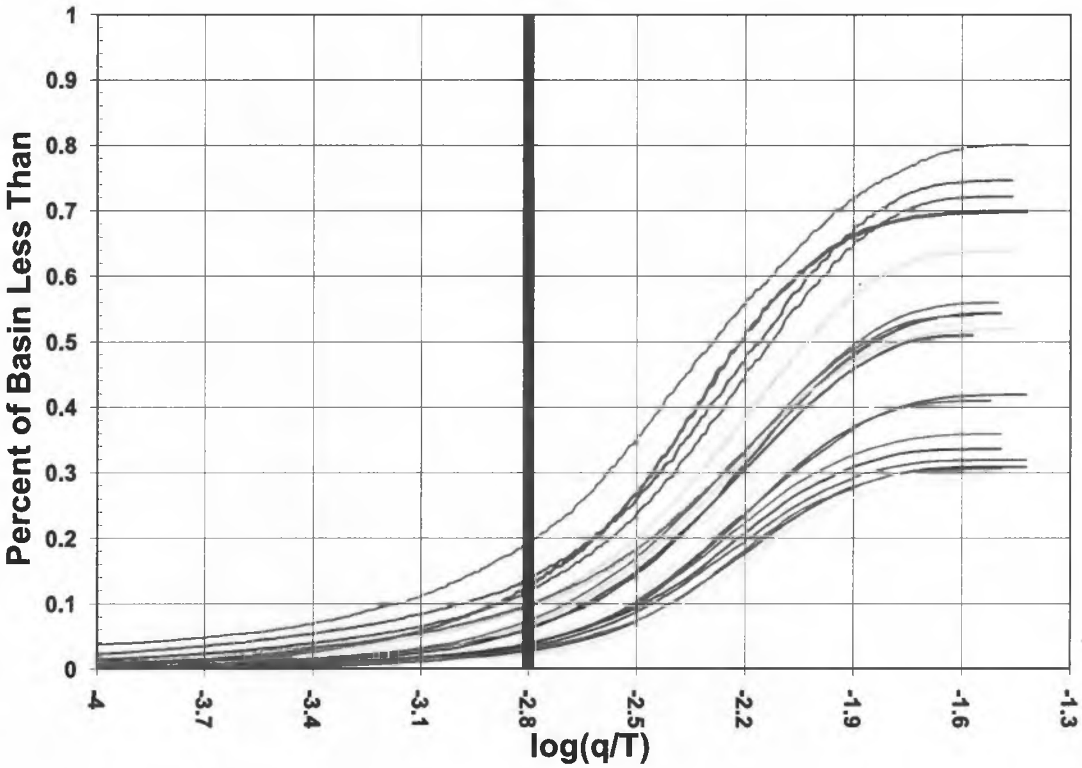

Figure 4-8 Sub-basin Cumulative Distribution of Instability (*log[q/T]*)

Each line represent to cumulative distribution of cell values for SHALSTAB model output *log[q/T],* for sampled basins. Highly negative values represent highly instable terrain. The positive values that sum the distribution to one were removed for clarity. The threshold of -2.8 *log[q/T]* (red line) was selected as the threshold based on (Dietrich et al., 1998), and the area under the curves to the left of the -2.8 *log[q/T]* threshold line was totalled for all sample sub basins. Warm colors represent No-CoBo basins while cool colors represent CoBo basins.

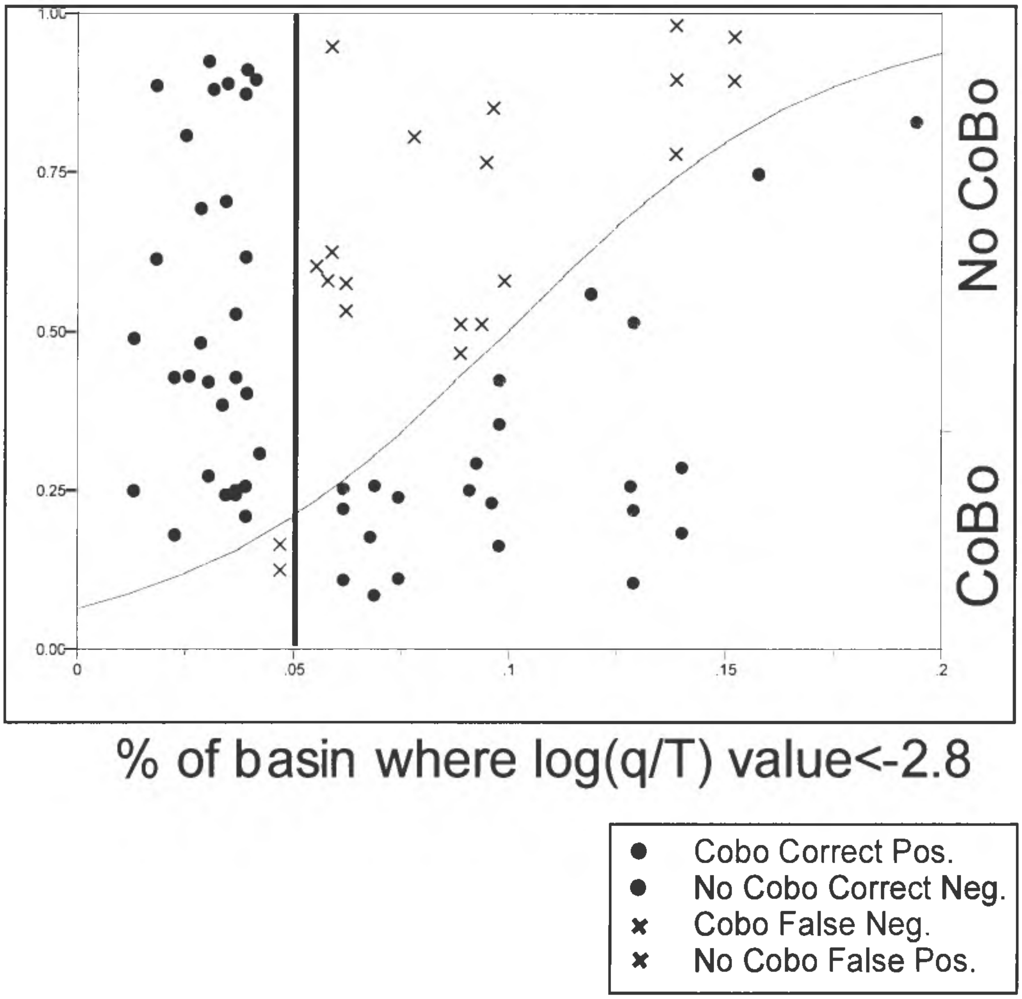

Figure 4-9 Logit, Basin Instability (SHALSTAB) vs. Observed CoBo

Part A presents the logit of the calibration dataset relating upstream fraction of unstable terrain plotted against channel CoBo state (CoBo vs. no CoBo). The P-value < 0.0001, therfore the relationship is significant. The data indicate a threshold of 0.06 optimizes the model performance statistics.

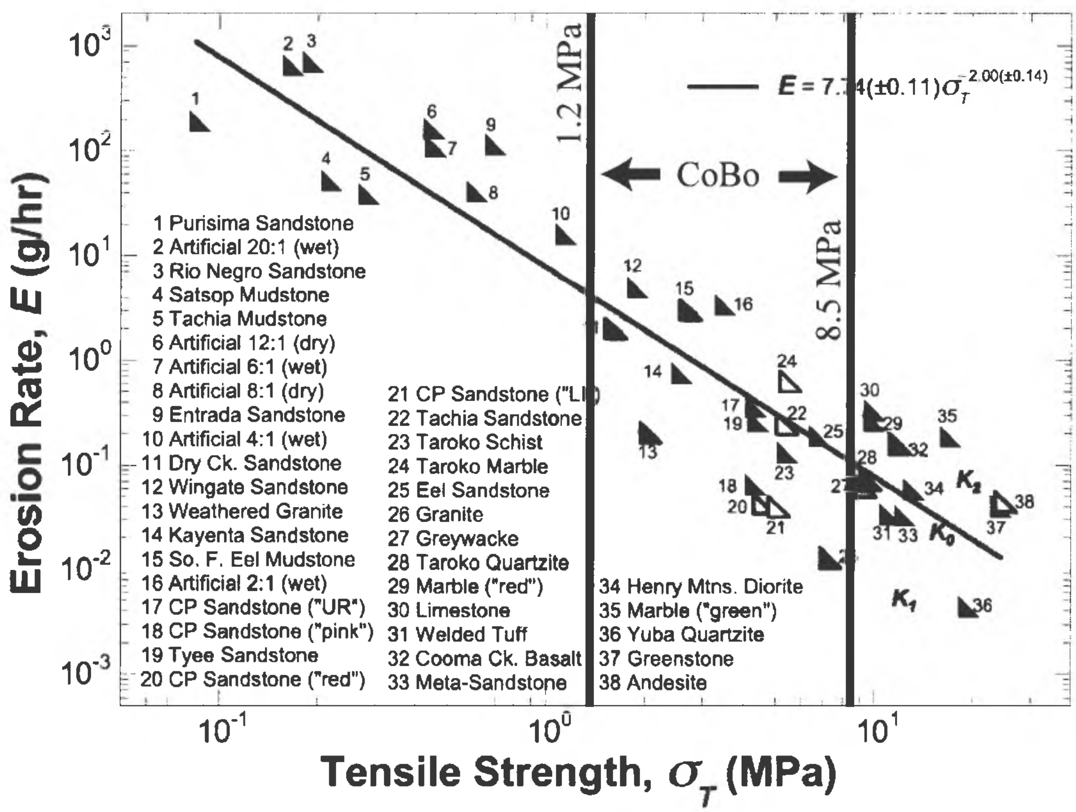

Figure 4-10 Rock Strength relative to data collected by *Beyeler and Sklar* [2010]

The vertical red lines represent the maximum and minimum tensile strengths of CoBo clasts observed within the Pescadero Creek basinHere we observe that the CoBo clasts sampled within the Pescadero Creek Basin fall within the stronger spectrum of the lithologies sampled by *Sklar and Dietrich* [2001]. Note that the minimum and maximum sampled rock strength sampled from CoBo clasts within the Pescadero Creek basin is 1.16 MPa and 8.9 MPa respectively.

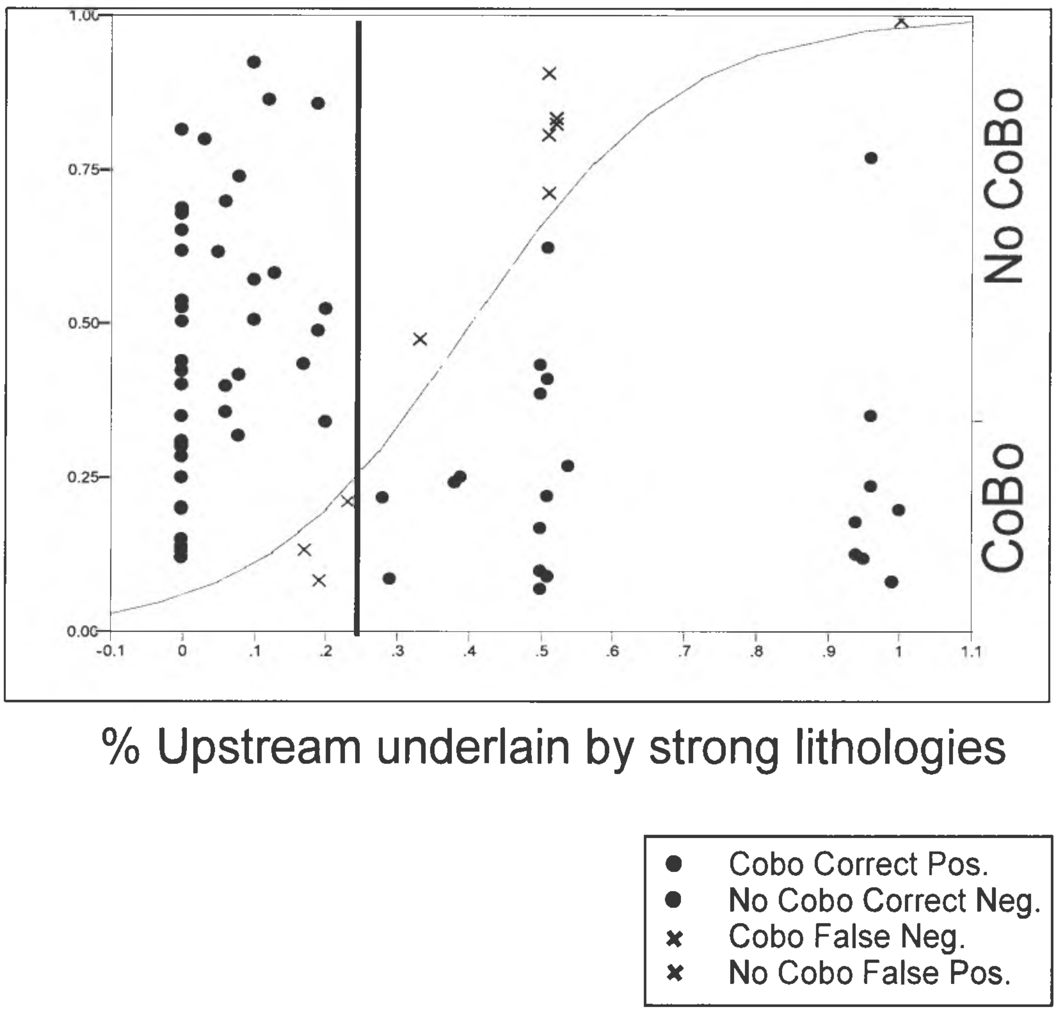

Figure 4-11 Logit, Upstream Percent Underlain by Durable Bedrock vs. Observed CoBo

Part A presents the Logistic regression plot of the calibration data for the rock strength parameter percent of upstream basin underlain by durable lithologies. P-value < 0.0001, therfore the relationship is significant. The data indicate a threshold of 0.25 optimizes the predictive statistics (see Figure 4-8 for reciever operator characteristics). Then applied as a secondary filter in tandem with the slope-area envelope a threshold of 0.20 optimizes the model statistics.

Figure 4-12 Little Boulder Creek, Refugia Sampling

I sampled a 165m reach on LIttle Boulder Creeek, at approximately 2.7km drainage area. The reach averaged slope is 0.045 m/m.

Figure 4-13 Oil Creek, Refugia Sampling

I sampled a 153m reach on Oil Creeek, at approximately 9.3 km^2 drainage area. The reach averaged slope is 0.045 m/m.

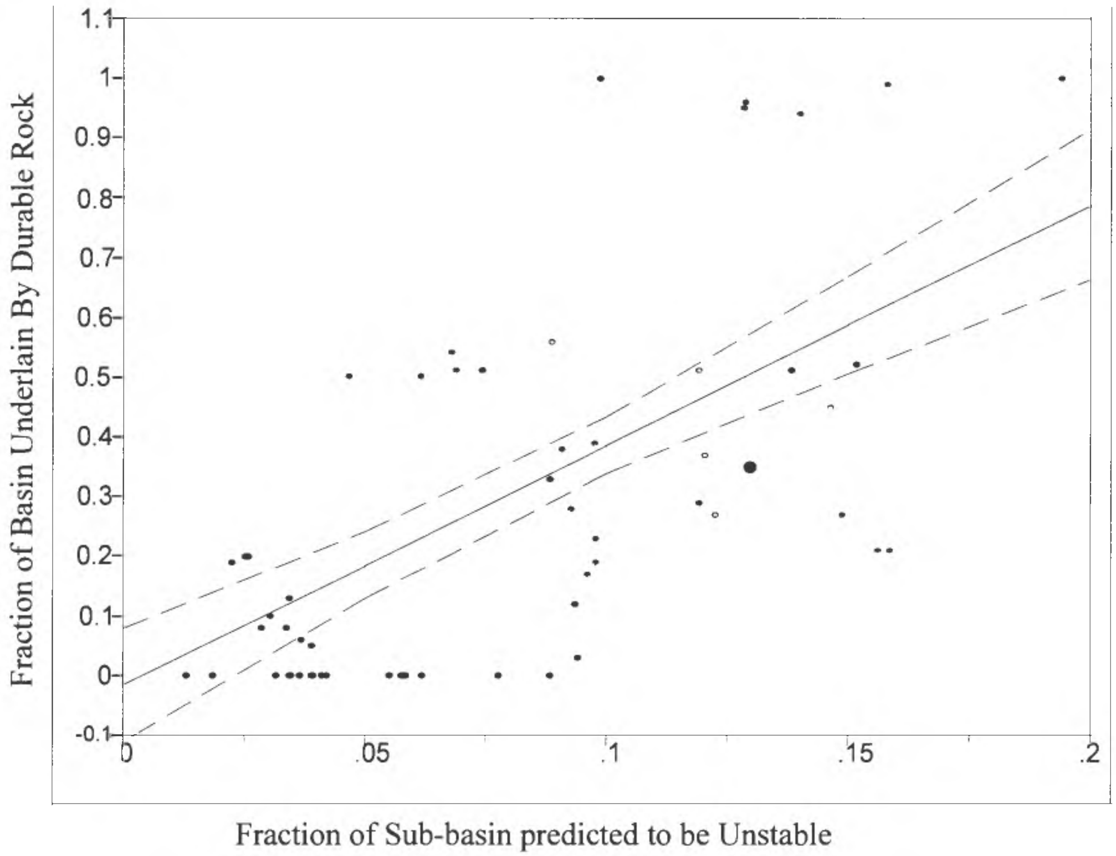

Figure 5-1 SHALSTAB vs. Bedrock Durability

Comparison of rock strength vs. percent of basin prone to shallow landsliding. R^2 is very low (0.38), but the relationship is statistically significant. Basins with more durable rock are more likely to be prone to debris flows. Additionally, because more durable rock generally hold a steeper angle of repose, there is there is a threshold response to the 45^{o} angle of internal friction used in SHALSTAB.

Reach#	CoBo	Basin	Watershed	DEM S (m/m)	DA(km^2)	Log10(DA [km^2])	% of basin <-2.8	Lamb d50, ED Hyd Geom
83	CoBo	NF Lambert	Pescadero	0.076	1.12	0.0492	0.098	223
114	No CoBo	Lambert	Pescadero	0.22	0.125	-0.9031		223
119	CoBo	lambert	Pescadero	0.066	0.928	-0.0325	0.047	229
126	No CoBo	Lambert	Pescadero	0.51	0.15	-0.8239		444
128	CoBo	lambert	Pescadero	0.135	1.77	0.2480	0.047	393
138	CoBo	lambert	Pescadero	0.091	1.82	0.2601	0.062	295
139	No CoBo	lambert	Pescadero	0.185	0.15	-0.8239		208
145	CoBo	lambert	Pescadero	0.091	2	0.3010	0.062	305
150	CoBo	lambert	Pescadero	0.13	2.03	0.3075	0.062	402
157	CoBo	lambert	Pescadero	0.23	2.05	0.3118	0.069	623
164	CoBo	lambert	Pescadero	0.22	2.07	0.3160	0.069	596
177	CoBo	lambert	Pescadero	0.26	2.14	0.3304	0.075	696
183	CoBo	Lambert	Pescadero	0.22	2.15	0.3324	0.075	604
187	No CoBo	Lambert	Pescadero	0.4	2.17	0.3365	0.075	942
193	No CoBo	Lambert	Pescadero	0.4	2.21	0.3444	0.075	943
198	No CoBo	Lambert	Pescadero	0.503	2.22	0.3464	0.075	1127
201	No CoBo	Lambert	Pescadero	0.514	2.22	0.3464	0.075	1147
205	No CoBo	Lambert	Pescadero	0.532	2.22	0.3464	0.075	1177
213	No CoBo	Lambert	Pescadero	0.382	2.22	0.3464	0.089	918
223	CoBo	NF Lambert	Pescadero	0.15	2.03	0.3075	0.147	436
228	CoBo	Lambert	Pescadero	0.194	2.25	0.3522	0.089	554
237	CoBo	Lambert	Pescadero	0.151	2.25	0.3522	0.089	460
238	CoBo	NF Lambert	Pescadero	0.262	2.03	0.3075	0.147	671
258	CoBo	NF Lambert	Pescadero	0.24	2.04	0.3096	0.147	620
259	CoBo	Lambert	Pescadero	0.151	2.36	0.3729	0.089	468
268	CoBo	Lambert	Pescadero	0.149	2.37	0.3747	0.119	463
288	CoBo	Lambert	Pescadero	0.149	4.41	0.6444	0.119	576
309	CoBo	Lambert	Pescadero	0.104	4.44	0.6474	0.119	443
313	No CoBo	Lambert	Pescadero	0.25	0.13	-0.8861		249
351	CoBo	Lambert	Pescadero	0.083	4.62	0.6646	0.119	377
375	CoBo	Peters	Pescadero	0.055	9.45	0.9754	0.121	359
382	CoBo	Devils Gulch	Pescadero	0.087	4.76	0.6776	0.123	394
430	CoBo	Devils Gulch	Pescadero	0.079	7.76	0.8899	0.123	367
447	CoBo	Peters	Pescadero	0.075	9.54	0.9795	0.121	454
560	No CoBo	McCormick	Pescadero	0.073	1.28	0.1072	0.032	220
661	No CoBo	McCormick	Pescadero	0.033	1.35	0.1303	0.039	124
772	No CoBo	McCormick	Pescadero	0.033	1.72	0.2355	0.039	135
902	No CoBo	Bradley	Pescadero	0.014	0.49	-0.3098	0.013	45
953	No CoBo	McCormick	Pescadero	0.044	1.79	0.2529	0.039	171
1023	No CoBo	McCOrmick	Pescadero	0.13	0.075	-1.1249		124
1040	No CoBo	McCormick	Pescadero	0.046	1.89	0.2765	0.039	177
1086	No CoBo	Bradley	Pescadero	0.014	1.62	0.2095	0.035	70
1087	No CoBo	Bradley	Pescadero	0.014	0.977	-0.0101	0.013	57
1144	No CoBo	tarwater	Pescadero	0.108	0.488	-0.3116	0.025	210
1202	No CoBo	McCormick	Pescadero	0.08	0.5	-0.3010		170
1210	No CoBo	McCormick	Pescadero	0.072	0.41	-0.3872		151
1231	No CoBo	tarwater	Pescadero	0.076	1.13	0.0531	0.023	216
1234	No CoBo	Bradley	Pescadero	0.023	2.04	0.3096	0.035	108
1303	No CoBo	tarwater	Pescadero	0.096	1.15	0.0607	0.023	258
1320	No CoBo	Jones Gulch	Pescadero	0.3	0.27	-0.5686	0.055	361
1323	No CoBo	Jones Gulch	Pescadero	0.24	0.27	-0.5686		303
1333	No CoBo	Jones Gulch	Pescadero	0.022	0.8	-0.0969	0.078	77
1356	No CoBo	Jones Gulch	Pescadero	0.025	1.46	0.1644	0.037	106

Reach#	CoBo	Basin	Watershed	DEM S (m/m)	DA(km^2)	Log10(DA [km^2])	% of basin <-2.8	Lamb d50, ED Hyd Geom
1369	No CoBo	Bradley	Pescadero	0.075	0.11	-0.9586		110
1402	No CoBo	tarwater	Pescadero	0.04	1.16	0.0645	0.026	134
1408	No CoBo	Jones Gulch	Pescadero	0.022	1.14	0.0569	0.062	88
1452	No CoBo	w. of McCor	Pescadero	0.076	0.49	-0.3098		163
1478	No CoBo	Jones Gulch	Pescadero	0.022	1.53	0.1847	0.062	97
1505	No CoBo	Jones Gulch	Pescadero	0.056	2.28	0.3579	0.041	222
1528	No CoBo	Jones Gulch	Pescadero	0.08	1.68	0.2253	0.059	263
1619	No CoBo	Jones Gulch	Pescadero	0.074	1.81	0.2577	0.059	254
1694	No CoBo	Jones Gulch	Pescadero	0.13	1.89	0.2765	0.058	390
1716	No CoBo	McCormick	Pescadero	0.031	3	0.4771	0.042	193
1731	No CoBo	tarwater	Pescadero	0.036	1.86	0.2695	0.035	148
1800	No CoBo	tarwater	Pescadero	0.036	2.35	0.3711	0.031	160
1885	No CoBo	tarwater	Pescadero	0.1	2.36	0.3729	0.031	346
1896	No CoBo	Slate	Pescadero	0.13	0.35	-0.4559		218
1903	No CoBo	tarwater	Pescadero	0.024	2.39	0.3784	0.031	118
1909	CoBo	main	Pescadero	0.003	101.17	2.0051	0.091	82
1912	No CoBo	Slate	Pescadero	0.14	0.94	-0.0269	0.152	328
1919	CoBo	Hoffman	Pescadero	0.138	0.86	-0.0655	0.140	307
1940	No CoBo	Slate	Pescadero	0.15	0.42	-0.3768		256
1943	No CoBo	Slate	Pescadero	0.18	0.039	-1.4089		129
1951	No CoBo	Slate	Pescadero	0.139	0.98	-0.0088	0.152	324
1971	No CoBo	Slate	Pescadero	0.25	0.14	-0.8539		255
1973	No CoBo	Slate	Pescadero	0.53	0.13	-0.8861		432
1974	No CoBo	Slate	Pescadero	0.34	0.12	-0.9208		310
1975	No CoBo	Bradley	Pescadero	0.043	0.29	-0.5376		100
1978	No CoBo	main	Pescadero	0.0026	108	2.0334	0.089	84
1997	No CoBo	tarwater	Pescadero	0.023	2.58	0.4116	0.029	121
1998	No CoBo	Main	Pescadero	0.0026	101	2.0043	0.089	83
2003	No CoBo	Peters	Pescadero	0.08	0.17	-0.7696		116
2012	No CoBo	Evans	Pescadero	0.049	1.55	0.1903	0.034	175
2015	No CoBo	Main	Pescadero	0.002	99.7	1.9987		82
2038	CoBo	Hoffman	Pescadero	0.1	0.76	-0.1192	0.140	235
2041	No CoBo	Slate	Pescadero	0.14	1.63	0.2122	0.139	404
2086	No CoBo	Peters	Pescadero	0.062	0.05	-1.3010		86
2095	No CoBo	Slate	Pescadero	0.11	1.64	0.2148	0.139	359
2107	No CoBo	tarwater	Pescadero	0.024	4.05	0.6075	0.029	141
2121	No CoBo	Slate	Pescadero	0.112	2.07	0.3160	0.139	365
2138	No CoBo	Bradley	Pescadero	0.013	8.2	0.9138	0.019	117
2229	No CoBo	tarwater	Pescadero	0.024	4.2	0.6232	0.037	144
2434	No CoBo	tarwater	Pescadero	0.032	4.21	0.6243	0.037	178
2489	CoBo	main	Pescadero	0.006	114.99	2.0607	0.093	158
2530	No CoBo	tarwater	Pescadero	0.032	4.47	0.6503	0.037	181
2787	CoBo	Slate	Pescadero	0.059	3.42	0.5340	0.119	264
2857	No CoBo	Tarwater	Pescadero	0.031	4.53	0.6561	0.039	181
2953	No CoBo	Dark Gulch	Pescadero	0.12	0.63	-0.2007	0.099	257
3126	CoBo	Slate	Pescadero	0.03	4.4	0.6435	0.098	175
3130	No CoBo	tarwater	Pescadero	0.044	8.64	0.9365	0.039	239
3153	No CoBo	E. of Tarwate	Pescadero	0.035	0.79	-0.1024		106
3203	No CoBo	Peters	Pescadero	0.023	21.6	1.3345		248
3352	CoBo	Slate	Pescadero	0.0234	5.12	0.7093	0.098	152
3357	No CoBo	Main (gage)	Pescadero	0.003	117	2.0682		89
3462	CoBo	Oil	Pesc	0.057	6.6	0.8195	0.159	322

Reach#	CoBo	Basin	Watershed	DEM S (m/m)	DA(km^2)	Log10(DA [km^2])	% of basin <-2.8	Lamb d50, ED Hyd Geom
3566	CoBo	Oil	Pesc	0.057	6.8	0.8325	0.159	325
3696	No CoBo	Peters	Pescadero	0.044	24.9	1.3962	0.094	426
3710	CoBo	Slate	Pescadero	0.04	5.62	0.7497	0.096	232
3779	No CoBo	Peters	Pescadero	0.0057	25.1	1.3997		92
3819	No CoBo	Main	Pescadero	0.006	77.5	1.8893		148
3836	No CoBo	Slate	Pescadero	0.062	5.68	0.7543	0.096	328
4118	CoBo	Hooker	Pescadero	0.06	1.19	0.0755	0.158	185
4169	No CoBo	Peters	Pescadero	0.0057	25.3	1.4031		92
4179	No CoBo	S. of Peters	Pescadero	0.1	0.37	-0.4318		174
4222	No CoBo	Main	Pescadero	0.005	49.1	1.6911		100
4262	CoBo	Oil	Pescadero	0.05	8.4	0.9243	0.156	317
4270	No CoBo	Main	Pescadero	0.005	75.3	1.8768		116
4308	CoBo	Oil	Pescadero	0.052	8.5	0.9294	0.156	331
4321	CoBo	Oil	Pescadero	0.052	9.3	0.9685	0.149	342
4572	CoBo	Fall	Pescadero	0.09	1.2	0.0792	0.194	252
4690	No CoBo	Main	Pescadero	0.007	47.5	1.6767		133
4740	No CoBo	Iverson	Pescadero	0.16	0.35	-0.4559		250
4942	No CoBo	Main	Pescadero	0.007	45.4	1.6571		132
5094	No CoBo	Main	Pescadero	0.01	45.1	1.6542		168
5828	No CoBo	Oil	Pescadero	0.018	12.3	1.0899	0.130	168
5964	No CoBo	Oil	Pescadero	0.018	12.3	1.0899	0.130	169
7030	No CoBo	Main	Pescadero	0.016	13.7	1.1367		168
7071	CoBo	Waterman	Pescadero	0.04	4.4	0.6435	0.068	216
7146	CoBo	LBC	Pescadero	0.067	2.67	0.4265	0.128	265
7165	CoBo	LBC	Pescadero	0.12	2.67	0.4265	0.129	423
7205	CoBo	LBC	Pescadero	0.069	2.57	0.4099	0.129	270
7241	CoBo	LBC	Pescadero	0.103	2.56	0.4082	0.129	362
7775	No CoBo	Little Butano	Pescadero	0.017	7.1	0.8513	0.095	131
7889	No CoBo	Bradley	Pescadero	0.016	6.64	0.8222	0.019	123

Reach#	Lamb threshold ed Hyd Geom	sa-parallel	just qt	sa-parallel small	SA YES and qt	lith prediction	lith plus SA	E Model 3
83	Yes	SA YES	Y	SA YES	Pred COBO	Y	Pred COBO	0.25
114	Yes	SA NO		SA NO	Pred NoCoBo		Pred NoCoBo	
119	Yes	SA YES	N	SA YES	Pred NoCoBo	Y	Pred COBO	-0.42
126	Yes	SA NO		SA NO	Pred NoCoBo		Pred NoCoBo	
128	Yes	SA YES	N	SA YES	Pred NoCoBo	Y	Pred COBO	-0.42
138	Yes	SA YES	Y	SA YES	Pred COBO	Y	Pred COBO	-0.09
139	Yes	SA NO		SA NO	Pred NoCoBo		Pred NoCoBo	
145	Yes	SA YES	Y	SA YES	Pred COBO	Y	Pred COBO	-0.09
150	Yes	SA YES	Y	SA YES	Pred COBO	Y	Pred COBO	-0.09
157	Yes	SA YES	Y	SA YES	Pred COBO	Y	Pred COBO	0.12
164	Yes	SA YES	Y	SA YES	Pred COBO	Y	Pred COBO	0.12
177	Yes	SA YES	Y	SA YES	Pred COBO	Y	Pred COBO	0.24
183	Yes	SA YES	Y	SA YES	Pred COBO	Y	Pred COBO	0.24
187	Yes	SA NO	Y	SA NO	Pred NoCoBo	Y	Pred NoCoBo	0.24
193	Yes	SA NO	Y	SA NO	Pred NoCoBo	Y	Pred NoCoBo	0.24
198	Yes	SA NO	Y	SA NO	Pred NoCoBo	Y	Pred NoCoBo	0.24
201	Yes	SA NO	Y	SA NO	Pred NoCoBo	Y	Pred NoCoBo	0.24
205	Yes	SA NO	Y	SA NO	Pred NoCoBo	Y	Pred NoCoBo	0.24
213	Yes	SA NO	Y	SA NO	Pred NoCoBo	Y	Pred NoCoBo	0.75
223	Yes	SA YES	Y	SA YES	Pred COBO	Y	Pred COBO	1.57
228	Yes	SA YES	Y	SA YES	Pred COBO	Y	Pred COBO	0.75
237	Yes	SA YES	Y	SA YES	Pred COBO	Y	Pred COBO	0.75
238	Yes	SA YES	Y	SA YES	Pred COBO	Y	Pred COBO	1.57
258	Yes	SA YES	Y	SA YES	Pred COBO	Y	Pred COBO	1.57
259	Yes	SA YES	Y	SA YES	Pred COBO	Y	Pred COBO	0.75
268	Yes	SA YES	Y	SA YES	Pred COBO	Y	Pred COBO	1.22
288	Yes	SA YES	Y	SA YES	Pred COBO	Y	Pred COBO	1.22
309	Yes	SA YES	Y	SA YES	Pred COBO	Y	Pred COBO	1.22
313	Yes	SA NO		SA NO	Pred NoCoBo		Pred NoCoBo	
351	Yes	SA YES	Y	SA YES	Pred COBO	Y	Pred COBO	1.22
375	Yes	SA YES	Y	SA NO	Pred COBO	Y	Pred COBO	0.67
382	Yes	SA YES	Y	SA YES	Pred COBO	Y	Pred COBO	0.31
430	Yes	SA YES	Y	SA YES	Pred COBO	Y	Pred COBO	0.31
447	Yes	SA YES	Y	SA NO	Pred COBO	Y	Pred COBO	0.67
560	Yes	SA YES	N	SA YES	Pred NoCoBo	N	Pred NoCoBo	-2.79
661	No	SA NO	N	SA NO	Pred NoCoBo	N	Pred NoCoBo	-2.63
772	Yes	SA NO	N	SA NO	Pred NoCoBo	N	Pred NoCoBo	-2.63
902	No	SA NO	N	SA NO	Pred NoCoBo	N	Pred NoCoBo	-3.20
953	Yes	SA YES	N	SA YES	Pred NoCoBo	N	Pred NoCoBo	-2.63
1023	No	SA NO		SA NO	Pred NoCoBo		Pred NoCoBo	
1040	Yes	SA YES	N	SA YES	Pred NoCoBo	N	Pred NoCoBo	-2.63
1086	No	SA NO	N	SA NO	Pred NoCoBo	N	Pred NoCoBo	-2.73
1087	No	SA NO	N	SA NO	Pred NoCoBo	N	Pred NoCoBo	-3.20
1144	Yes	SA NO	N	SA NO	Pred NoCoBo	N	Pred NoCoBo	-2.11
1202	Yes	SA NO		SA NO	Pred NoCoBo		Pred NoCoBo	
1210	Yes	SA NO		SA NO	Pred NoCoBo		Pred NoCoBo	
1231	Yes	SA YES	N	SA YES	Pred NoCoBo	N	Pred NoCoBo	-2.21
1234	No	SA NO	N	SA NO	Pred NoCoBo	N	Pred NoCoBo	-2.73
1303	Yes	SA YES	N	SA YES	Pred NoCoBo	N	Pred NoCoBo	-2.21
1320	Yes	SA NO	N	SA NO	Pred NoCoBo	N	Pred NoCoBo	-2.27
1323	Yes	SA NO		SA NO	Pred NoCoBo		Pred NoCoBo	
1333	No	SA NO	Y	SA NO	Pred NoCoBo	N	Pred NoCoBo	-1.78
1356	No	SA NO	N	SA NO	Pred NoCoBo	N	Pred NoCoBo	-2.68

Reach#	Lamb threshold ed Hyd Geom	sa-parallel	just qt	sa-parallel small	SA YES and qt	lith prediction	lith plus SA	E Model 3
1369	No	SA NO		SA NO	Pred NoCoBo		Pred NoCoBo	
1402	Yes	SA NO	N	SA NO	Pred NoCoBo	N	Pred NoCoBo	-2.10
1408	No	SA NO	Y	SA NO	Pred NoCoBo	N	Pred NoCoBo	-2.13
1452	Yes	SA NO		SA NO	Pred NoCoBo		Pred NoCoBo	
1478	No	SA NO	Y	SA NO	Pred NoCoBo	N	Pred NoCoBo	-2.13
1505	Yes	SA YES	N	SA YES	Pred NoCoBo	N	Pred NoCoBo	-2.58
1528	Yes	SA YES	N	SA YES	Pred NoCoBo	N	Pred NoCoBo	-2.20
1619	Yes	SA YES	N	SA YES	Pred NoCoBo	N	Pred NoCoBo	-2.20
1694	Yes	SA YES	N	SA YES	Pred NoCoBo	N	Pred NoCoBo	-2.22
1716	Yes	SA YES	N	SA YES	Pred NoCoBo	N	Pred NoCoBo	-2.56
1731	Yes	SA NO	N	SA NO	Pred NoCoBo	N	Pred NoCoBo	-2.19
1800	Yes	SA NO	N	SA NO	Pred NoCoBo	N	Pred NoCoBo	-2.41
1885	Yes	SA YES	N	SA YES	Pred NoCoBo	N	Pred NoCoBo	-2.41
1896	Yes	SA NO		SA NO	Pred NoCoBo		Pred NoCoBo	
1903	No	SA NO	N	SA NO	Pred NoCoBo	N	Pred NoCoBo	-2.41
1909	No	SA NO	Y	SA NO	Pred NoCoBo	Y	Pred NoCoBo	0.06
1912	Yes	SA YES	Y	SA YES	Pred COBO	Y	Pred COBO	1.98
1919	Yes	SA YES	Y	SA YES	Pred COBO	Y	Pred COBO	3.44
1940	Yes	SA NO		SA NO	Pred NoCoBo		Pred NoCoBo	
1943	Yes	SA NO		SA NO	Pred NoCoBo		Pred NoCoBo	
1951	Yes	SA YES	Y	SA YES	Pred COBO	Y	Pred COBO	1.98
1971	Yes	SA NO		SA NO	Pred NoCoBo		Pred NoCoBo	
1973	Yes	SA NO		SA NO	Pred NoCoBo		Pred NoCoBo	
1974	Yes	SA NO		SA NO	Pred NoCoBo		Pred NoCoBo	
1975	No	SA NO		SA NO	Pred NoCoBo		Pred NoCoBo	
1978	No	SA NO	Y	SA NO	Pred NoCoBo	Y	Pred NoCoBo	-0.19
1997	No	SA NO	N	SA NO	Pred NoCoBo	N	Pred NoCoBo	-2.53
1998	No	SA NO	Y	SA NO	Pred NoCoBo	N	Pred NoCoBo	-1.55
2003	No	SA NO		SA NO	Pred NoCoBo		Pred NoCoBo	
2012	Yes	SA YES	N	SA YES	Pred NoCoBo	N	Pred NoCoBo	-2.42
2015	No	SA NO		SA NO	Pred NoCoBo		Pred NoCoBo	
2038	Yes	SA YES	Y	SA YES	Pred COBO	Y	Pred COBO	3.44
2041	Yes	SA YES	Y	SA YES	Pred COBO	Y	Pred COBO	1.64
2086	No	SA NO		SA NO	Pred NoCoBo		Pred NoCoBo	
2095	Yes	SA YES	Y	SA YES	Pred COBO	Y	Pred COBO	1.64
2107	Yes	SA NO	N	SA NO	Pred NoCoBo	N	Pred NoCoBo	-2.53
2121	Yes	SA YES	Y	SA YES	Pred COBO	Y	Pred COBO	1.64
2138	No	SA NO	N	SA NO	Pred NoCoBo	N	Pred NoCoBo	-3.08
2229	Yes	SA NO	N	SA NO	Pred NoCoBo	N	Pred NoCoBo	-2.43
2434	Yes	SA YES	N	SA YES	Pred NoCoBo	N	Pred NoCoBo	-2.43
2489	Yes	SA NO	Y	SA NO	Pred NoCoBo	Y	Pred NoCoBo	-0.31
2530	Yes	SA YES	N	SA YES	Pred NoCoBo	N	Pred NoCoBo	-2.43
2787	Yes	SA YES	Y	SA YES	Pred COBO	Y	Pred COBO	0.32
2857	Yes	SA YES	N	SA YES	Pred NoCoBo	N	Pred NoCoBo	-2.42
2953	Yes	SA NO	Y	SA NO	Pred NoCoBo	Y	Pred NoCoBo	2.78
3126	Yes	SA YES	Y	SA YES	Pred COBO	N	Pred COBO	-0.40
3130	Yes	SA YES	N	SA YES	Pred NoCoBo	N	Pred NoCoBo	-2.63
3153	No	SA NO		SA NO	Pred NoCoBo		Pred NoCoBo	
3203	Yes	SA NO		SA NO	Pred NoCoBo		Pred NoCoBo	
3352	Yes	SA YES	Y	SA YES	Pred COBO	N	Pred NoCoBo	-0.56
3357	No	SA NO		SA NO	Pred NoCoBo		Pred NoCoBo	
3462	Yes	SA YES	Y	SA NO	Pred COBO	N	Pred COBO	0.85

Reach#	Lamb threshold ed Hyd Geom	sa-parallel	just qt	sa-parallel small	SA YES and qt	lith prediction	lith plus SA	E Model 3
3566	Yes	SA YES	Y	SA NO	Pred COBO	N	Pred COBO	0.85
3696	Yes	SA NO	Y	SA NO	Pred NoCoBo	N	Pred NoCoBo	-0.94
3710	Yes	SA YES	Y	SA YES	Pred COBO	N	Pred NoCoBo	-0.68
3779	No	SA NO		SA NO	Pred NoCoBo		Pred NoCoBo	
3819	Yes	SA NO		SA NO	Pred NoCoBo		Pred NoCoBo	
3836	Yes	SA YES	Y	SA NO	Pred COBO	N	Pred NoCoBo	-0.68
4118	Yes	SA YES	Y	SA YES	Pred COBO	Y	Pred COBO	4.03
4169	No	SA NO		SA NO	Pred NoCoBo		Pred NoCoBo	
4179	Yes	SA NO		SA NO	Pred NoCoBo		Pred NoCoBo	
4222	No	SA NO		SA NO	Pred NoCoBo		Pred NoCoBo	
4262	Yes	SA YES	Y	SA NO	Pred COBO	N	Pred COBO	0.80
4270	No	SA NO		SA NO	Pred NoCoBo		Pred NoCoBo	
4308	Yes	SA YES	Y	SA NO	Pred COBO	N	Pred COBO	0.80
4321	Yes	SA YES	Y	SA NO	Pred COBO	Y	Pred COBO	0.88
4572	Yes	SA YES	Y	SA YES	Pred COBO	Y	Pred COBO	4.87
4690	Yes	SA NO		SA NO	Pred NoCoBo		Pred NoCoBo	
4740	Yes	SA NO		SA NO	Pred NoCoBo		Pred NoCoBo	
4942	Yes	SA NO		SA NO	Pred NoCoBo		Pred NoCoBo	
5094	Yes	SA NO		SA NO	Pred NoCoBo		Pred NoCoBo	
5828	Yes	SA NO	Y	SA NO	Pred NoCoBo	Y	Pred NoCoBo	0.79
5964	Yes	SA NO	Y	SA NO	Pred NoCoBo	Y	Pred NoCoBo	0.79
7030	Yes	SA NO		SA NO	Pred NoCoBo		Pred NoCoBo	
7071	Yes	SA YES	Y	SA YES	Pred COBO	Y	Pred COBO	0.22
7146	Yes	SA YES	Y	SA YES	Pred COBO	Y	Pred COBO	3.22
7165	Yes	SA YES	Y	SA YES	Pred COBO	Y	Pred COBO	3.28
7205	Yes	SA YES	Y	SA YES	Pred COBO	Y	Pred COBO	3.28
7241	Yes	SA YES	Y	SA YES	Pred COBO	Y	Pred COBO	3.28
7775	Yes	SA NO	Y	SA NO	Pred NoCoBo	N	Pred NoCoBo	-1.29
7889	No	SA NO	N	SA NO	Pred NoCoBo	N	Pred NoCoBo	-3.08

Reach#	E model 3 output	Field S (m/m)	Field BFW (m)	Field BFD (m)	GPS point / pourpt	% Tmb	% Tvq	% Tb	%Tla	% Tsr	Tsl	% Tpt	% Tm
83	CoBo				Lam1	0.08	0.31	0	0.6	0	0	0	0
114													
119	No CoBo	0.0854			p5	0.19	0.31	0	0.3	0	0.19	0	0
126													
128	No CoBo				p5	0.19	0.31	0	0.3	0	0.19	0	0
138	No CoBo				P1	0.22	0.28	0	0.2	0	0.21	0	0
139													
145	No CoBo				P1	0.22	0.28	0	0.2	0	0.21	0	0
150	No CoBo	0.155	2.5	0.3	P1	0.22	0.28	0	0.2	0	0.21	0	0
157	CoBo	0.21			p2	0.24	0.27	0	0.2	0	0.21	0	0
164	CoBo	0.34			p2	0.24	0.27	0	0.2	0	0.21	0	0
177	CoBo	0.105	2.5	0.3	p3	0.25	0.26	0	0.2	0	0.22	0	0
183	CoBo	0.105	2.5	0.3	P3	0.25	0.26	0	0.2	0	0.22	0	0
187	CoBo	0.44			WPT050	0.25	0.26	0	0.2	0	0.22	0	0
193	CoBo	0.44			WPT050	0.25	0.26	0	0.2	0	0.22	0	0
198	CoBo	0.44			WPT050	0.25	0.26	0	0.2	0	0.22	0	0
201	CoBo	0.44			WPT050	0.25	0.26	0	0.2	0	0.22	0	0
205	CoBo	0.44			WPT050	0.25	0.26	0	0.2	0	0.22	0	0
213	CoBo	0.44			WPT051	0.23	0.278	0.05	0.2	0	0.22	0	0
223	CoBo	0.105	3.5	0.4	WPT53	0.16	0.29	0	0.5	0	0.04	0	0
228	CoBo	0.44			WPT051	0.23	0.278	0.05	0.2	0	0.22	0	0
237	CoBo	0.193			WPT058	0.23	0.278	0.05	0.2	0	0.22	0	0
238	CoBo	0.105	3.5	0.4	WPT53	0.16	0.29	0	0.5	0	0.04	0	0
258	CoBo	0.105	3.5	0.4	WPT53	0.16	0.29	0	0.5	0	0.04	0	0
259	CoBo				WPT058	0.23	0.278	0.05	0.2	0	0.22	0	0
268	CoBo				WPT052	0.21	0.27	0.03	0.4	0	0.13	0	0
288	CoBo				WPT052	0.21	0.27	0.03	0.4	0	0.13	0	0
309	CoBo	0.105	4	0.5	WPT054	0.21	0.27	0.03	0.4	0	0.13	0	0
313													
351	CoBo	0.083			WPT055	0.21	0.27	0.03	0.4	0	0.13	0	0
375	CoBo	0.039	7	0.9	WPT056	0.18	0.19	0	0.5	0	0.16	0	0
382	CoBo	0.052	3	0.5	Dev1	0.15	0.12	0	0.5	0	0.19	0	0
430	CoBo	0.052	3	0.5	Dev2	0.15	0.12	0	0.5	0	0.19	0	0
447	CoBo	0.039	9	0.8	WPT057	0.18	0.19	0	0.5	0	0.16	0	0
560	No CoBo				Mc005	0	0	0	0	0	0	1	0
661	No CoBo				Mc004	0	0	0	0	0	0	1	0
772	No CoBo				Mc004	0	0	0	0	0	0	1	0
902	No CoBo				Brad4	0	0	0	0	0	0	0.9	0
953	No CoBo				Mc002	0	0	0	0	0	0	1	0
1023													
1040	No CoBo				Mc002	0	0	0	0	0	0	1	0
1086	No CoBo				Brad3	0	0	0	0	0	0	0.6	0
1087	No CoBo				Brad4	0	0	0	0	0	0	0.9	0
1144	No CoBo				tar6	0.2	0	0	0	0	0	0.8	0
1202													
1210													
1231	No CoBo				Tar1	0.19	0	0	0	0	0	0.8	0
1234	No CoBo				Brad2	0	0	0	0	0	0	0.9	0
1303	No CoBo				Tar1	0.19	0	0	0	0	0	0.8	0
1320	No CoBo				jg7	0	0	0	0	0	0	1	0
1323													
1333	No CoBo				jg6	0	0	0	0	0	0	1	0
1356	No CoBo				JG3	0	0	0	0	0	0	1	0

Reach#	E model 3 output	Field S (m/m)	Field BFW (m)	Field BFD (m)	GPS point / pourpt	% Tmb	% Tvq	% Tb	%Tla	% Tsr	Tsl	% Tpt	% Tm
1369													
1402	No CoBo				tar7	0.2	0	0	0	0	0	0.8	0
1408	No CoBo				JG1	0	0	0	0	0	0	1	0
1452													
1478	No CoBo				JG1	0	0	0	0	0	0	1	0
1505	No CoBo				JG2	0	0	0	0	0	0	1	0
1528	No CoBo				JG4	0	0	0	0	0	0	1	0
1619	No CoBo				JG4	0	0	0	0	0	0	1	0
1694	No CoBo				JG5	0	0	0	0	0	0	1	0
1716	No CoBo				MC6	0	0	0	0	0	0	0.7	0
1731	No CoBo				Tar2	0.13	0	0	0	0	0	0.9	0
1800	No CoBo				tar5	0.1	0	0	0	0	0	0.9	0
1885	No CoBo				tar5	0.1	0	0	0	0	0	0.9	0
1896													
1903	No CoBo				tar5	0.1	0	0	0	0	0	0.9	0
1909	CoBo				atHoff	0.07	0.1	0.21	0.2	0	0	0.2	0
1912	CoBo				Slate018	0.12	0.4	0	0.5	0	0	0	0
1919	CoBo				Hoff	0	0	0.94	0	0	0	0	0
1940													
1943													
1951	CoBo				Slate018	0.12	0.4	0	0.5	0	0	0	0
1971					WPT020								
1973					WPT020								
1974					WPT020								
1975													
1978	No CoBo				main1	0.07	0.1	0.16	0.2	0	0	0.3	0
1997	No CoBo				Tar3	0.08	0	0	0	0	0	0.9	0
1998	No CoBo				main1	0	0	0	0	0	0	0	0
2003													
2012	No CoBo		1.2	0.4	Evans1	0.08	0	0	0	0	0	0.6	0.29
2015													
2038	CoBo				Hoff	0	0	0.94	0	0	0	0	0
2041	CoBo				15	0.2	0.31	0	0.5	0	0	0	0
2086													
2095	CoBo		2.3	0.4	15	0.2	0.31	0	0.5	0	0	0	0
2107	No CoBo				tar3	0.08	0	0	0	0	0	0.9	0
2121	CoBo				15	0.2	0.31	0	0.5	0	0	0	0
2138	No CoBo				Brad	0	0	0	0	0	0	0.8	0
2229	No CoBo				tar8	0.06	0	0	0	0	0	0.9	0
2434	No CoBo				tar8	0.06	0	0	0	0	0	0.9	0
2489	No CoBo				Main3	0	0.09	0.19	0.2	0	0	0.3	0.06
2530	No CoBo				tar8	0.06	0	0	0	0	0	0.9	0
2787	CoBo	0.06	3	1	39	0.15	0.14	0	0.7	0	0	0	0
2857	No CoBo				Tar4	0.05	0	0	0	0	0	1	0
2953	CoBo				DG1	0	0	1	0	0	0	0	0
3126	No CoBo	0.03			WPT040	0.12	0.11	0	0.8	0	0	0	0
3130	No CoBo				Tar4	0	0	0	0	0	0	0	0
3153													
3203													
3352	No CoBo	0.05	3.25	0.8	41	0.1	0.09	0	0.8	0	0	0	0
3357													
3462	CoBo	0.047	5	0.8	Oil8	0.04	0.17	0	0.8	0	0	0	0.04

Reach#	E model 3 output	Field S (m/m)	Field BFW (m)	Field BFD (m)	GPS point / pourpt	% Tmb	% Tvq	% Tb	%Tla	% Tsr	Tsl	% Tpt	% Tm
3566	CoBo	0.047	5	0.8	Oil8	0	0.21	0	0.7	0	0	0	0.05
3696	No CoBo	0.01	8.2	1	Peters4	0.12	0	0	0.4	0	0	0.2	0.15
3710	No CoBo	0.035			WPT045	0.09	0.08	0	0.8	0	0	0	0
3779													
3819													
3836	No CoBo	0.135			47	0.09	0.08	0	0.8	0	0	0	0
4118	CoBo		3	0.6	WPT028	0	0	0.99	0	0	0	0	0
4169													
4179													
4222													
4262	CoBo	0.024	6	1	Oil7	0.04	0.17	0	0.8	0	0	0	0.04
4270													
4308	CoBo	0.024	6	1	Oil7	0.04	0.17	0	0.8	0	0	0	0.04
4321	CoBo		6	1	Oil6	0.05	0.22	0	0.7	0	0	0	0.04
4572	CoBo	0.065	2.5	0.3	Fall-WPT031	0	0	1	0	0	0	0	0
4690													
4740													
4942													
5094													
5828	CoBo	0.0176	7	1.5	Oil5	0.12	0.23	0	0.6	0.01	0	0	0.07
5964	CoBo	0.0176	7	1.5	Oil5	0.12	0.23	0	0.6	0.01	0	0	0.07
7030													
7071	CoBo				WatermanD	0.18	0.36	0	0.2	0.09	0	0.1	0.13
7146	CoBo	0.025			LB1	0	0	0.95	0	0	0	0	0
7165	CoBo				lb2	0	0	0.96	0	0	0	0	0
7205	CoBo				lb2	0	0	0.96	0	0	0	0	0
7241	CoBo				lb2	0	0	0.96	0	0	0	0	0
7775	No CoBo				LBut	0	0	0.03	0	0	0	0	0
7889	No CoBo				brad	0	0	0	0	0	0	0.8	0

Reach#	% Tpp	% Tsc	% other	bedrock total	Percent Strong	Percent Weak	Percent Unknown	model testing	OID_	FNODE_
83	0	0	0.01	1	0.39	0.6	0	model	83	72
114									114	116
119	0	0	0.05	1	0.5	0.26	0.19	model	119	122
126									126	128
128	0	0	0.05	1	0.5	0.26	0.19	model	128	126
138	0	0	0.07	1	0.5	0.22	0.21	model	138	136
139									139	134
145	0	0	0.07	1	0.5	0.22	0.21	model	145	146
150	0	0	0.07	1	0.5	0.22	0.21	model	150	152
157	0	0	0.07	1	0.51	0.21	0.21	model	157	157
164	0	0	0.07	1	0.51	0.21	0.21	model	164	164
177	0	0	0.06	1	0.51	0.21	0.22	model	177	177
183	0	0	0.06	1	0.51	0.21	0.22	model	183	185
187	0	0	0.06	1	0.51	0.21	0.22	test1	187	192
193	0	0	0.06	1	0.51	0.21	0.22	test1	193	196
198	0	0	0.06	1	0.51	0.21	0.22	test1	198	202
201	0	0	0.06	1	0.51	0.21	0.22	test1	201	207
205	0	0	0.06	1	0.51	0.21	0.22	test1	205	210
213	0	0	0.011	1	0.558	0.212	0.219	test1	213	215
223	0	0	0.01	1	0.45	0.5	0.04	test1	223	232
228	0	0	0.011	1	0.558	0.212	0.219	test1	228	225
237	0	0	0.011	1	0.558	0.212	0.219	test1	237	239
238	0	0	0.01	1	0.45	0.5	0.04	test1	238	234
258	0	0	0.01	1	0.45	0.5	0.04	test1	258	249
259	0	0	0.011	1	0.558	0.212	0.219	test1	259	248
268	0	0	0	1	0.51	0.36	0.13	test1	268	271
288	0	0	0	1	0.51	0.36	0.13	test1	288	279
309	0	0	0	1	0.51	0.36	0.13	test1	309	298
313									313	315
351	0	0	0	1	0.51	0.36	0.13	test1	351	326
375	0	0	0.02	1	0.37	0.45	0.16	test1	375	367
382	0	0	0.01	1	0.27	0.53	0.19	test1	382	397
430	0	0	0.01	1	0.27	0.53	0.19	test1	430	443
447	0	0	0.02	1	0.37	0.45	0.16	test1	447	388
560	0	0	0	1	0	1	0	model	560	508
661	0	0	0.01	1	0	0.99	0	model	661	581
772	0	0	0.01	1	0	0.99	0	model	772	677
902	0	0	0.14	1	0	0.86	0	model	902	833
953	0	0	0.02	1	0	0.98	0	model	953	793
1023									1023	1013
1040	0	0	0.02	1	0	0.98	0	model	1040	977
1086	0.35	0	0.1	1	0	0.9	0	model	1086	1026
1087	0	0	0.14	1	0	0.86	0	model	1087	958
1144	0	0	0	1	0.2	0.8	0	model	1144	1119
1202									1202	1230
1210									1210	1236
1231	0	0	0	1	0.19	0.81	0	model	1231	1218
1234	0	0	0.09	1	0	0.91	0	model	1234	1237
1303	0	0	0	1	0.19	0.81	0	model	1303	1260
1320	0	0	0	1	0	1	0	model	1320	1344
1323									1323	1304
1333	0	0	0	1	0	1	0	model	1333	1272
1356	0	0	0.03	1	0	0.97	0	model	1356	1065

Reach#	% Tpp	% Tsc	% other	bedrock total	Percent Strong	Percent Weak	Percent Unknown	model testing	OID_	FNODE_
1369									1369	1340
1402	0	0	0	1	0.2	0.8	0	model	1402	1330
1408	0	0	0	1	0	1	0	model	1408	1360
1452									1452	1381
1478	0	0	0	1	0	1	0	model	1478	1433
1505	0	0	0.02	1	0	0.98	0	model	1505	1391
1528	0	0	0	1	0	1	0	model	1528	1504
1619	0	0	0	1	0	1	0	model	1619	1558
1694	0	0	0	1	0	1	0	model	1694	1647
1716	0.21	0	0.09	1	0	0.91	0	model	1716	1446
1731	0	0	0	1	0.13	0.87	0	model	1731	1532
1800	0	0	0	1	0.1	0.9	0	model	1800	1764
1885	0	0	0	1	0.1	0.9	0	model	1885	1835
1896									1896	1883
1903	0	0	0	1	0.1	0.9	0	model	1903	1913
1909	0	0	0.16	1	0.38	0.46	0	model	1909	1938
1912	0	0	0	1	0.52	0.48	0	model	1912	1904
1919	0	0.05	0.01	1	0.94	0	0.05	model	1919	1949
1940									1940	1925
1943									1943	1974
1951	0	0	0	1	0.52	0.48	0	model	1951	1942
1971									1971	2005
1973									1973	2007
1974									1974	2008
1975									1975	1824
1978	0	0	0.19	1	0.33	0.48	0	model	1978	2014
1997	0	0	0	1	0.08	0.92	0	model	1997	1933
1998	0	0	0	0	0	0	0	model	1998	1820
2003									2003	2038
2012	0	0	0	1	0.08	0.63	0.29	model	2012	1993
2015									2015	1935
2038	0	0.05	0.01	1	0.94	0	0.05	model	2038	2071
2041	0	0	0	1	0.51	0.49	0	model	2041	2041
2086									2086	2118
2095	0	0	0	1	0.51	0.49	0	model	2095	2089
2107	0	0	0	1	0.08	0.92	0	model	2107	2042
2121	0	0	0	1	0.51	0.49	0	model	2121	2128
2138	0	0	0.24	1	0	0.76	0	model	2138	2011
2229	0	0	0	1	0.06	0.94	0	model	2229	2220
2434	0	0	0	1	0.06	0.94	0	model	2434	2261
2489	0	0	0.16	1	0.28	0.5	0.06	model	2489	2365
2530	0	0	0	1	0.06	0.94	0	model	2530	2466
2787	0	0	0	1	0.29	0.71	0	model	2787	2758
2857	0	0	0	1	0.05	0.95	0	model	2857	2566
2953	0	0	0	1	1	0	0	model	2953	2993
3126	0	0	0	1	0.23	0.77	0	model	3126	3098
3130	0	0	0	0	0	0	0	model	3130	2949
3153									3153	3070
3203									3203	3136
3352	0	0	0.02	1	0.19	0.79	0	model	3352	3274
3357									3357	3056
3462	0	0	0	1	0.21	0.75	0.04	test1	3462	3464

Reach#	% Tpp	% Tsc	% other	bedrock total	Percent Strong	Percent Weak	Percent Unknown	model testing	OID_	FNODE_
3566	0	0	0	1	0.21	0.74	0.05	test1	3566	3491
3696	0	0	0.15	1	0.12	0.58	0.15	model	3696	3622
3710	0	0	0.02	1	0.17	0.81	0	model	3710	3668
3779									3779	3746
3819									3819	3832
3836	0	0	0.02	1	0.17	0.81	0	model	3836	3734
4118	0	0	0.01	1	0.99	0	0	model	4118	4145
4169									4169	3803
4179									4179	4139
4222									4222	4248
4262	0	0	0	1	0.21	0.75	0.04	test1	4262	4116
4270									4270	4196
4308	0	0	0	1	0.21	0.75	0.04	test1	4308	4289
4321	0	0	0.01	1	0.27	0.68	0.04	test1	4321	4334
4572	0	0	0	1	1	0	0	model	4572	4598
4690									4690	4717
4740									4740	4769
4942									4942	4974
5094									5094	5119
5828	0	0	0.01	1	0.35	0.56	0.08	test1	5828	5735
5964	0	0	0.01	1	0.35	0.56	0.08	test1	5964	5854
7030									7030	7052
7071	0	0	0	1.01	0.54	0.25	0.22	model	7071	7025
7146	0	0	0.05	1	0.95	0	0	model	7146	7167
7165	0	0	0.04	1	0.96	0	0	model	7165	7187
7205	0	0	0.04	1	0.96	0	0	model	7205	7227
7241	0	0	0.04	1	0.96	0	0	model	7241	7264
7775	0	0.87	0.1	1	0.03	0	0.87	model	7775	7777
7889	0	0	0.24	1	0	0.76	0	model	7889	1694

Reach#	TNODE_	LENGTH	Theissen (km^2)	BF WIDTH	BF DEPTH
83	87	160.09	1.24	4.50	0.39
114	120	55.38	0.13	1.85	0.21
119	126	128.73	1.76	5.15	0.43
126	134	23.73	0.15	1.96	0.22
128	136	89.99	1.82	5.22	0.44
138	146	86.54	1.84	5.24	0.44
139	146	42.91	0.15	1.98	0.22
145	152	46.17	2.03	5.45	0.45
150	157	92.50	2.05	5.47	0.45
157	164	51.81	2.07	5.49	0.45
164	171	55.03	2.08	5.50	0.45
177	185	45.40	2.14	5.57	0.46
183	192	54.87	2.15	5.57	0.46
187	196	10.89	2.21	5.64	0.46
193	202	19.86	2.21	5.64	0.46
198	207	24.23	2.22	5.64	0.46
201	210	23.71	2.22	5.64	0.46
205	215	22.90	2.22	5.64	0.46
213	225	31.91	2.22	5.65	0.46
223	234	19.73	2.03	5.45	0.45
228	239	62.87	2.25	5.67	0.46
237	248	20.20	2.25	5.68	0.46
238	249	46.47	2.03	5.45	0.45
258	270	51.70	2.04	5.46	0.45
259	271	60.45	2.37	5.79	0.47
268	279	18.44	2.37	5.79	0.47
288	298	63.54	4.43	7.39	0.55
309	320	116.80	4.47	7.41	0.55
313	324	48.43	0.13	1.87	0.22
351	362	121.77	4.63	7.52	0.56
375	388	185.41	9.48	9.94	0.68
382	369	140.87	4.79	7.61	0.56
430	397	154.18	4.72	7.58	0.56
447	458	161.59	9.57	9.98	0.68
560	581	167.46	1.31	4.59	0.40
661	677	174.91	1.37	4.68	0.40
772	793	194.33	1.75	5.14	0.43
902	926	138.20	0.50	3.16	0.31
953	977	275.10	1.85	5.26	0.44
1023	1050	92.62	0.07	1.48	0.18
1040	1066	157.22	1.91	5.32	0.44
1086	1115	456.45	1.73	5.12	0.43
1087	1115	270.83	1.01	4.16	0.37
1144	1173	64.08	0.49	3.13	0.31
1202	1227	147.72	0.48	3.11	0.31
1210	1230	168.28	0.45	3.02	0.30
1231	1260	72.85	1.14	4.35	0.39
1234	1235	361.50	2.09	5.52	0.45
1303	1330	127.38	1.15	4.37	0.39
1320	1348	40.78	0.26	2.45	0.26
1323	1351	51.80	0.27	2.46	0.26
1333	1360	105.29	0.82	3.82	0.35
1356	1383	463.30	1.56	4.92	0.42

Reach#	TNODE_	LENGTH	Theissen (km^2)	BF WIDTH	BF DEPTH
1369	1395	146.22	0.17	2.06	0.23
1402	1428	165.00	1.17	4.39	0.39
1408	1433	195.40	1.19	4.43	0.39
1452	1477	159.63	0.50	3.16	0.31
1478	1504	243.90	1.59	4.96	0.42
1505	1534	215.91	2.30	5.73	0.46
1528	1558	152.13	1.78	5.18	0.43
1619	1647	161.73	1.84	5.24	0.44
1694	1727	93.19	1.91	5.32	0.44
1716	1749	346.99	5.29	7.92	0.58
1731	1764	243.52	1.89	5.30	0.44
1800	1835	94.88	2.36	5.78	0.47
1885	1913	121.34	2.39	5.81	0.47
1896	1925	74.54	0.35	2.75	0.28
1903	1933	53.65	2.40	5.82	0.47
1909	1820	276.99	101.17	25.03	1.28
1912	1942	84.75	0.95	4.06	0.37
1919	1938	31.13	0.86	3.90	0.36
1940	1971	79.76	0.41	2.92	0.29
1943	1957	56.66	0.04	1.19	0.16
1951	1981	78.42	0.98	4.11	0.37
1971	2004	48.80	0.14	1.94	0.22
1973	2006	22.91	0.13	1.85	0.21
1974	2007	35.40	0.13	1.84	0.21
1975	2009	278.53	0.41	2.93	0.29
1978	1599	518.33	108.06	25.68	1.30
1997	2033	157.62	2.60	6.00	0.48
1998	2014	771.76	106.63	25.55	1.29
2003	1946	157.81	0.19	2.14	0.24
2012	2044	53.90	1.55	4.91	0.42
2015	1938	1005.98	100.07	24.92	1.27
2038	1966	122.28	0.81	3.81	0.35
2041	2074	48.33	1.64	5.01	0.42
2086	2038	196.89	0.13	1.85	0.21
2095	2128	63.43	2.07	5.50	0.45
2107	2138	123.13	3.95	7.06	0.54
2121	2151	34.34	2.17	5.59	0.46
2138	2166	248.61	8.22	9.40	0.65
2229	2261	65.31	4.22	7.25	0.55
2434	2466	225.30	4.29	7.30	0.55
2489	2519	585.27	115.24	26.33	1.32
2530	2566	161.60	4.50	7.43	0.56
2787	2826	112.75	3.45	6.70	0.52
2857	2900	389.62	4.60	7.50	0.56
2953	2963	37.49	0.69	3.57	0.34
3126	3163	188.79	4.37	7.35	0.55
3130	3167	252.93	4.80	7.62	0.57
3153	3189	265.07	0.81	3.80	0.35
3203	3238	192.06	21.64	13.72	0.85
3352	3383	160.21	5.13	7.83	0.58
3357	3230	893.33	118.67	26.64	1.33
3462	3491	50.07	6.61	8.64	0.62

Reach#	TNODE_	LENGTH	Theissen (km^2)	BF WIDTH	BF DEPTH
3566	3593	164.46	6.77	8.72	0.62
3696	3721	136.88	25.08	14.53	0.88
3710	3734	122.35	5.63	8.11	0.59
3779	3803	76.49	25.15	14.54	0.88
3819	3601	808.09	78.05	22.62	1.19
3836	3857	196.57	5.76	8.18	0.59
4118	3968	203.04	1.21	4.46	0.39
4169	4196	436.47	25.39	14.60	0.88
4179	4210	128.11	0.38	2.83	0.29
4222	4196	119.29	49.58	18.95	1.05
4262	4289	245.74	8.46	9.51	0.66
4270	3980	1212.39	75.30	22.31	1.18
4308	4334	108.70	8.53	9.54	0.66
4321	4347	123.98	9.33	9.88	0.68
4572	4470	135.33	1.22	4.47	0.39
4690	4390	577.90	47.54	18.64	1.04
4740	4733	76.56	0.35	2.75	0.28
4942	4635	790.90	46.80	18.53	1.04
5094	4932	590.72	45.06	18.26	1.03
5828	5854	155.65	12.10	10.93	0.72
5964	5986	137.97	12.30	11.00	0.73
7030	6970	204.07	16.47	12.33	0.79
7071	7093	156.69	4.44	7.39	0.55
7146	7112	183.07	2.70	6.09	0.48
7165	7167	97.61	2.67	6.06	0.48
7205	7187	176.54	2.64	6.04	0.48
7241	7227	117.99	2.57	5.98	0.48
7775	7791	96.42	7.11	8.88	0.63
7889	1891	200.04	6.64	8.65	0.62